

Dissertation zur Erlangung des Doktorgrades
der Fakultät für Chemie und Pharmazie
der Ludwig-Maximilians-Universität München



Role of cGMP-dependent protein kinase
in
brown fat cell differentiation

von
Bernd-Bodo Haas
aus Michelstadt

2008

Für meine Familie

Erklärung

Diese Dissertation wurde im Sinne von §13 Abs. 3 bzw. 4 der Promotionsordnung vom 29. Januar 1998 von Prof. Dr. Alexander Pfeifer betreut.

Ehrenwörtliche Versicherung

Diese Dissertation wurde selbstständig, ohne unerlaubte Hilfe erarbeitet.

München, am 04.06.2008

Bernd-Bodo Haas

Dissertation eingereicht am	04.06.2008
1. Gutachter	Prof. Dr. A. Pfeifer
2. Gutachter	Prof. Dr. M. Biel
Mündliche Prüfung am	14.07.2008

Danksagung

An erster Stelle möchte ich mich bei meiner Frau Zitlali bedanken, die mich während meiner ganzen Promotion immer unterstützt und ermuntert hat. Sie hat mit viel Toleranz, Geduld und Liebe meine vielen Wochenenden im Labor und am Computer ertragen. Darauf bin ich stolz und möchte dies auch an dieser Stelle zum Ausdruck bringen. Ich danke meiner kleinen Tochter Emilia Nayeli für das Dasein auf dieser Erde und jedes Lächeln, das sie mir nach einem anstrengendem Labortag schenkt.

Ein weiterer herzlicher Dank geht an meine Eltern und meinen Bruder Heiko, ohne deren Unterstützung ich jetzt nicht das wäre, was ich heute bin. Ihr standet mir immer mit Rat und Tat und familiärem Zusammenhalt zur Seite! Dabei gilt auch ein besonderer Dank meiner Omi, die mich schon zu Schulzeiten auf den richtigen akademischen Weg gebracht hat. Meinen Onkels Rolf und Bernd Klauer und ihren Familien, die mich während des Studiums in Heidelberg und der Promotion in München tatkräftig unterstützt haben.

Ich danke Herrn Prof. Dr. Alexander Pfeifer, der meine Promotion betreut hat. Durch ihn habe ich wissenschaftliches Arbeiten erst richtig erlernt und schätzen gelernt. Ich bedanke mich, für anregende bis hin zu aufregenden und aufgeregten wissenschaftlichen Diskussionen, bei denen trotz allem Ernstes der nötige Humor nie gefehlt hat. Herr Prof. Pfeifer war zu jeder Stunde für alle Fragen und Probleme offen und hat mich stets intensiv und mit vollem Engagement betreut.

Vielen Dank an Herrn Prof. Dr. Martin Biel für die Übernahme des zweiten Gutachtens und die gute Zusammenarbeit mit seinem Labor während unserer Zeit in München.

Ebenso danke ich Prof. Dr. Reinhard Fässler für die vielen Hilfen, Ratschläge und Labormaterialien, die uns sein Labor zur Verfügung gestellt hat, die maßgeblich zum Fortschritt dieser Arbeit beigetragen haben.

Ganz besonders danke ich meinen Arbeitskollegen, vorne weg Dr. Andreas Hofmann, der mir nicht nur im Arbeitsalltag immer mit Rat und Tat zur Seite stand, sondern mir auch privat bei all zu oft „nur einem Bier“ ein guter Freund und Kumpel geworden ist. Meiner ehemaligen Kollegin Katharina Hennecke für die lustige Zeit in München und die Aufbauhilfe zum Laboreinstieg in Bonn. Daniela Scholz für das Einlernen in München, die tolle Zusammenarbeit und vielen lustigen Abende jetzt auch in Bonn. Stefanie Kipschull für viele gelungene

Experiment und stetige Unterstützung. Ohne euch Zwei wäre es nur halb so lustig und produktiv im Labor! Meiner treuen Kollegin Katja Jennissen, mit der ich Büro und Laboralltag teile, für die gute Zusammenarbeit, das Korrekturlesen dieser Arbeit und hin und wieder ein aufmunterndes Lächeln, dass sagt: „Alles wird gut, Bodo!“

Regina Müller danke ich für die Unterstützung im Labor. Ebenso danke ich Diana Messow, Andrea Kabermann, Heidi Sebald, Beate Syttkus, Tiong Ti Lim, Maike Schulte, Jutta Müllich und Christina Stichnote für die gute Zusammenarbeit.

Zu guter Letzt bedanke ich mich bei meine ehemaligen Münchner Kollegen, besonders Dr. Christian Eckert, meinem Fernsehquiz-Partner und WG-Kollegen, Drs. Heidi Geiger und Ludwig Baumann für die wunderbare Zeit in München, die mir immer in Erinnerung bleiben wird. Christina Griesmeier, dem Prakti, Dr. Stylianos Michalakis und Prof. Dr. Christian Wahl für tolle Zusammenarbeit und lustige Stunden.

BAT rules und alles wird gut!!!

Erklärung	I
Danksagung	II
Table of Contents	IV
Abbreviations	VII
1. Introduction	1
1.1. The NO/cGMP signaling cascade	1
1.2. Structure, expression and function of PKGs	2
1.2.1. Physiological role of PKGI	4
1.2.2. Brown adipose tissue – BAT	6
1.2.2.1. Insulin signaling in BAT	8
1.2.3. Adipogenic differentiation - Mesenchymal stem cells.....	9
1.3. Aim of the PhD thesis	11
2. Materials and Methods	12
2.1. Common chemicals	12
2.2. Animals	12
2.3. Histological analysis	12
2.3.1. Preparation of paraffin sections.....	13
2.3.2. Hematoxylin/Eosin staining	13
2.4. Immunological methods.....	14
2.4.1. Materials immunological analysis.....	14
2.4.2. Immunostaining of brown adipose tissue sections	15
2.4.3. F-Actin staining of adherent cells in culture	16
2.4.4. Staining of mitochondria by MitoTracker fluorescence	17
2.4.5. Microscopy	18
2.4.5.1. Fluorescence microscopy	18
2.4.5.2. Electron microscopy.....	18
2.5. Cell culture methods	19
2.5.1. Materials cell culture	19
2.5.2. Isolation and culture of primary BAT-derived mesenchymal stem cells.....	19
2.5.2.1. immortalization of primary BAT-MSCs.....	20
2.5.3. Cell culture and trypsinization of cell lines.....	21
2.5.3.1. Cryo-preservation of cells	21
2.5.3.2. Thawing of cryo-preserved cells	21
2.5.4. Adipogenic differentiation of immortalized brown adipocytes	22
2.5.4.1. Oil Red O staining of differentiated adipocytes.....	22
2.5.4.2. Triglyceride determination of differentiated adipocytes.....	23
2.5.5. Osteogenic differentiation of immortalized brown adipocytes	24
2.5.5.1. Alkaline phosphatase staining of osteoblasts	25
2.5.6. Luciferase reporter assays	25
2.6. Biochemical Methods.....	26
2.6.1. Materials biochemistry	26
2.6.2. Preparation of total protein lysates from adherent cells.....	26
2.6.3. Preparation of total protein lysates from tissues	27
2.6.4. Quantification of proteins with the Bradford protein assay	28
2.6.5. Immunoprecipitation	28
2.6.6. Rhotekin pull down assay	29
2.6.6.1. Preparation of GBP-GTP fusion proteins.....	29
2.6.6.2. Loading of glutathione beads and pull down	30
2.6.7. One-dimensional SDS-polyacrylamid-gelectrophoresis (SDS-PAGE).....	31

2.6.8.	Western blotting and immunodetection	32
2.6.9.	Coomassie staining of SDS-PAGE gels.....	34
2.7.	Molecular Biological Methods.....	35
2.7.1.	Materials molecular biology.....	35
2.7.2.	Phenol/Chloroform extraction of tail DNA.....	35
2.7.3.	Bacteriological tools.....	36
2.7.3.1.	Preparation of competent bacteria.....	36
2.7.3.2.	Transformation of competent bacteria	37
2.7.3.3.	Cryo-preservation of bacteria.....	37
2.7.3.4.	Preparation of plasmid DNA from bacterial cultures - Mini Preparation ...	37
2.7.3.5.	Preparation of plasmid DNA from bacterial cultures – Maxi Preparation..	37
2.7.4.	Enzymatic manipulation of DNA.....	38
2.7.4.1.	Digestion of DNA with restriction enzymes	38
2.7.4.2.	Dephosphorylation of plasmid DNA.....	38
2.7.4.3.	Phosphorylation of DNA fragments.....	39
2.7.4.4.	Blunting of DNA fragments.....	39
2.7.4.5.	Ligation of DNA fragments	39
2.7.5.	Agarose gel electrophoresis	40
2.7.5.1.	Extraction of DNA from agarose gels.....	40
2.7.6.	Generation of lentiviral expression constructs.....	41
2.7.6.1.	Plasmids and cDNAs.....	41
2.7.6.2.	Expression vectors.....	41
2.7.6.3.	Generation of caPKGI expression construct	42
2.7.6.4.	Generation of control expression construct.....	42
2.7.7.	Generation of lenti-/retrovirus.....	42
2.7.7.1.	Calcium phosphate transfection of HEK293-T cells.....	42
2.7.7.2.	Harvest of viral supernatant	43
2.7.7.3.	Infection of cells with lenti-/retroviral vectors.....	43
2.7.8.	Isolation of RNA from cells and tissues and reverse transcription (RT)	44
2.7.9.	Polymerase chain reaction (PCR)	44
2.7.9.1.	Primers PCR.....	45
2.7.9.2.	PCR reactions.....	46
2.7.9.3.	PCR programs	47
2.7.9.4.	Real-time PCR (SYBR Green).....	48
2.7.9.5.	Primers Real-time PCR.....	48
2.7.9.6.	Real-time PCR reactions	49
2.7.9.7.	Real-time PCR program.....	49
2.7.9.8.	Quantification of Real-time PCR data	50
2.7.10.	DNA chip hybridization.....	50
2.8.	Statistical analysis	50
3.	Results	51
3.1.	Characterization of BAT-derived mesenchymal stem cells.....	51
3.1.1.	Expression of the NO/cGMP signaling cascade in BAT-MSCs.....	53
3.2.	PKGI mediates cGMP-induced mitochondrial biogenesis in BAT-MSCs.....	53
3.3.	PKGI regulates accumulation of fat and expression of adipogenic makers during fat cell differentiation	55
3.3.1.	Microarray (CHIP) analysis of differentiated brown fat cells.....	57
3.4.	PKGI effects on adipogenic differentiation are mediated via the RhoA/ROCK pathway	60
3.5.	Insulin signaling is impaired in PKGI ^{-/-} brown adipocytes.....	62
3.6.	Akt downstream signaling is impaired in PKGI ^{-/-} brown adipocytes	66

3.7.	Brown adipose tissue of PKGI ^{-/-} mice exhibits reduced fat accumulation and expression of fat specific markers	68
4.	Discussion	70
4.1.	NO/cGMP effects on mitochondrial biogenesis and thermogenesis.....	70
4.2.	Potential cGMP-activated signaling pathways.....	70
4.3.	cGMP effects on mitochondrial biogenesis and UCP-1 expression are mediated by PKGI	72
4.4.	PKGI is necessary for brown fat cell differentiation	73
4.5.	PKGI at the cross-roads of three signaling pathways	74
4.6.	Role of PKGI in BAT <i>in vivo</i>	75
5.	Summary	77
6.	Appendix	80
7.	Curriculum vitae	84
8.	Publications and Abstracts	86
8.1.	Publications	86
8.2.	Abstracts.....	86
9.	References	87

Abbreviations

3T3-L1	white preadipocyte cell line
ABC	avidin-biotin-peroxidase complex
ALP	alkaline phosphatase
Akt	protein kinase B / PKB
ANP	atrial natriuretic peptide
APS	ammonium peroxodisulfate
aP2	fatty acid binding protein 4 (Fabp-4)
AT	adipose tissue
ATP	adenosine triphosphate
BAT	brown adipose tissue
BAT-MSCs	brown adipose tissue derived mesenchymal stem cells
BCIP	8-bromo-4-chloro-3-indoyl-phosphate
BES	<i>N,N</i> -bis(2-hydroxyethyl)-2-aminoethansulfonicacid
BBS	BES-buffered saline
BM	bone marrow
bp	base pair
BSA	bovine serum albumine
Ca ²⁺	calcium ion
CaCl ₂	calcium chloride
cAMP	cyclic adenosine-3', 5'-monophosphate
caPKGI	constitutively active PKGI
cDNA	complementary DNA
C/EBPβ	CCAAT/enhancer-binding protein β
Cidea	cell death-inducing DNA fragmentation factor α subunit-like effector A
CIP	calf intestinal phosphatase
cGMP	cyclic guanosine-3', 5'-monophosphate
CMV	cytomegalovirus promoter
CNG	cyclic nucleotide-gated channel
Cre	Cre-recombinase
CRE	cAMP-responsive element
CREB	cAMP-responsive element-binding protein
DAB	3-3' diaminobenzidine
DAPI	4',6-diamidin-2-phenylindol-dihydrochloride

Abbreviations

DMEM	Dulbecco's Modified Eagle Medium
DMSO	dimethyl sulfoxide
DNA	deoxyribonucleic acid
dsDNA	double-strand DNA
dNTPs	deoxynucleotide triphosphate
DTT	1,4-dithiothreitol
ECL	enhanced chemiluminescence
<i>E. coli</i>	<i>Escherichia coli</i>
EtOH	ethanol
EDTA	ethylene diamine tetraacetic acid
F-actin	filamentous actin
FACS	fluorescence activated cell sorting
FBS	foetal bovine serum
FFA	free fatty acids
fl	floxed allele
FN	fibronectin
GA	glutaraldehyde
gag	<i>gag</i> -gene of HIV-1
GAPDH	glycerol aldehyde-3-phosphate dehydrogenase
GBD	GTPase binding domain
Gpd-1	glycerol-3-phosphate dehydrogenase
GDP	guanosine diphosphate
GTP	guanosine triphosphate
h	hours
HBSS	Hanks' balanced salt solution
H/E	hematoxylin/eosin
HEK293-T	human embryonic kidney cells
HEPES	N-(2-hydroxyethyl)-piperazine-N'-2-ethansulfonic acid
HIB1B	brown preadipocyte cell line
HIV	human immune deficiency virus
HRP	horseradish peroxidase
HPRT	hypoxanthine-guanine-phosphoribosyltransferase
HSL	hormone-sensitive lipase
IBMX	3-isobutyl-methyl-xanthine

Abbreviations

IF	immunofluorescence
ins	insulin
IP	immunoprecipitation
IP ₃	inositol-1,4,5-triphosphate
IPTG	isopropyl-β-D-galactopyranoside
IRAG	IP ₃ receptor-associated cGMP kinase substrate
IRS	insulin receptor substrate
K	potassium
kb	kilo base
KCl	potassium chloride
kDa	kilo Dalton
KH ₂ PO ₄	potassium dihydrogenphosphate
k.o.	knock out
LB ⁺	Luria-Bertani Medium with glucose
LBamp	Luria-Bertani Medium with ampicillin
LiCl	lithium chloride
loxP	34bp cis-active sequence, target-sequence of the Cre-recombinase
LTD	long term depression
LTP	long term potentiation
LTR	long terminal repeat
LV-	lentiviral vector
LV-caPKGI	lentiviral vector containing constitutively active PKGI
LV-cntr	lentiviral vector containing no promoter and no transgene
LV-CreSD	lentiviral vector containing self-deleting (SD) Cre-recombinase
LV-PGKTA _g	lentiviral vector containing a PGKTA _g expression cassette
ml/μl	milliliter/microliter
MAPK	mitogen-activated kinase
M/mM/μM	molar/millimolar/micromolar
MBS	myosin binding subunit of MLCP
MEFs	murine embryonic fibroblasts
MeOH	methanol
Mg	magnesium
MgCl ₂	magnesium chloride
mg/μg	milligram/microgram

Abbreviations

min	minutes
MLC	myosin light chain
MLCP	myosin light chain phosphatase 1
mRNA	messenger RNA
MSC	mesenchymal stem cell
MuLV	murine leukaemia-virus
Myr-	myristoylated
n/N	number
Na	sodium
NA	noradrenalin
NaCl	sodium chloride
NaF	sodium fluoride
Na ₂ HPO ₄	disodium hydrogenphosphate
NaN ₃	sodium azid
Na ₃ VO ₄	sodium orthovanadate
NBT	nitro blue tetrazolium
NCS	normal chicken serum
NH ₄ OAc	ammonium acetate
nm	nanometer
nM	nanomolar
NO	nitric oxid
NOS	NO-synthase
Ocn	osteocalcin
OD	optical density
o/n	overnight
p	passage
PAGE	polyacrylamid gel electrophoresis
PBS	phosphate-buffered saline
PCR	polymerase chain reaction
PDE	phosphodiesterase
Pen/Strep	penicilline/streptomycine
pGC	particulate guanylyl cyclase
PKA	cAMP-dependent kinase, protein kinase A
Plin	perilipin

Abbreviations

PFA	paraformaldehyde
PGK	phosphoglycerate kinase promoter
PI3K	phosphoinositide 3-kinase
PKG	cGMP-dependent kinase, protein kinase G
PNK	polynucleotide kinase
pol	<i>pol</i> -gene of HIV-1
PPAR γ	peroxisome proliferator-activated receptor γ
PGC-1 α	peroxisome proliferator-activated receptor γ coactivator 1 α
PVDF	polyvinylidene fluoride
RBD	rhotekin-binding domain
RhoGDI	Rho GDP-dissociation inhibitor
RIPA	radio immunoprecipitation assay
RNA	ribonucleic acid
RNase	ribonuclease
ROCK	Rho kinase
rpm	rotations per minute
RRE	<i>rev</i> response element, binding domain of <i>rev</i>
RRL	lentiviral vector plasmid
RSV	respiratory syncytial virus
RT	room temperature
RT-PCR	reverse transcription-PCR
SDS	sodium dodecyl sulfate
s.e.m.	standard error of the mean
Ser	serine
sGC	soluble guanylyl cyclase
SIN	self-inactivating
SV40	simian virus 40
SVF	stromal vascular fraction
T3	triiodothyronine
TAg	SV40 large tumor antigen
Taq	<i>Thermophilus aquaticus</i> polymerase
TBE	Tris-borate-EDTA
TBS	Tris-buffered saline
TE	Tris-EDTA buffer

Abbreviations

TEMED	N, N, N', N'-tetramethylethylenediamine
Thr	threonine
Tris	2-Amino-2-hydroxymethyl-propane-1,3-diol
Tyr	tyrosine
U3	U3 region of the HIV LTR
U5	U5 region of the HIV LTR
UCB	umbilical cord blood
UCP-1	uncoupling protein-1
VASP	vasodilator-stimulated-phospho-protein
VSV-G	<i>env</i> -protein of the vesicular stomatitis virus
WAT	white adipose tissue
WB	Western blot
WPRE	post-transcriptional regulatory element of the woodchuck hepatitis virus
wt	wild type
XL-1/XL-21	competent <i>E. coli</i> bacteria

1. Introduction

1.1. The NO/cGMP signaling cascade

The Nitric Oxide (NO)/cyclic guanosine-3', 5'-monophosphate (cGMP) signaling cascade plays an important role in the regulation of a variety of physiological responses such as smooth muscle relaxation, inhibition of platelet aggregation and synaptic plasticity.

The messenger molecule NO is produced by NO-synthases (NOS) which catalyze the oxidation of the terminal nitrogen of the guanidino group of the amino acid arginine (Lloyd-Jones and Bloch, 1996; Loscalzo and Welch, 1995). Three different isoforms can be distinguished. Two constitutively Ca^{2+} /Calmodulin-dependent isoforms are expressed in neurons (nNOS, NOS-1) and in endothelial cells (eNOS, NOS-3). A third isoform is found in many cell types, e.g. in macrophages, vascular smooth muscle cells and endothelial cells. Due to its activation by cytokines and lipopolysaccharides this isoform is called inducible NOS (iNOS, NOS-2). Activated iNOS is independent from the Ca^{2+} -concentration and produces NO over longer periods and at greater amounts. NO diffuses through the membrane into the target cell where it activates the NO-sensitive or soluble guanylyl cyclase (sGC). sGC catalyzes the formation of the second messenger cGMP from guanosine-5'-triphosphate (GTP) (Furchgott and Vanhoutte, 1989). cGMP can also be generated by the membrane bound, particulate guanylyl cyclases (GC-A, GC-B, GC-C), which are stimulated by natriuretic peptides, like atrial natriuretic peptide (ANP) (Garbers and Lowe, 1994).

Most of the known NO effects are mediated by cGMP (Schmidt and Walter, 1994). Mammalian cells have three major types of cGMP receptors: cGMP-regulated ion channels (cyclic nucleotide-gated channels, CNG channels) (Biel et al., 1999), cGMP-dependent phosphodiesterases (PDEs) (Sonnenburg and Beavo, 1994) and cGMP-dependent protein kinases (PKGs) (Figure 1). The increase in cGMP is terminated by the action of cGMP-degrading PDEs.

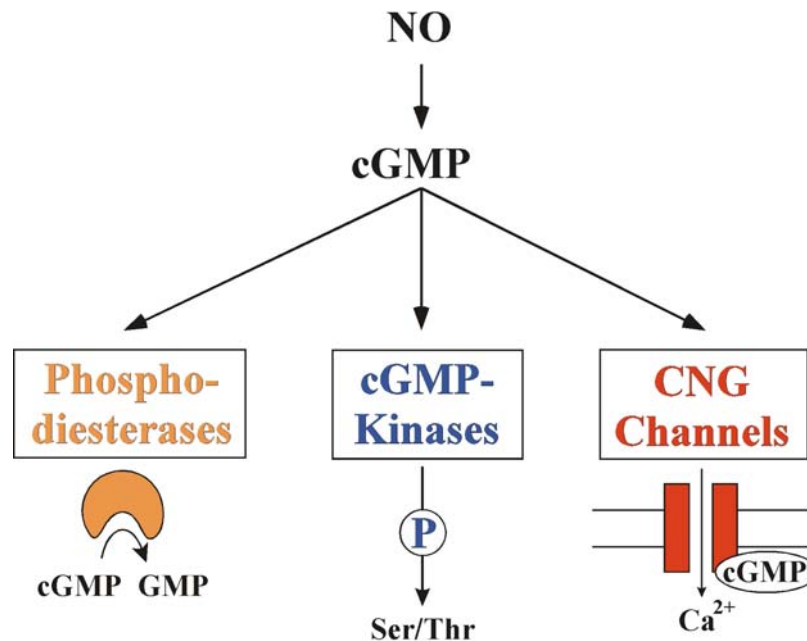


Figure 1. The NO/cGMP signaling cascade and the three major cGMP receptors.

1.2. Structure, expression and function of PKGs

Important mediators of cGMP are the cGMP-dependent protein kinases or PKGs. They belong to the family of serine/threonine kinases and are present in a variety of species. In mammals two PKG genes, *prkg1* and *prkg2* that encode PKGI and PKGII are found. PKGI and PKGII are structurally similar but differ in their subcellular localization, tissue distribution and function (Hofmann et al., 1992).

PKGI is a soluble 75 – 77 kDa protein. The first 100 amino acids of the N-terminus of PKGI are encoded by two alternatively spliced exons that produce the isoforms PKGI α and PKGI β , which are differentially expressed (see also Table 1). The enzymes are activated at submicromolar to micromolar concentrations of cGMP (Gamm and Uhler, 1995; Ruth et al., 1997). Due to the distinct N-terminus to PKGI β , PKGI α has a higher affinity to cGMP at one of the binding pockets.

PKGs are structurally related to cAMP-dependent protein kinase (PKA), the best characterized member of the serine/threonine kinase family (Su et al., 1995). While the regulatory and catalytic units of both kinases are highly conserved, their quaternary structures are distinct. The regulatory and catalytic units of PKG are contained within the same polypeptide chain and the holoenzyme is a homodimer. In contrast, PKA forms a tetrameric holoenzyme complex, composed of separate catalytic and regulatory subunits. cAMP-binding to the regulatory subunits leads to the dissociation and activation of the catalytic subunits.

PKGs are composed of three functional domains: a N-terminal (A) domain, a regulatory (R) domain, and a catalytic (C) domain (Figure 2). The regulatory domain contains two binding pockets for cGMP. The catalytic domain contains a Mg-ATP and a substrate peptide-binding pocket, and is responsible for the transfer of the γ -phosphate residue of ATP to the serine/threonine residues of the substrate protein. In the absence of cGMP, the catalytic domain of PKGI is blocked by a N-terminal autoinhibitory domain which is located between the dimerization domain and the cGMP-binding sites. After binding of 2 moles cGMP/1 mole of enzyme, PKGI α is autophosphorylated at Thr59 and PKGI β at Ser64 and Ser80, respectively. This induces a conformational change of PKGI and the substrate can interact with the substrate-binding site and the catalytic domain leading to the phosphorylation of the substrate. (Hofmann et al., 2000; Pfeifer et al., 1999).

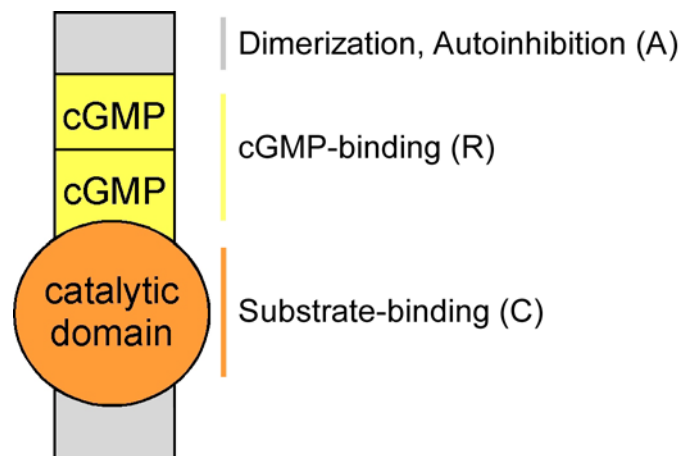


Figure 2. Structure of the PKGs.

PKG consist of three domains. The N-terminus (A) is responsible for dimerization and autoinhibiton. The regulatory domain (R) leads to the activation of the kinase by cGMP-binding and the catalytic domain (C) is responsible for substrate binding and catalysis.

Initially, PKGI was found in invertebrates (Kuo and Greengard, 1970). Two years later cGMP-induced kinase activity was detected in cell extracts of the cerebellum of rats (Hofmann and Sold, 1972) and was then further found in a variety of tissues of mammals. The highest amount of PKGI was found in the Purkinje cells of the cerebellum (Lohmann et al., 1981), in smooth muscles (Keilbach et al., 1992) and in thrombocytes (Waldmann et al., 1986). Furthermore, PKGI is expressed in the hippocampus (Kleppisch et al., 1999), endothelial cells of blood vessels (Draijer et al., 1995), heart (Kumar et al., 1999), kidney (Joyce et al., 1986), spinal ganglions (Qian et al., 1996), the neuromuscular end-plate (Chao et al., 1997) and in neutrophile granulocytes and macrophages (Pryzwansky et al., 1995).

Table 1. Expression of PKGI and its isoforms in tissues.

Tissue	Isoform	Reference
heart, lung	PKGI α >> PKGI β	Kumar et al., 1999
immune cells	PKGI α >> PKGI β	Pryzwansky et al., 1995, Werner et al., 2005
cerebellum	PKGI α > PKGI β	Lohmann et al., 1981
aorta, trachea, uterus	PKGI α << PKGI β	Keilbach et al., 1992, Geiselhoringer et al., 2004
thrombocytes	PKGI α << PKGI β	Waldmann et al., 1986
smooth muscle	PKGI α = PKGI β	Keilbach et al., 1992
neurons	PKGI α = PKGI β	Qian et al., 1996, Chao et al., 1997
hippocampus	PKGI α = PKGI β	Kleppisch et al., 1999
kidney	PKGI α = PKGI β	Joyce et al., 1986

PGKII is also a homodimeric protein of a molecular mass of 87 kDa. Due to myristoylation at the N-terminus PGKII is membrane bound and is found in brain, bone, kidney and the intestinal mucosa (Hofmann et al., 2000; Pfeifer et al., 1999).

1.2.1. Physiological role of PKGI

PKGI regulates a broad spectrum of physiological functions. Thus far, PKGI function was most intensively studied in the cardiovascular and neuronal systems.

The smooth muscle tone in blood vessels and blood pressure are influenced by a variety of factors including NO and natriuretic peptides (Palmer et al., 1987). Both reduce smooth muscle tone by stimulating the cGMP production via the activation of sGC or pGC, respectively. PKGI reduces smooth muscle tone by two major mechanisms. cGMP/PKGI decreases vascular tone by lowering cytosolic calcium (Ca²⁺)-levels or by regulation of the contractile filament via Ca²⁺-independent mechanisms. The liberation of Ca²⁺ from the sarcoplasmic reticulum can be inhibited by the phosphorylation of the inositol-1,4,5-triphosphate receptor (IP₃R) (Komalavilas and Lincoln, 1996) and/or the inhibition of the agonist-induced generation of IP₃. It has been shown that the thrombin-induced IP₃ synthesis and the liberation of Ca²⁺ from the sarcoplasmic reticulum are inhibited by PKGI (Ruth et al., 1993). Furthermore, PKGI β phosphorylates the IP₃ receptor-associated cGMP kinase substrate (IRAG) (Schlossmann et al., 2000), thereby inhibiting IP₃-dependent Ca²⁺-release. In addition, Ca²⁺-dependent high-conductance potassium channels (BK_{Ca} channels), which are involved in the generation of the membrane potential in vascular smooth muscle cell (VSMCs), are activated by PKGI (Fukao et al., 1999; Taniguchi et al., 1993). Phosphorylation of the BK_{Ca} channels leads to a

hyperpolarization causing a reduction of the Ca^{2+} -influx by closing voltage-dependent Ca^{2+} -channels (Alioua et al., 1998). Thus, activation of PKGI leads to a reduction of the Ca^{2+} -concentration in VSMCs, which in turn, leads to relaxation of the smooth muscle and vasodilatation. Furthermore, Ca^{2+} -independent mechanisms have been identified. PKGI α causes the dephosphorylation of the myosin light chain (MLC) through the myosin-phosphatase 1 (MLCP) by phosphorylating the regulatory myosin-binding subunit (MBS) of the MLCP (Surks et al., 1999). PKGI-dependent phosphorylation of MBS at Ser695 increases MLCP activity (Wooldridge et al., 2004). This mechanism would allow a reduction in MLC phosphorylation and smooth muscle relaxation at constant Ca^{2+} -concentrations. Another mechanism of PKGI-dependent smooth muscle relaxation is mediated via the small GTPase RhoA. PKGI phosphorylation of RhoA at Ser188 induces translocation from the membrane to the cytosol whereby RhoA is inactivated. Thus, PKGI inhibits the downstream RhoA effector Rho kinase (ROCK) and consequently activates MLCP to dephosphorylate MLC (Etter et al., 2001; Sauzeau et al., 2000).

In addition to smooth muscle relaxation, PKGI has also a pivotal role in thrombocyte aggregation. Platelets express high amounts of PKGI β (Table 1), which is activated in response to NO and has an anti-aggregatory function (Gambaryan et al., 2004; Marshall et al., 2004; Massberg et al., 1999). Destruction of the endothelial cell layer leads to platelet adhesion and aggregation. Endothelial cells release prostacyclin and NO, which increase cAMP and cGMP levels in platelets and, thereby, inhibit clot formation. In PKGI-deficient mice, collagen-induced platelet aggregation was not inhibited by NO or cGMP analogs, whereas aggregation was prevented by cAMP-elevating agents (Massberg et al., 1999), demonstrating that PKGI is essential for NO/cGMP effects in platelets. Two PKGI substrates have been identified in platelets: vasodilator-stimulated-phospho-protein (VASP) and IRAG. In VASP-deficient mice, cAMP and cGMP-dependent inhibition of platelet aggregation was reduced. Other cAMP and cGMP-dependent effects in platelets, such as inhibition of agonist-induced increases in cytosolic Ca^{2+} -concentrations and granule secretion, were not dependent on the presence of VASP (Aszodi et al., 1999; Hauser et al., 1999). In addition, the interaction of platelets with the endothelium *in vivo* has been found to be increased (Massberg et al., 2004). Platelets from IRAG-deficient mice (Geiselhoringer et al., 2004) have a severe defect in the cGMP-mediated prevention of aggregation, indicating that IRAG is also an essential component of this pathway.

PKGI also has important physiological function in the neuronal system. The analysis of the trajectories of sensory axons in the spinal cord of mouse embryos revealed that axons lacking

PKGI extended predominantly into a single direction (Schmidt et al., 2002). This branching defect resulted in a reduced number of sensory axons in the spinal cord of newborn PKGI mutants and a substantial impairment of the nociceptive flexion reflexes compared with their wild type littermates. These findings indicate that PKGI is required for the correct guidance and connectivity of axons originating from dorsal root ganglia sensory neurons.

Changes in the strength of the synaptic transduction are potential mechanisms for learning and memory (Carey and Lisberger, 2002; Chen and Tonegawa, 1997). Two important phenomena of synaptic plasticity are long term potentiation (LTP) and long term depression (LTD). Both are involved in synaptic transmission, which can be induced *in vivo* and *in vitro* through activation of pre-synaptic fibers. PKGI has been implicated in the generation of LTP in cultured hippocampal pyramidal cells and hippocampal slices (Arancio et al., 1995; Zhuo et al., 1994). In contrast to these findings, hippocampal LTP was normal in PKGI-deficient mice (Kleppisch et al., 1999). Additionally, hippocampus-specific PKGI knock out mice showed normal basal synaptic transmission and normal early phase of LTP within the first hour after a single tetanus in the hippocampus (Kleppisch et al., 2003). However, protein synthesis-dependent late phase of LTP was impaired after multiple episodes of strong theta burst stimulation in adult hippocampus-specific PKGI knock out mice (Kleppisch et al., 2003). NO has also been proposed to be involved in the induction of LTD (Shibuki and Okada, 1991) and Purkinje cells contain high levels of PKGI α (Table 1). Purkinje cell-specific disruption of the PKGI gene caused a nearly complete loss of cerebellar LTD (Feil et al., 2003), identifying PKGI as an essential component in the signaling pathway underlying the induction of LTD at parallel fibers signaling to Purkinje cell synapses.

1.2.2. Brown adipose tissue – BAT

Adipose tissue plays an important role in energy storage and has great influence on whole-body homeostasis. Two types of adipose tissue exist in mammals: White adipose tissue (WAT) and brown adipose tissue (BAT). WAT stores energy in the form of lipids whereas BAT can dissipate energy through adaptive thermogenesis (Barnard, 1977; Rothwell and Stock, 1979). WAT and BAT are normally localized in anatomically distinct areas in mammals. BAT is mainly found in the interscapular neck region and in supraclavicular regions of new born mammals. BAT is also histologically different from WAT. Whereas white fat cells usually contain one major - unilocular - lipid droplet filling up almost the whole cytoplasm, brown fat cells contain several small - multilocular - lipid droplets (Cinti, 2005). In addition, brown

adipocytes contain high numbers of mitochondria containing cristae. BAT is highly vascularized and highly innervated by the sympathetic nervous system. The differences in lipid content and mitochondrial abundance in white and brown fat cells, as well as in vascularization of the tissues, are the reasons for the color differences between WAT and BAT. The thermogenic capacity of BAT is due to expression of UCP-1 exclusively in brown adipocytes. UCP-1 is a facultative proton transporter localized at the mitochondrial inner membrane, where it uncouples the oxidation of fuel substrates from the production of ATP, thereby generating heat (Figure 3).

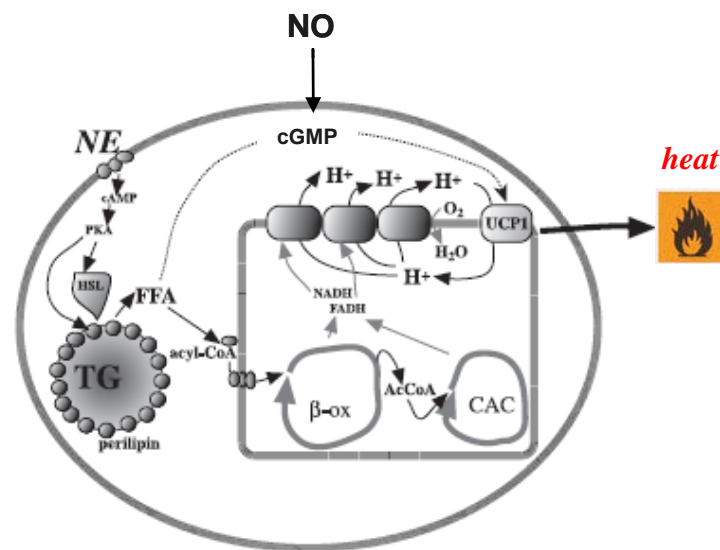


Figure 3. Uncoupling of mitochondrial ATP synthesis by UCP-1 (modified after Cannon and Nedergaard, 2004).

NE, noradrenalin; HSL, hormone-sensitive lipase; TG, triglycerides; FFA, free fatty acids; β -ox, β -oxidation; CAC, citric acid cycle.

In rodents, expression of UCP-1 is highly responsive to external stimuli such as food intake and changes in temperature. Food intake and exposure to cold induce sympathetic activation and the release of noradrenalin (NA) which in turn activates adrenergic receptors of brown fat cells. Recently, NO has been demonstrated to induce mitochondrial biogenesis in brown adipose tissue through activation of cGMP-dependent mechanisms (Nisoli et al., 2003; Nisoli et al., 1998). In addition, calorie restriction induces eNOS expression in a variety of tissues including white fat (Nisoli et al., 2005).

Although BAT content decreases after birth, recent studies using positron emission tomography indicate that adult humans possess metabolically active BAT (Nedergaard et al., 2007).

1.2.2.1. Insulin signaling in BAT

Insulin induces diverse biological actions by binding to and activating its tyrosine kinase receptors (Kasuga et al., 1982; Ullrich et al., 1985). Brown fat cells express a high number of insulin and IGF-I receptors (Lorenzo et al., 1993; Teruel et al., 1996). These receptors transduce signals by phosphorylation of several cellular substrates, especially insulin receptor substrate (IRS) proteins 1, 2, 3 and 4 (White, 2003; White and Kahn, 1994). Following insulin stimulation, IRS proteins are phosphorylated at multiple tyrosine residues, resulting in the interaction with SH2 domain-containing proteins such as the p85 subunit of phosphoinositide 3-kinase (PI3K), the protein tyrosine phosphatase SHPTP2, and the growth factor receptor-bound-2 (Grb-2/Sem5). These events lead to activation of various downstream signaling pathways (Backer et al., 1992; Skolnik et al., 1993; Sun et al., 1993; Sun et al., 1995).

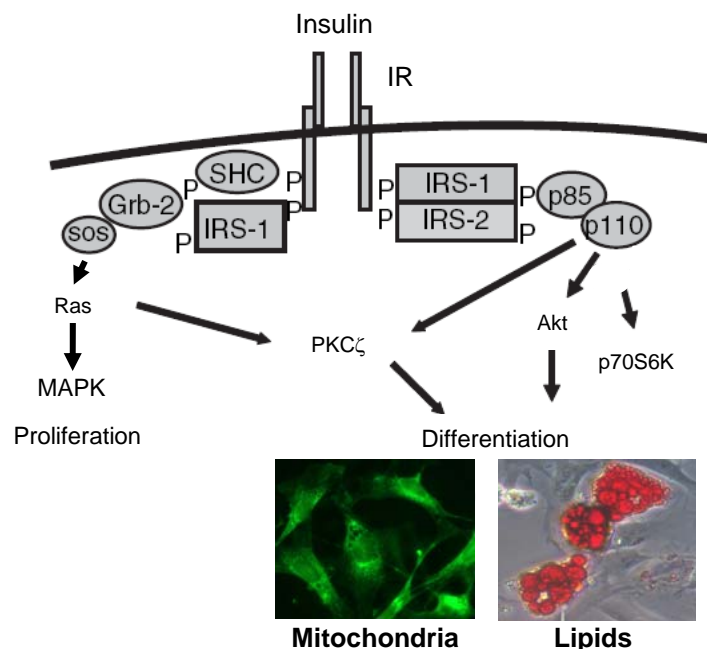


Figure 4. Insulin signaling pathways in brown adipocytes (modified after Valverde et al., 2005).

IRS-1/PI3K/Akt pathway is essential for insulin-induced lipid synthesis, mitochondrial biogenesis and UCP-1 expression in brown adipocytes. MitoTracker staining of BAT-MSCs (2.4.4), mitochondria are stained green (bottom, left); Oil Red O staining (2.5.4.1) of differentiated brown adipocytes, lipids are stained red (bottom right).

Insulin promotes both adipogenic and thermogenic differentiation. The main pathway involved in insulin induction of adipogenic differentiation is the IRS-1/PI3K/Akt (PKB) cascade, which up-regulates the expression of adipogenic-related genes at the transcriptional level (Teruel et al., 1996; Valverde et al., 1992). In addition, the IRS-1/PI3K pathway activates the UCP-1 promoter leading to increased UCP-1 expression (Lorenzo et al., 1993) in BAT.

1.2.3. Adipogenic differentiation - Mesenchymal stem cells

Stem cells can be divided in three groups depending on their differentiation potential: 1) Totipotent stem cells which are found in zygotes and give rise to the embryo and the trophoblast (embryonic stem cells). 2) Pluripotent stem cells derive from the blastocyst and can differentiate into all three germ layers (embryonic stem cells). 3) Multipotent stem cells differentiate in cells of different tissues and are responsible for building up and self-renewal of the tissue (adult stem cells).

Mesenchymal stem cells (MSCs) are multipotent adult stem cells, which can give rise to a variety of lineages of mesenchymal origin including the adipogenic, osteogenic, chondrogenic, myogenic, endothelial and hematopoietic lineages (depending on the *in vitro* culture conditions) (Guilak et al., 2004; Hattori et al., 2004; Safford et al., 2004; Zuk et al., 2002). They are found in bone marrow (BM) (Pittenger et al., 1999), scalp tissue (Shih et al., 2005), placenta (In 't Anker et al., 2004), umbilical cord blood (UCB) (Bieback et al., 2004) and in various fetal tissues (Campagnoli et al., 2001) as well as in adipose tissue (AT) (Zuk et al., 2001).

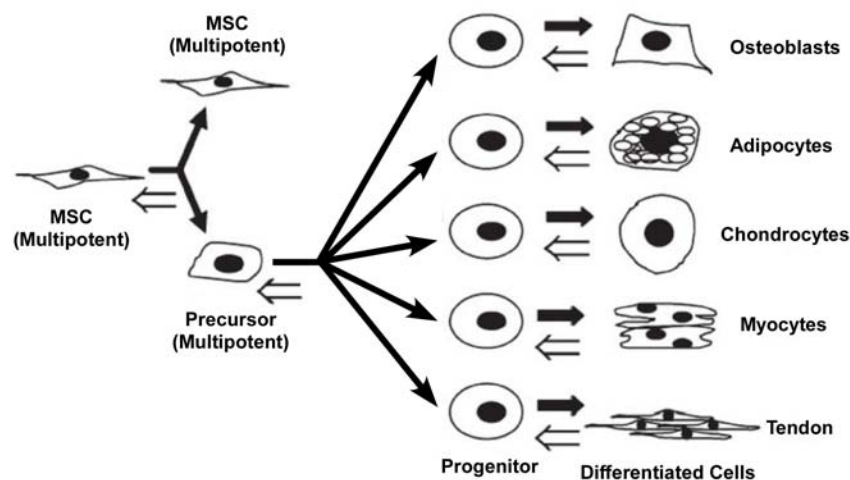


Figure 5. Schematic model of mesenchymal stem cell differentiation (modified after Baksh et al., 2004).

Adipose tissue-derived mesenchymal stem cells (AT-MSCs), are considered to be the multipotent fraction of adherent cells, which, after isolation of the adipose stromal vascular fraction (SVF), attach to plastic culture dishes and remain there as a heterogeneous population of fibroblast-like cells. They can be isolated from either white or brown adipose tissue with similar differentiation potentials (Prunet-Marcassus et al., 2006).

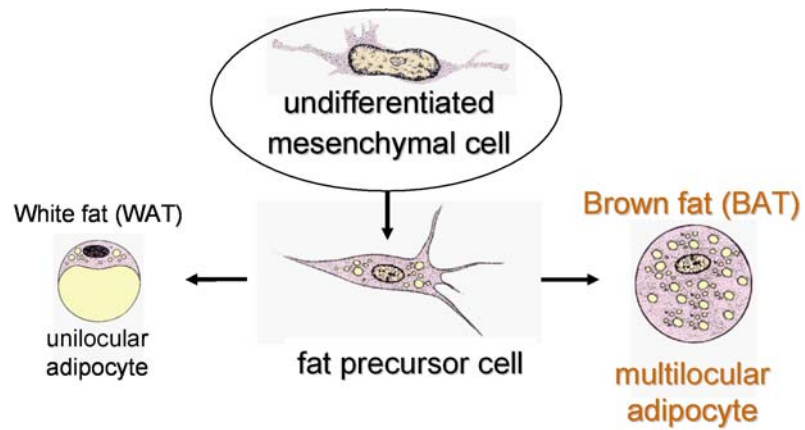


Figure 6. White and brown adipocytes derive from the same mesenchymal precursor cells (modified after Junqueira and Carneiro, 2002).

MSCs used in this study were derived from brown adipose tissue (**brown adipose tissue-derived mesenchymal stem cells, BAT-MSCs**) (2.5.2) and were differentiated into brown adipocytes and osteoblasts, depending on the culture conditions (2.5.4 and 2.5.5).

1.3. Aim of the PhD thesis

The NO/cGMP signaling cascade has been implicated in regulating mitochondrial biogenesis in BAT (Nisoli et al., 2003; Nisoli et al., 1998). However, the mechanism underlying cGMP-induced mitochondrial biogenesis is unclear. In addition, brown fat thermogenesis and brown fat differentiation (adipogenesis) can be differentially regulated (Uldry et al., 2006).

cGMP can signal via three major receptors including PDEs, CNG channels and PKGs. The overall goal of this study was to investigate which of the cGMP receptors is/are responsible for NO/cGMP induced mitochondrial biogenesis. Therefore, the following questions were raised:

- 1) Which components of the NO/cGMP signaling cascade are expressed in BAT?
- 2) Which cGMP receptor(s) regulate mitochondrial biogenesis in BAT?
- 3) What role plays PKG in BAT?
- 4) Does the cGMP signaling pathway regulate BAT differentiation?

In order to determine the role of PKGI in BAT mitochondrial biogenesis and differentiation *in vitro*, PKGI knock out and PKGI floxed mice were used to establish brown adipocyte cell lines, which could further be modified by using lenti- and retroviral vectors to overexpress target proteins. To further investigate the role of PKGI in BAT *in vivo*, the consequences of PKGI-deletion in BAT were analyzed.

2. Materials and Methods

2.1. Common chemicals

All chemicals used in this study, if not further specified were purchased from the following companies: Carl Roth GmbH (Karlsruhe), Merck, Calbiochem (Darmstadt), Sigma-Aldrich (München) and VWR (Darmstadt). Water used in this study was purified and distilled with an EASYpure UV/UF system (WeteA, Wilhelm Werner GmbH, Leverkusen).

2.2. Animals

All mouse strains were maintained and bred in the animal facilities of the Department Pharmazie, Ludwig-Maximilians-Universität, München and the Institut für Pharmakologie und Toxikologie, Bonn. The mice had free access to standard rodent diets and water. The light cycle was set for 12 h. For breeding mice at age of 8 weeks were used. At an age of 3 weeks after birth, mice were separated by sex, marked with ear tags and housed in separate cages.

PKGI knock out mice (Pfeifer et al., 1998) were kept in the heterozygous state on a C57BL/6N background. PKGI floxed mice were kindly provided by Prof. Reinhard Fässler, MPI für Biochemie, Martinsried and kept in the homozygous state on a C57BL/6N background.

2.3. Histological analysis

Equipment

Fluorescence microscope, Axioskop 2 with an Atto Arc light source, HBO-lamp (100W), AxioCam camera and AxioVision software, Zeiss, Jena

Light microscope, DMIL, Leica, Wetzlar

Microtome, HM335E, Microm, Walldorf

Stereo microscope, Advance ICD, Bresser, Rhede

Mounting media

Roti[®]-Histokitt, Roth (Cat. No. 6638.1)

PermaFluor[®], Beckman Coulter, Krefeld (Cat. No. PN IM 0752)

2.3.1. Preparation of paraffin sections

Paraffin wax is the most widely used embedding medium since it is solid enough to support the tissue but yet soft enough to enable rather thin sections to be cut. The most widely used fixatives are paraformaldehyde (PFA) and glutaraldehyde (GA) which react with basic amino acid residues thereby cross-linking neighboring proteins.

Mice of different ages were sacrificed and dissected under a stereo light microscope (Bresser). The isolated brown adipose tissue was collected in PBS and transferred to PFA solution (4% PFA/PBS) and incubated for 30 min at room temperature (RT). Next, tissue samples were dehydrated by subsequent washes in ethanol of ascending concentrations (50%, 70%, 80%, 90%, and 100%) for 1 h each incubated 2 times in xylol for 30 min and placed in paraffin solution 3 times for 1 h at 55° C. The tissue was placed in embedding forms and was embedded with fluid paraffin. Paraffin blocks were stored until cutting at 4° C. Paraffin blocks were cut in 4 µm thick sections using a microtome (Microm). Quality and orientation of the tissue was frequently checked under a light microscope (Leica). Slides were dried at RT for 1 - 2 h and finally stored at 4° C.

PBS

NaCl 8 g
Na₂HPO₄ 1.44 g
KH₂PO₄..... 0.24 g
KH₂PO₄..... 0.24 g
KCl..... 0.2 g
filled up to 1000 ml with H₂O and adjusted to pH 7.4 with HCl

Paraformaldehyde solution

Paraformaldehyde (PFA)..... 4 g
dissolved in PBS pH 7.4, boiled for 1 min and cooled on ice

2.3.2. Hematoxylin/Eosin staining

This technique is a widespread histological stain, which can demonstrate a large number of different tissue structures. The major oxidization product of hematoxylin is hematin which is responsible for the color properties. It stains cell nuclei with good intranuclear detail in blue,

while eosin stains the cytoplasm and connective tissue in varying shades and intensities with a pink color.

In order to perform a hematoxylin/eosin stain, paraffin sections were treated 2 times for 2 min in xylol (deparaffinization) followed by incubation in 100%, 90%, 80%, 70%, 50% and PBS for 2 min (rehydration). Slides were then treated for 1 min with hematoxylin (Mayers hemalaun) and blued in tap water. Subsequently, slides were stained with eosin for 1 min and washed again in tap water. Sections were dehydrated in 50%, 70%, 80%, 90%, 100%, ethanol for 2 min each, washed 2 times 5 min in xylol and finally mounted with Roti®-Histokitt.

Mayers hemalaun, Merck (Cat.No. 1.09249)

Eosin G, Merck (Cat.No. 1.09844)

2.4. Immunological methods

2.4.1. Materials immunological analysis

Flow cytometer, FACSCalibur® with CellQuest® software, Becton Dickinson, USA

VECTASTAIN® ABC Kit, Vector Laboratories, UK (Cat. No. PK-4000)

ACLAR transparencies, Plano, Wetzlar (Cat. No. 10501-10)

Glass coverslips, VWR (Cat. No. 0111520)

Antibodies, see below:

Name	Manufacturer.....	Cat. No.....	WB	IF	IP
Actin.....	Sigma.....	A-5441	1:5000.....	---	---
Akt.....	Cell Signaling.....	9272.....	1:1000.....	---	---
Akt pSer473	Cell Signaling.....	9271	1:1000.....	---	---
aP2.....	Santa Cruz	sc-18661	1:1000.....	---	---
C/EBPβ.....	Santa Cruz	sc-150	1:1000.....	---	---
CD11b-PE	BD Pharmingen	553311	---	1:800.....	---
CD44-PE	BD Pharmingen	553134	---	1:200.....	---
CD45-PE	BD Pharmingen	553081	---	1:400.....	---
CD49e-PE	BD Pharmingen	557447	---	1:200.....	---
CD73-PE	BD Pharmingen	550741	---	1:200.....	---
CD105-PE	Santa Cruz	sc-18838 PE... ..	---	1:200.....	---
CD106-PE	Santa Cruz	sc-19982 PE... ..	---	1:200.....	---

Name	Manufacturer	Cat. No.	WB	IF	IP
CREB	Cell Signaling	9192	1:1000	---	---
CREB pSer133	Cell Signaling	9191	1:1000	---	---
goat-HRP	Chemicon	AP309P	1:5000	---	---
IRS-1	Santa Cruz	sc-7200	1:1000	---	1 μ g
IRS-1 pSer636/639	Cell Signaling	2388	1:1000	---	---
MitoTracker®GreenFM	Molecular Probes	M-7514	---	1:20000	---
mouse-HRP	Dianova	115-035-146	1:10000	---	---
Myc-tag (9B11)	Cell Signaling	2276	1:1000	---	---
PI3K p85 α	Cell Signaling	4257	1:1000	---	---
PPAR γ	Santa Cruz	sc-7273	1:1000	---	---
PGKI	self made	MPI (Ussar)	1:2000	1:600	---
p38	Cell Signaling	9212	1:1000	---	---
p38 pThr180/Tyr182	Cell Signaling	9215	1:1000	---	---
pTyr (Y-20)	Santa Cruz	sc-508	1:1000	---	---
rabbit-biotin	Dianova	---	1:10000	---	---
rabbit-HRP	Cell Signaling	7074	1:10000	---	---
phalloidin Alexa 546	Molecular Probes	A22283	---	1:40	---
RhoA	Santa Cruz	sc-418	1:1000	---	---
Sca-1-PE	BD Pharmingen	553336	---	1:200	---
Tubulin	Dianova	DLN-09992	1:1000	---	---
UCP-1	Santa Cruz	sc-6529	1:500	---	---

2.4.2. Immunostaining of brown adipose tissue sections

Immunostaining on brown adipose tissue was carried out on 4 μ m dewaxed and rehydrated paraffin sections as described before (2.3.2). To quench endogenous peroxidases, sections were treated with peroxidase solution for 30 min, blocked with blocking solution for 30 min at RT and washed three times with washing solution. The primary antibody against PGKI was diluted in blocking solution (1:600) and sections were incubated overnight (o/n) at RT. After subsequent washing with washing solution, the secondary anti-rabbit-biotin antibody was applied for 1 h at RT. After washing again with TBS the VECTASTAIN® ABC Kit (Vector Laboratories) was applied according to the manufactures instructions for 30 min and was developed with 3-3' diaminobenzidine (DAB). After reaction with oxidizing reagents like

peroxidases DAB produces an intense brownish color. Finally, sections were dehydrated as described above (2.3.2) and mounted in Roti®-Histokitt.

TBS

NaCl 150 mM

Tris-HCl 50 mM

filled up to 1000 ml with H₂O and adjusted to pH 7.4 with HCl

Peroxidase solution

30% H₂O₂ 8 g

Methanol..... 40%

Blocking solution

Normal chicken serum (NCS).....2% *VectorLaboratories (Cat.No.S300)*

dissolved in TBS pH 7.4

Washing solution (1% BSA)

Bovine serum albumin (BSA) 1 mg

TBS 1 ml

2.4.3. F-Actin staining of adherent cells in culture

Phallotoxins, isolated from the deadly *Amanita phalloides* mushroom, are bicyclic peptides that differ by two amino acid residues. They can be used interchangeably in most applications and bind competitively to the same sites in F-actin. Phalloidin and phalloidin contain an unusual thioether bridge between a cysteine and tryptophan residue that forms an inner ring structure. Fluorescent and biotinylated phallotoxins stain F-actin at nanomolar concentrations. Glass coverslips placed in 6-well plates were coated o/n at 4° C with fibronectin (FN) (10 µg/ml). The next day wells were placed at 37° C for 1 h, washed with PBS and cells were plated at a density of 1.8 x 10⁵ cells/well. The next day cells were serum starved for 24 h, pre-incubated with 200 µM 8-pCPT-cGMP (2.5.4) for 2 h and induced with 10% FBS for 30 min as indicated. After one wash with PBS cells were fixed with 4% PFA, permeabilized with 0.1% Triton-X 100, blocked with 1% BSA/PBS for 30 min and stained with phalloidin-Alexa 546 for 20 min at RT. After washing with PBS and nuclear staining with 4', 6-diamidino-2-

phenylindole (DAPI) for 5 min, coverslips were mounted on glass slides using PermaFluor® mounting medium.

Fibronectin (FN) solution, Sigma (Cat. No. F-1141)

2.4.4. Staining of mitochondria by MitoTracker fluorescence

In order to stain the mitochondria of the cells a mitochondria selective dye (MitoTracker® GreenFM) was used. The cell permeant MitoTracker® probe passively diffuses across the plasma membrane and accumulates in active mitochondria. It contains a mildly thiolreactive chloromethyl moiety that appears to be responsible for keeping the dye associated with the mitochondria.

Cells were incubated in their culture media containing 50 nM MitoTracker®GreenFM working solution for 30 - 45 min at 37° C. They were then washed with PBS, trypsinized, washed once with PBS and were finally resuspended in PBS. The MitoTracker fluorescence was analyzed by flow cytometry on a FACSCalibur® using CellQuest® software (Becton Dickinson). Data are expressed as relative fluorescence intensity of the geometric mean fluorescent signal versus unstained sample.

MitoTracker® GreenFM working solution (50 nM)

MitoTracker® Green FM stock solution..... 1 µl

Growth medium..... 20 ml

MitoTracker® GreenFM stock solution (1 mM)

MitoTracker® Green FM..... 50 µg

DMSO..... 74.4 µl

dissolved and stored at -20° C

FACS buffer

NaCl 8.12 g

KH₂PO₄..... 0.26 g

Na₂HPO₄..... 2.35 g

KCl 0.28 g

Na₂EDTA..... 0.36 g

LiCl..... 0.43 g
NaN₃ 0.2 g
 filled up to 1000 ml with H₂O and adjusted to pH 7.37

2.4.5. Microscopy

2.4.5.1. Fluorescence microscopy

Fluorescence images were collected by using a fluorescence microscope (Axioskop 2, Zeiss) with a camera (AxioCam, Zeiss) using filter sets described in Table 2. AxioVision software (Zeiss) was used for image acquisition and evaluation.

Table 2. Filter sets used at the Axioskop 2 microscope

Name	#	Excitation	Emission	Fluorochrome
Filter set 01	(488001-0000)	BP 365/12	LP 397	DAPI
Filter set 10	(488010-0000)	BP 450-490	LP 515-565	eGFP
Filter set 38	(1031-350)	BP 470/40	BP 525/50	eGFP
Filter set 15	(488015-0000)	BP 546/12	LP 590	TRITC
Filter set 31	(1031-350)	BP 565/30	LP 620/60	TRITC

2.4.5.2. Electron microscopy

Cells were differentiated on ACLAR transparencies (Plano), fixed in 2% GA and 2% PFA in 0.1 M cacodylate buffer pH 7.4 and subsequently rinsed in 0.1 M PBS. Further processing was done by Prof. Wilhelm Bloch at the Abteilung für Molekulare und Zelluläre and Sportmedizin, Deutsche Sporthochschule, Köln according to the following protocol:

Preparations were postfixated with 2% osmium tetroxide in 0.1 M PBS for 2 h at 4° C. Before embedding in araldite (Ciba-Geigy, Switzerland) the cells were dehydrated in a graded series of ethanol. Ultrathin sections (60 nm) were mounted on formvar-coated copper grids, stained with 0.2% uranyl acetate and leadcitrate, and then examined with a EM 902 A electron microscope (Zeiss). Single cross sectional areas of at least 50 mitochondria per group were measured on EM pictures photographed with a high-speed TEM camera (Mega View III; SIS, Münster) using the morphometric software iTEM 5.0 (SIS, Münster).

2.5. Cell culture methods

2.5.1. Materials cell culture

Centrifuge, Biofuge Primo, Heraeus, Hanau

Incubator, HeraCell 150, Heraeus, Hanau

Laminar air flow, HeraSafe, Heraeus, Hanau

5 ml pipette, Sarstedt, Nümbrecht (Cat. No. 86.1253.001)

10 ml pipette, Sarstedt, Nümbrecht (Cat. No. 86.1254.001)

25 ml pipette, Sarstedt, Nümbrecht (Cat. No. 86.1685.001)

24-well plate, Sarstedt, Nümbrecht (Cat. No. 83.1839.001)

6-well plate, Sarstedt, Nümbrecht (Cat. No. 86.1836.001)

100 mm dish, Sarstedt, Nümbrecht (Cat. No. 83.1802.001)

140 mm dish, Sarstedt, Nümbrecht (Cat. No. 83.1803.001)

15 ml Falcon tube, Sarstedt, Nümbrecht (Cat. No. 62.554.001)

50 ml Falcon tube, Sarstedt, Nümbrecht (Cat. No. 62.548.004)

Cryogenic vials, Sarstedt, Nümbrecht (Cat. No. 72.379.992)

DMEM Glutamax + 4500 mg/l Glucose, Gibco, Karlsruhe (Cat. No. 61965059)

Foetal bovine serum, Biochrom AG, Berlin (Cat. No. S0115)

Neubauer counting chamber, Labomedic, Giessen

Nylon meshes, Millipore, Schwalbach

Sterile filter 0.22 µm, VWR (Cat. No. 514-0061)

Trypan blue 0.4% solution, Sigma (Cat. No. T-8154)

Trypsin, Biochrom AG, Berlin (Cat. No. 25300096)

Penicillin, Streptomycin (P/S), Biochrom AG, Berlin (Cat. No. A2213)

2.5.2. Isolation and culture of primary BAT-derived mesenchymal stem cells

BAT-MSCs were isolated from interscapular brown fat of new born mice (Nechad, 1983). The interscapular brown adipose tissue was dissected out and placed into collagenase digestion buffer. After 30 min at 37° C in a shaking water bath, tissue remnants were removed by filtration through a 100 µm nylon mesh and placed on ice for 30 min. The infranatant containing the BAT-MSCs was filtered through a 30 µm nylon mesh and centrifuged at 700 x g for 10 min. The pellet was resuspended in dissection/differentiation medium. Cells were

counted with trypan blue (1:1) in a Neubauer counting chamber and 5.7×10^5 cells were seeded on 6-well plates (day 0) and grown at 37° C, 5% CO₂ and 95% H₂O. For differentiation, the medium was exchanged every 24 h until day 7.

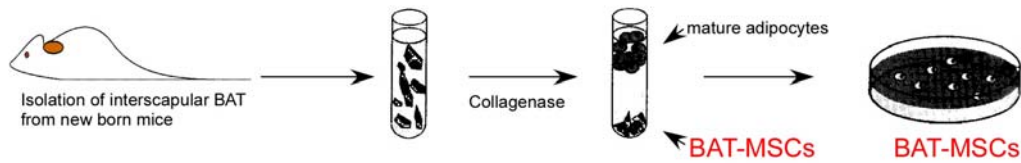


figure 7. Isolation scheme of BAT-MSCs from interscapular BAT of new born mice.

Collagenase digestion buffer

NaCl 0.72 g

KCl 37.3 mg

Ca₂Cl..... 19.1 mg

Glucose..... 99.1 mg

HEPES..... 2.38 g

dissolved in 100 ml H₂O adjusted to pH 7.4, sterile filtered and stored at 4° C

the following substances were added before use:

BSA 1.5%

Collagenase II 2 mg/ml *Worthington, UK (Cat. No. CLS2)*

sterile filtered

Dissection/differentiation medium (DMEM)

FBS 10%

P/S 1%

Insulin..... 4 nM *Sigma (Cat. No. I-9278)*

Triiodothyronine-Na..... 4 nM *Sigma (Cat. No. T-6397)*

HEPES..... 10 mM

Sodium ascorbate 25 µg/ml

2.5.2.1. Immortalization of primary BAT-MSCs

For immortalization, the primary BAT-MSCs (passage 0, p 0) were infected as described (2.7.7.3) with a lentivirus containing the SV40 large T antigen one day after isolation (day 1) and expanded in growth medium at 37° C, 5% CO₂ and 95% H₂O. Cells were used for experiments between p 1 and p 5.

Growth medium (DMEM)

FBS..... 10%
P/S..... 1%

2.5.3. Cell culture and trypsinization of cell lines

Cells were maintained in growth medium as described (2.5.2.1). In order to take cells into suspension cells were washed once in pre-warmed PBS and detached from the wells by incubation with trypsinization solution for approximately 5 min at 37° C. Detached cells were resuspended in growth medium.

Trypsinization solution (1 x trypsin)

10 x Trypsin/EDTA..... 10 ml
PBS..... 90 ml

2.5.3.1. Cryo-preservation of cells

In order to store cell lines for a longer period of time cells were trypsinized and resuspended in pre-warmed growth medium (2.5.3.). The cell suspension was centrifuged for 5 min at 160 x g. The pellet was resuspended in growth medium and 500 µl of cell suspension was mixed with 500 µl freezing medium in cryogenic vials (10% DMSO final), put on ice for 15 min and were finally stored at -80° C. After one day cryo-cultures were transferred to liquid nitrogen (-196° C).

Freezing medium (20% DMSO)

Growth medium..... 8 ml
DMSO..... 2 ml

2.5.3.2. Thawing of cryo-preserved cells

Frozen cells were quickly placed in a water bath at 37° C until the freezing medium was thawed. Cells were then added to pre-warmed growth medium (approximately 10 times the volume of the cryo-culture) and centrifuged for 5 min at 160 x g. The cell pellet was resuspended in growth medium and seeded in a well of appropriate size.

2.5.4. Adipogenic differentiation of immortalized brown adipocytes

To differentiate the immortalized cells into brown adipocytes, 1.8×10^5 cells were seeded on 6-wells or 3.8×10^4 cells on 24-wells (day -4) and after 48 h the medium was exchanged with differentiation medium (day -2). Adipogenesis was induced by treating confluent cultures (day 0) with induction medium for 48 h. After this induction phase (day 2) the cells were returned to differentiation medium, which was replenished every second day until day 7 when cells were considered brown adipocytes (Figure 9B).

Differentiation medium (DMEM)

FBS..... 10%

P/S..... 1%

Insulin..... 20 nM

Triiodothyronine-Na..... 1 nM

Induction medium (DMEM)

FBS..... 10%

P/S..... 1%

Insulin..... 20 nM

Triiodothyronine-Na..... 1 nM

Dexamethason..... 1 μ M *Sigma (Cat. No. D-4902)*

Isobutylmethylxanthine..... 0.5 mM *Sigma (Cat. No. I-5879)*

The following substances were included into the media as indicated:

PKG activation: 8-pCPT-cGMP, Biolog, Bremen (Cat. No. C009-10E)

ROCK inhibition: Y-27632, Calbiochem (Cat. No. 688000)

2.5.4.1. Oil Red O staining of differentiated adipocytes

Oil Red O is a widely used dye to visualize lipids in tissues or cells. After accumulation in fat droplets the lipids appear red.

Differentiated adipocytes were washed once with PBS and fixed with 4% PFA for 15 min at RT. After two additional washes with PBS cells were then stained with Oil Red O working solution for 4 h at RT and were washed three times with water.

Oil Red O stock solution (5 mg/ml)

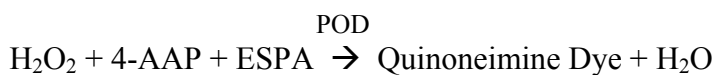
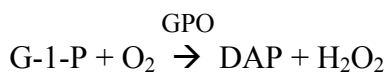
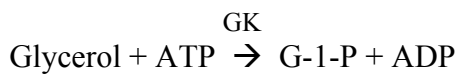
Oil Red O..... 0.5 g *Sigma (Cat. No. O-9755)*
Isopropyl alcohol 99%..... 100 ml
dissolved with a magnetic stir bar o/n, stored at RT

Oil Red O working solution (3 mg/ml)

Oil Red O stock solution..... 6 ml
H₂O..... 4 ml
mixed one day before use, filtered the next day through a paper filter

2.5.4.2. Triglyceride determination of differentiated adipocytes

Triglycerides (TGs) are esters of fatty acids and glycerol. Methods for TG determination generally involve enzymatic or alkaline hydrolysis of triglycerides to glycerol and free fatty acids followed by either chemical or enzymatic measurement of the glycerol released. The procedure involves hydrolysis of the triglycerides to glycerol and free fatty acids. The glycerol produced is then measured by coupled enzyme reactions:



ATP	adenosine-5'-triphosphate
G-1-P	glycerol-1-phosphate
ADP	adenosine-5'-diphosphate
GK	glycerol kinase
GPO	glycerol phosphate oxidase
DAP	dihydroxyacetone phosphate
H ₂ O ₂	hydrogen peroxide
POD	peroxidase
4-AAP	4-aminoantipyrine
ESPA	sodium <i>N</i> -ethyl- <i>N</i> -(3-sulfopropyl) <i>m</i> -anisidine

The increase in absorbance at 540 nm is directly proportional to the free glycerol concentration of the sample.

Differentiated adipocytes growing on 6-well plates were washed once with PBS and after addition of 100 µl TG-Tx-lysis buffer to the cells, wells were immediately frozen at -80° C. Wells were thawed on ice and cells were resuspended and sonicated to hydrolyse TGs to glycerol and free fatty acids. After centrifugation for 10 min, 15000 x g, 4° C, 2 µl were used for protein content determination using the Bradford method (2.6.4). 800 µl free glycerol reagent was added to the remaining part, a blank (100 µl TG-Tx-lysis buffer) and a glycerol standard (10 µl glycerol standard in 90 µl TG-Tx-lysis buffer). After incubation for 5 min at 37° C, absorbtion at 450 nm was measured against water. The TG content was calculated from the resulting values and normalized to the protein content of the sample:

$$\text{Glycerol content} = (A_{\text{sample}} - A_{\text{blank}}) / (A_{\text{standard}} - A_{\text{blank}}) \times \text{concentration of standard (mg/ml)}$$

TG-Tx-lysis buffer

NaCl 150 mM
Tris-HCl 10 mM pH 8.0
Triton-X 100 0.05%

sterile filtered and stored at 4° C

40 µl/ml Complete® protease inhibitor cocktail (2.6) was added before use

Glycerol standard (0.26 mg/ml)

Glycerol..... 26 mg
H₂O..... 100 ml

Free glycerol reagent, Sigma (Cat. No. F-6428)

2.5.5. Osteogenic differentiation of immortalized brown adipocytes

For osteogenic differentiation of immortalized brown adipocytes 1.8 x 10⁵ cells were seeded on 6 wells (day -2) and after 48 h the medium was exchanged with osteoblast differentiation medium. The cells were differentiated until day 7 or day 14 exchanging the medium every second day (Figure 9C).

Osteoblast differentiation medium (DMEM)

<i>FBS</i>	10%	
<i>P/S</i>	1%	
<i>Ascorbate-2-phosphate</i>	250 μ M	
<i>β-glycero-phosphate</i>	10 mM	
<i>All-trans retinoic acid</i>	2.5 μ M	Calbiochem (Cat No.5547258)

2.5.5.1. Alkaline phosphatase staining of osteoblasts

Alkaline phosphatases are a group of enzymes predominantly found in the liver and in the bone. Osteoblasts express high amounts of alkaline phosphatases and can therefore be identified by the use of the NBT/BCIP reporter system. At regions of high phosphatase activity NBT (Nitro blue tetrazolium chloride) and BCIP (5-bromo-4-chloro-3-indolyl phosphate) form a complex resulting in blue precipitates.

Cells were washed once with PBS and fixed with 4% PFA for 15 min at RT. After two additional washes with PBS cells were incubated with BCIP/NCIB solution in DIG III buffer for 1 h at 37° C. The reaction was stopped by the addition of TE buffer pH 8.0 for 10 min. After 3 additional washes with water cells were visualized.

DIG III buffer

<i>Tris-HCl</i>	100 mM	pH 9.5
<i>NaCl</i>	100 mM	
<i>MgCl₂</i>	50 mM	

NBT/BCIP solution

<i>NBT/BCIP stock solution</i>	200 μ l	Sigma (Cat. No. 72091)
<i>DIG III buffer</i>	10 ml	

TE buffer

<i>Tris-HCl</i>	10 mM	pH 8.0
<i>EDTA</i>	1 mM	pH 8.0

2.5.6. Luciferase reporter assays

Luciferase reporter assays were performed by Dr. Stephan Herzig, Deutsches Krebsforschungszentrum, Heidelberg. The following protocol was applied: Cells from the

brown preadipocyte cell line HIB1B were transiently transfected with caPKGI or cntr (2.7.6.3 and 2.7.6.4) together with the promoter reporter constructs by lipofectamine according to the manufacturer's instructions. 24 h after transfection, cells were exposed to insulin (500 nM) for 18 h. Cell extracts were prepared 48 h after transfection, and luciferase assays were performed as described (Herzig et al., 2001), normalizing to activity from cotransfected beta-galactosidase expression plasmid.

2.6. Biochemical Methods

2.6.1. Materials biochemistry

Centrifuges: Biofuge Primo, Heraeus, Hanau

5415R, Eppendorf, Hamburg

Sigma 8k with 12510-H rotor, Sartorius, Göttingen

Film processor, CP100, Agfa, Köln

ECL-reagent, ECL, Amersham Biosciences, UK (Cat. No. 1059250/243)

Electrophoresis/Blotting system, Mini Trans Blot System, BioRad, München

Thermomixer, 5350, Eppendorf, Hamburg

Power supply, Consort E835, Peqlab, Erlangen

Photometer, Biophotometer, Eppendorf, Hamburg

Chemiluminescence films, Hyperfilm®, Amersham Biosciences, UK (Cat. No. 28906837)

Protease inhibitor cocktails: Complete®, Roche, Mannheim (Cat. No. 11697498)

Complete® EDTA-free, Roche, Mannheim (Cat. No. 11873580)

Protein standard, Precision plus All Blue Standard, BioRad, München (Cat. No. 161-0373)

PVDF membranes, Immobilon®P 0.45µm, Millipore, Schwalbach (Cat. No. IPVH 00010)

Ultra-Turrax®, T8, IKA, Staufen

2.6.2. Preparation of total protein lysates from adherent cells

Before cell lysis, cells were washed in ice-cold PBS. The appropriate amount of ice-cold cell lysis buffer (RIPA) was added to the wells and cells were scraped with a cell scraper. Cell lysates were centrifuged at 15000 x g for 15 min at 4° C and the protein concentration of the supernatant was determined using the Bradford protein assay (2.6.4). After the protein concentrations were adjusted, the appropriate amount of 6 x Laemmli buffer (Laemmli, 1970)

was added and samples incubated for 5 min at 97° C. Samples were either frozen at -20° C or directly subjected to SDS PAGE (2.6.7).

Cell lysis buffer (RIPA)

<i>Tris-HCl</i>	<i>10 mM</i>	<i>pH 7.4</i>
<i>NaCl</i>	<i>150 mM</i>	
<i>NP-40</i>	<i>1%</i>	
<i>Desoxy-cholic acid-Na</i>	<i>1%</i>	
<i>SDS</i>	<i>0.1%</i>	
<i>sterile filtered and stored at 4° C</i>		
<i>before use the following substances were added:</i>		
<i>Complete® EDTA-free</i>	<i>40 µl/ml</i>	
<i>NaF</i>	<i>10 mM</i>	
<i>Na₃VO₄</i>	<i>1 mM</i>	

6 x Laemmli buffer

<i>0.5 M Tris-HCl</i>	<i>7 ml</i>	<i>pH 6.8</i>
<i>87% Glycerol</i>	<i>3 ml</i>	
<i>DTT</i>	<i>0.93 g</i>	
<i>SDS</i>	<i>10%</i>	
<i>Bromphenol blue</i>	<i>1.2 mg</i>	

The following volumes of cell lysis buffer were used:

<i>24-well plate</i>	<i>50 - 100 µl</i>
<i>6-well plate</i>	<i>70 - 200 µl</i>
<i>100 mm dish</i>	<i>0.3 - 1 ml</i>
<i>14 mm dish</i>	<i>0.5 - 2 ml</i>

2.6.3. Preparation of total protein lysates from tissues

Mice were sacrificed and tissues were dissected out and either snap-frozen in liquid nitrogen for longer storage or directly processed. Therefore, tissues were placed in ice-cold Tx-lysis buffer and disrupted using an Ultra-Turrax®. The protein was further isolated as described above (2.6.2).

Tx-lysis buffer

Tris-HCl 50 mM pH 7.4

NaCl 150 mM

CaCl₂ x 2 H₂O..... 2 mM

Triton-X 100..... 0.5%

sterile filtered and stored at 4° C

before use the following substances were added:

Complete®..... 40 µl/ml

NaF..... 10 mM

Na₃VO₄..... 1 mM

2.6.4. Quantification of proteins with the Bradford protein assay

The Bradford assay is based on the Coomassie brilliant blue G-250 dye which specifically interacts with arginine, tryptophan, tyrosine, histidine and phenylalanine residues (Bradford, 1976). While the free dye displays an absorbance maximum at 470 nm the bound dye has an absorbance maximum at 595 nm. The protein content is determined using a BSA standard ranging from 1 to 30 µg as a reference. 2 µl - 5 µl of protein lysates were diluted to 100 µl with 0.15 M NaCl solution. 1 ml Coomassie solution was added, incubated for 2 min and the absorbance was measured at 595 nm.

Coomassie solution

Coomassie brilliant blue G-250..... 50 mg Merck (Cat. No. 1.15444.0025)

EtOH 95%..... 25 ml

Phosphoric acid 85%..... 50 ml

filled up to 500 ml with H₂O, stored at 4° C protected from light

2.6.5. Immunoprecipitation

Before cell lysis, cells were washed once in ice-cold PBS. Cell lysis buffer (2.6.2) was added, cells were scraped with a cell scraper, vortexed and centrifuged at 15000 x g for 10 min at 4° C. The protein concentration of the supernatant was determined using the Bradford protein assay (2.6.4). Typically lysates with a concentration of 0.5 - 1.5 mg/ml were used. For immunoprecipitation (IP) of endogenous proteins lysates were incubated with rabbit polyclonal antibodies and protein A sepharose beads by incubating for 2 h at 4° C (1 - 4 µg

antibody per IP). After binding, beads were washed 3 times with lysis buffer and once with PBS. Beads were resuspended in 40 μ l 2 x Laemmli buffer (2.6.2) and boiled for 5 min at 97° C.

Protein A sepharose CL-4B, Amersham Biosciences, UK (Cat. No. 17-0780-01)

2.6.6. Rhotekin pull down assay

As in contrast to a normal Western blot, which detects the total (GTP- and GDP-bound) amount of the respective Rho-GTPase, the pull down assay only measures the amount of active (GTP-bound) Rho-GTPase. This is accomplished by utilizing the GTPase binding domain (GBD) of a specific effector molecule, which recognizes the active, but not the inactive form of its GTPase. This GBD is expressed as a fusion protein with glutathion-S-transferase to allow immobilization on glutathion coated sepharose beads. The 'loaded' beads are subsequently incubated with the cell extracts of interest, washed, and directly submitted to SDS-PAGE. The bound (active) GTPases are finally detected by Western blot (2.6.7).

2.6.6.1. Preparation of GBP-GTP fusion proteins

For measuring active RhoA the GTPase binding domain of rhotekin (aa 7 - 89) is used (Reid et al., 1999; Ren et al., 1999). This domain is fused to the C-terminus of GST (~26 kDa) and expressed from a pGEX-2T vector in *E. coli* BL21-Gold. 3 ml pre-culture (LBamp, 37° C) (2.7.3) of BL21 bacteria containing the GST-rhotekin-GBD pGEX-2T vector were inoculated o/n. The next morning 2 ml of o/n pre-culture were diluted in 100 ml LBamp and were grown at 37° C for ~2 h, until OD₆₀₀ was 0.5 - 0.6.

The culture was allowed to cool to RT and protein synthesis was induced by adding 100 μ l 1 M Isopropyl- β -D-thiogalactopyranoside (IPTG) solution (final 1 mM IPTG). After growing at 26° C for 6 h (reducing the temperature helps to keep protein soluble and avoids protein aggregation; general: temperature can be reduced to 18° C with o/n expression) bacteria were spun down in two 50 ml Falcon tubes at 5000 rpm for 10 min at 4° C. Pellets were washed in 20 ml Buffer A (ice cold) and were combined into one Falcon tube. The pellet was frozen in liquid nitrogen and stored at -80° C. To extract the proteins the pellet was thawed at 37° C, 5 ml of ice-cold Buffer A+ was added and sonicated 4 x 15 sec with ~30 sec on ice in between. 50 μ l Triton-X 100 (1% final) was added and tumbled 20 min at 4° C. 550 μ l (10% final) glycerol was added, distributed into Eppendorf tubes and centrifuged at 15000 x g for 15 min at 4° C. Supernatants were pooled and 20 μ l aliquots were taken for SDS-PAGE check (12%;

Coomassie stain 2.6.9). The bacterial extracts were frozen in 500 µl aliquots in liquid nitrogen and stored at -80° C for up to 3 months.

IPTG solution (1 M)

IPTG 2.38 g
dissolved in 10 ml H₂O ,sterile filtered and stored in aliquots at - 20° C

Buffer A

Tris-HCl 50 mM *pH 7.4*
MgCl₂ 5 mM
NaCl 50 mM
autoclaved and stored at RT

Buffer A+

Buffer A 10 ml
PMSF..... 1 mM
DTT..... 1 mM
Complete® EDTA-free..... 400 µl

pGEX-2T vector, Amersham Biosciences, UK

E. coli BL21-Gold, Stratagene, USA (Cat. No. 230130)

2.6.6.2. Loading of glutathione beads and pull down

Subconfluent cultures of BAT-MSCs (day -2) were serum starved for 24 h, washed in ice-cold PBS and lysed with NP-40 lysis buffer. Lysates were cleared by centrifugation at 15000 x g for 10 min at 4° C and incubated (0.5 – 2 mg) with GST-rhotekin and glutathione sepharose beads for 1 h at 4° C to capture GTP bound Rho proteins. After three washes with NP-40 lysis buffer, beads were boiled in 2 x reducing sample buffer and were subjected to Western blot analysis (2.6.7) with anti-RhoA antibody. Whole-cell lysates (5% of input) were analyzed in parallel.

NP-40 lysis buffer

Tris-HCl 50 mM *pH 7.4*
MgCl₂ 5 mM

NaCl 200 mM
NP-40 1%
Glycerol..... 10%
sterile filtered and stored at 4° C
before use the following substances were added:
Complete® EDTA-free 40 µl/ml
NaF..... 1 mM
Na₃VO₄..... 1 mM

2 x reducing sample buffer

0.5 M Tris-HCl..... 7 ml pH 6.8
87% Glycerol..... 3 ml
SDS..... 10%
Bromphenol blue 1.2 mg
filled up to 30 ml with H₂O
before use, β-mercaptoethanol was added to a final concentration of 4%

Glutathione sepharose 4 fast flow, Amersham Biosciences, UK (Cat. No. 17-5132-01)

2.6.7. One-dimensional SDS-polyacrylamid-gelectrophoresis (SDS-PAGE)

SDS-PAGE under denaturing conditions is the most widely used method for separation of proteins, which can be subsequently visualized by silverstaining, protein dyes like Coomassie or Western blotting. After proteins are solubilized by boiling in the presence of sodium dodecyl sulphate (SDS) the individual proteins are separated electrophoretically. β-mercaptoethanol or dithiothreitol (DTT) is added during solubilization to reduce disulfide bonds.

To perform discontinuous gel electrophoresis differentially buffered separating and stacking gels are poured on top of each other. The proteins that pass first through a stacking gel get concentrated at the stacking/separating gel interface. In the separating gel the proteins are separated according to molecular size in denaturing gel (containing SDS).

Proteins were separated in the Minigel format (7.3 mm x 8.3 mm x 1.5 mm) by means of the Mini Trans Blot system (BioRad). After polymerization of the polyacrylamid gel and

assembly of the electrophoresis module, cooked protein samples (2.6.2; 2.6.3; 2.6.5; 2.6.6.2) were collected by centrifugation and loaded on the stacking gel. Finally, the electrophoresis was performed in SDS-PAGE running buffer at 100 V at RT.

<i>Separating gel (10 ml)</i>	<i>6%</i>	<i>8%</i>	<i>10%</i>	<i>12%</i>	
<i>H₂O</i>	<i>5.3 ml</i>	<i>4.6 ml</i>	<i>4.0 ml</i>	<i>3.3 ml</i>	
<i>Rotiphorese®Gel 30</i>	<i>2.0 ml</i>	<i>2.7 ml</i>	<i>3.3 ml</i>	<i>4.0 ml</i>	
<i>1.5 M Tris-HCl</i>	<i>2.5 ml</i>	<i>2.5 ml</i>	<i>2.5 ml</i>	<i>2.5 ml</i>	<i>pH 8.8</i>
<i>10% SDS</i>	<i>0.1 ml</i>	<i>0.1 ml</i>	<i>0.1 ml</i>	<i>0.1 ml</i>	
<i>20% APS</i>	<i>0.05 ml</i>	<i>0.05 ml</i>	<i>0.05 ml</i>	<i>0.05 ml</i>	
<i>TEMED</i>	<i>0.008 ml</i>	<i>0.006 ml</i>	<i>0.004 ml</i>	<i>0.004 ml</i>	

<i>Stacking gel (5 ml)</i>	<i>5%</i>	
<i>H₂O</i>	<i>3.4 ml</i>	
<i>Rotiphorese®Gel 30</i>	<i>0.83 ml</i>	
<i>1.0 M Tris-HCl</i>	<i>0.63 ml</i>	<i>pH 6.8</i>
<i>10% SDS</i>	<i>0.04 ml</i>	
<i>20% APS</i>	<i>0.02 ml</i>	
<i>TEMED</i>	<i>0.008 ml</i>	

10 x SDS PAGE running buffer

<i>Tris</i>	<i>30.3 g</i>
<i>Glycine</i>	<i>144 g</i>
<i>SDS</i>	<i>10 g</i>
<i>dissolved in 1000 ml H₂O, stored at RT</i>	

Rotiphorese®Gel 30 (37.5:1), Roth (Cat. No. 3029.1)

2.6.8. Western blotting and immunodetection

Western blotting is used to identify specific proteins by polyclonal or monoclonal antibodies. Proteins are first separated by SDS-PAGE and then electrically transferred onto a polyvinylidene fluoride (PVDF) membrane. Proteins bound to the surface of this membrane can be visualized by immunodetection reagents.

After separation of proteins by SDS-PAGE (2.6.7) the stacking gel was removed while the separating gel was placed in transfer buffer. After short equilibration of the polyacrylamid gel and a methanol activated PVDF membrane in transfer buffer a transfer sandwich was assembled.

Proteins were then electrically transferred with different currents, times and temperatures depending on the protein size to be transferred.

<i>Protein size.....</i>	<i>Voltage.....</i>	<i>Current.....</i>	<i>Time.....</i>	<i>Temperature</i>
<i>15 - 30 kDa.....</i>	<i>100 V</i>	<i>225 mA.....</i>	<i>45 min.....</i>	<i>4° C</i>
<i>30 - 50 kDa.....</i>	<i>100 V.....</i>	<i>250 mA.....</i>	<i>60 min.....</i>	<i>4 ° C</i>
<i>50 - 75 kDa.....</i>	<i>100 V.....</i>	<i>300 mA.....</i>	<i>60 min.....</i>	<i>4° C - RT</i>
<i>75 - 250 kDa..</i>	<i>100 V.....</i>	<i>300 mA.....</i>	<i>90 - 120 min.....</i>	<i>4° C - RT</i>

After disassembly of the transfer sandwich, membranes were washed for 15 sec in methanol and dried for 15 min or longer at RT. After drying, membranes were washed again for 15 sec in methanol and blocked for 1 h at RT in blocking buffer I or II. Blocked membranes were washed 3 times with TBS-T and incubated with the primary antibody either for 1 h at RT or o/n at 4° C in blocking buffer depending on the instructions of the antibody manufacturer. After three washes with TBS-T, the appropriated horseradish peroxidase (HRP)-coupled secondary antibody was applied for 1 h at RT. Finally, the membrane was washed another 3 times with TBS-T and was subjected to chemiluminescence based detection with an enhanced chemiluminescence (ECL) reagent and chemiluminescent films which were developed in an automatic film processor (CP100, Agfa).

Transfer buffer

<i>10 x SDS PAGE running buffer.....</i>	<i>100 ml</i>
<i>Methanol.....</i>	<i>200 ml</i>
<i>H₂O.....</i>	<i>700 ml</i>

10 x TBS

<i>Tris</i>	<i>24.3 g</i>
<i>NaCl</i>	<i>80 g</i>
<i>dissolved in 1000 ml H₂O, adjusted to pH 8.0 with HCl</i>	

TBS-T (0.1%)

<i>Tween-20</i>	<i>1 ml</i>
<i>10 x TBS</i>	<i>100 ml</i>
<i>H₂O</i>	<i>900 ml</i>

Blocking buffer I (5%)

<i>skimmed milk powder</i>	<i>5 g</i>
<i>TBS-T</i>	<i>100 ml</i>

Blocking buffer II (5%)

<i>BSA</i>	<i>5 g</i>
<i>TBS-T</i>	<i>100 ml</i>

2.6.9. Coomassie staining of SDS-PAGE gels

The Coomassie Blue dye can be used to stain proteins separated by SDS-PAGE gel electrophoresis.

After electrophoresis (2.6.7) the stacking gel was removed and the gel was placed in Coomassie solution for 30 min under agitation. The gel was destained o/n with three changes of destaining solution.

Coomassie solution

<i>Coomassie G-250</i>	<i>0.5%</i>
<i>Methanol</i>	<i>40%</i>
<i>Acetic acid 100%</i>	<i>10%</i>

Destaining solution

<i>Methanol</i>	<i>40%</i>
<i>Acetic acid 100%</i>	<i>10%</i>

2.7. Molecular Biological Methods

2.7.1. Materials molecular biology

Autoclave, Varioklav 135 T, Faust, Meckenheim

Ultra Centrifuge, Optima LE-80K with SW28 rotor and SW55 rotor, Beckman & Coulter, USA

Electrophoresis chamber, Peqlab, Erlangen

Incubator, Certomat IS, Sartorius, Göttingen

Microwave, Severin, Sundern

Real-time PCR machine, LightCycler®480, Roche, Mannheim

Thermocycler, T1, Biometra, Göttingen

UV light transilluminator, GelDoc®XR, BioRad, München

2.7.2. Phenol/Chloroform extraction of tail DNA

For genotyping of mice, a small biopsy of the mouse tail was digested with 500 µl proteinase K buffer in an Eppendorf tube at 55° C at 300 rpm in a thermomixer o/n. The next day, 500 µl phenol/chloroform (1:1, Rothi®-Phenol) was added, the DNA solution was mixed and centrifuged for 5 min at 15000 x g. The upper layer was taken off and added to 500 µl chloroform/isoamylalcohol solution (24:1), mixed and centrifuged again for 5 min at 15000 x g. The upper DNA-rich layer was taken off and DNA was precipitated by addition of 500 µl isopropyl alcohol. The white DNA precipitates were pelleted by centrifugation for 1 min at 15000 x g. Pellets were air-dried and subsequently dissolved in 50 - 100 µl H₂O.

Proteinase K buffer

<i>Tris-HCl</i>	<i>100 mM</i>	<i>pH 7.6</i>
<i>NaCl</i>	<i>200 mM</i>	
<i>EDTA</i>	<i>5 mM</i>	
<i>SDS</i>	<i>0.2%</i>	
<i>Proteinase K</i>	<i>0.1 mg/ml</i>	<i>Roche (Cat. No. 03115828)</i>

Rothi®-Phenol, Roth (Cat. No. 0038.2)

2.7.3. Bacteriological tools

Escherichia coli (*E. coli*) cultures were cultured in lysogeny broth (LB) rich medium. Media were prepared and autoclaved for 20 min at 120° C. Antibiotics were added after the solutions were cooled below 50° C.

LB+ medium

NaCl 5 g

Pepton..... 10 g

Yeast extract..... 5 g

Glucose..... 1 g

filled up to 1000 ml with H₂O, adjusted to pH 7.5, autoclaved and stored at 4° C

LB+ plates

LB+ medium..... 1000 ml

Agar-Agar..... 15 g

autoclaved, poured into 100 mm Petri dishes and stored at 4 °C

Additives

Ampicillin 50 µg/ml

Kanamycin..... 25 µg/ml

Tetracyclin..... 12.5 mg/ml

2.7.3.1. Preparation of competent bacteria

An *E. coli* (XL-1 Blue) bacterial culture was grown o/n in 10 ml LB+ with tetracycline (2.7.3) at 37° C shaking at 225 rpm in an incubator. The next morning, 100 ml of LB+ with tetracycline was inoculated with 2 ml o/n culture and grown until an OD₅₅₀ of 0.5 was reached. The bacterial culture was placed on ice for 10 min and then centrifuged at 1000 x g for 15 min at 4° C. The pellet was resuspended in 10 ml TSS and 2.9 ml glycerol (87%) was added. This bacterial suspension was aliquoted in volumes of 100 µl and immediately frozen in liquid nitrogen. Competent cells were stored at -80° C.

TSS

Polyethylene glycol 50 g

Pepton..... 5 g

Yeast extract..... 2.5 g

NaCl 2.5 g
DMSO..... 25 ml
1M MgCl₂..... 25 ml
sterile filtered and stored at 4° C

2.7.3.2. Transformation of competent bacteria

100 µl of competent bacteria were thawed on ice, DNA was added and incubated on ice for 30 min. Cells were then placed on 42° C for 45 sec (heat shock) in a water bath and subsequently placed on ice for 2 min. 900 µl pre-warmed LB+ medium (w/o antibiotics) was added and cells were incubated for 1 h at 37° C shaking at 225 rpm. Next, bacteria were pelleted by centrifugation at 3500 rpm for 5 min, resuspended in 100 µl LB+ medium and spreaded on LB plates with the appropriate antibiotics. Plates were incubated o/n at 37° C. Colonies appeared within 8 - 12 h depending on the transformed DNA construct.

2.7.3.3. Cryo-preservation of bacteria

In order to freeze bacterial cultures 250 µl glycerol (87%) was added to 750 µl bacterial o/n culture. Cryo-cultures were stored at -80° C.

2.7.3.4. Preparation of plasmid DNA from bacterial cultures - Mini Preparation

Bacterial colonies were inoculated with 7 ml LB+ medium containing the appropriate antibiotics o/n at 37° C and 225 rpm. To check the transformed plasmid DNA a protocol from Sambrook and Russel for alkaline lysis was used. This method allows a rapid isolation of plasmid DNA with a sufficient degree of purity for further restriction check cuts and sequencing.

2.7.3.5. Preparation of plasmid DNA from bacterial cultures - Maxi Preparation

Bacterial colonies were inoculated with 100 - 200 ml LB+ medium containing the appropriate antibiotics o/n at 37° C and 225 rpm. The next day, cultures were spun down at 5000 rpm for 20 min at 4° C (Sigma 8k, Sartorius). The DNA was extracted with either NucleoBond® PC 500 Kit (MACHERY-Nagel) or for endotoxin-free DNA preparations with the NucleoBond® PC 500 EF Kit (MACHERY-Nagel).

NucleoBond® PC 500 Kit, MACHERY-Nagel, Düren (Cat. No. 740574.25)

NucleoBond® PC 500 EF Kit, MACHERY-Nagel, Düren (Cat. No. 740550)

2.7.4. Enzymatic manipulation of DNA

Restriction enzymes are widely used in molecular biology in order to cleave DNA at specific sites. They can be divided into three groups. The type I restriction enzymes are complex multi subunit enzymes that cut the DNA randomly far from their recognition sequence. The type II enzymes bind to specific DNA sequences and cut the DNA within or close to this binding motif. The type III restriction enzymes are complex and cleave the DNA outside of their recognition sequence. Type II restriction enzymes are widely used as a molecular tool.

2.7.4.1. Digestion of DNA with restriction enzymes

All restriction and DNA-modifying enzymes used in this study were purchased from New England Biolabs (NEB), Schwalbach. Digestion was performed according to the instructions of the manufacturer using restriction buffers from Roche, Mannheim. In general the following reaction conditions were used:

DNA digestion

DNA.....1 - 4 μ g
Roche 10 x buffer (A - H) 3 μ l
Restriction enzyme..... 5 - 20 U
filled up to 30 μ l with H₂O, incubated for 1 - 3 h or o/n at 37° C

2.7.4.2. Dephosphorylation of plasmid DNA

Digestion of DNA with restriction enzymes generates a reactive 5'-phosphate group and a 3'-hydroxyl group. In order to prevent self-ligation of digested plasmids, the 5'-phosphate group was removed by the use of calf intestinal phosphatase (CIP). Digestion enzymes were heat-inactivated and the DNA subsequently incubated with CIP.

Dephosphorylation of DNA

DNA.....1 - 4 μ g
Roche 10 x buffer H..... 3 μ l
CIP 1 μ l
filled up to 30 μ l with H₂O, incubated for 1 h at 37° C

2.7.4.3. Phosphorylation of DNA fragments

T4 polynucleotide kinase (PNK) was used in order to generate reactive 5'-phosphate ends for subsequent ligation. PNK catalyzes the transfer of the γ -phosphate from ATP to 5'-hydroxyl-termini of polynucleotides.

Phosphorylation of DNA

DNA fragment 1 - 4 μ g
NEB 10 x ligation buffer..... 3 μ l *containing 1 mM ATP*
PNK..... 1 μ l
filled up to 30 μ l with H₂O, incubated for 45 min at 37° C

2.7.4.4. Blunting of DNA fragments

To generate blunt-ends of digestion products DNA was treated with T4 polymerase. The T4 polymerase fills in 5'-overhangs thereby generating blunt-ends.

Blunting of DNA

DNA fragment 1 - 4 μ g
NEB 10 x buffer 3..... 3 μ l
dNTPs..... 10 μ M
T4-polymerase..... 1 μ l
filled up to 30 μ l with H₂O, incubated for 45 min at 37° C

2.7.4.5. Ligation of DNA fragments

For DNA ligation, the generation of a phosphodiester bond between a 3'-hydroxyl group and a 5'-phosphate group, the following protocol was used.

DNA ligation

DNA backbone (vector)..... 20 - 50 ng *dephosphorylated*
DNA insert..... 60 - 150 ng *digested DNA*
NEB 10 x ligation buffer 1.5 μ l
T4 DNA ligase..... 1 μ l
filled up to 15 μ l with H₂O, incubated for 60 min at 25° C or o/n at 16° C, 10 μ l of the ligation products were used for transformation as described before (2.7.3.2)

2.7.5. Agarose gel electrophoresis

Agarose gel electrophoresis is a simple method for separating, identifying, or purifying DNA fragments. For gel preparation, the desired amount (between 0.7 and 2%) of agarose was added to 1x TBE buffer and boiled in the microwave. For 100 ml agarose solution, 8 µl ethidium bromide (800 ng/ml final) was added. The melted agarose was poured into casting platforms, allowed to harden at RT and placed into an electrophoresis chamber containing 1 x TBE buffer. Next, DNA was mixed with 6 x loading buffer and loaded on the agarose gel. Electrophoresis was performed at 80 - 120 V at RT. DNA bands were visualized under an UV light transilluminator (GelDoc®XR, BioRad) at 366 nm using QuantityOne® software (BioRad).

10 x TBE

Tris-HCl 0.9 M
Boric acid 0.9 M
EDTA 20 mM pH 8.0
filled up to 1000 ml with H₂O, stored at RT

6 x loading buffer

10 x TBE 60%
Ficoll type 400 18%
EDTA 0.12 mM pH 8.0
Bromphenol blue 0.15%
Xylencyanol FF 0.15%

Ethidium bromide 10 mg/ml, Roth (Cat. No. 2218.1)

2.7.5.1. Extraction of DNA from agarose gels

Extraction of DNA fragments from agarose gels was done by using the GFX®-Kit (GE Health Care) according to the manufacturer's instructions.

GFX®-Kit Illustra®, GE Health Care, UK (Cat. No. 28-9034-71)

2.7.6. Generation of lentiviral expression constructs

In order to stably express the protein of interest in cell lines, lentiviral expression constructs were generated which all uses the pRRL.SIN-18 vector system. This construct contains sequences from human immune deficiency virus-1 (HIV-1) and the expression cassette for the transgene. It represents a part of a lentiviral gene transfer system which integrates in the genome of the targeting cell. It contains no wild type copies of the HIV-long terminal repeats (LTRs): the 5' LTR is chimeric and contains an enhancer and promoter of the respiratory syncytial virus (RSV) instead of the U3-region of the wild type HIV (RRL). In the 3' LTR-region the U3-region was nearly completely deleted, including the TATA-box (nucleotide -418 to -18, relative to the U3/R border). Because the 3' U3-region is used as a template for the generation of both copies of the LTRs in the life cycle of the virus, this deletion in the U3-region leads to a transcriptional inactivation of both LTRs (self-inactivating (SIN)-vector) (Dull *et al.*, 1998).

The original virus plasmids were provided by Inder Verma (The Salk Institute for Biological Studies, Laboratory of Genetics, La Jolla, CA, USA).

2.7.6.1. Plasmids and cDNAs

cDNA	Backbone	Provided by	Reference
caPKGI (<i>bovine</i>)	pBluescript KS	A. Pfeifer	(Heil et al., 1987)
Myc-RhoL63	pCLMFG	J. Collard	---
Myc-RhoN19	pCLMFG	J. Collard	---
Myr-Flag-Akt.....	pBABE	Addgene	(Boehm et al., 2007)
Cre-SD	pRRL.SIN18.....	A. Pfeifer	(Pfeifer et al., 2001)
TAg.....	PKGpRRL.SIN18.....	A. Pfeifer	(Salmon et al., 2000)
GST-rotokin-GBD	pGEX-2T	R. Fässler.....	---

2.7.6.2. Expression vectors

Name	Approach.....	Resistance.....	Source
pBluescript KS.....	cloning	ampicillin	Stratagene
pGEX-2T	expression.....	ampicillin	Amersham Biosciences
pCLMFG	expression.....	ampicillin	A. Pfeifer
pBABE.....	expression.....	ampicillin/puromycin	Addgene
CMVpRRL.SIN18	expression/cloning.....	ampicillin	A. Pfeifer/I. Verma

2.7.6.3. Generation of caPKGI expression construct

CMVpRRL.SIN18-caPKGI (LV-caPKGI): Constitutively active PKGI (caPKGI) cDNA was released from caPKGI in pBluescript KS by digestion with PstI and NotI, blunt ended (2.7.4.4) and inserted into EcoRV digested pBluescript KS. Correct insertion was checked by EcoRI digestion. From there caPKGI cDNA was released again by digestion with BamHI and SalI and inserted into BamHI/SalI digested CMVpRRL.SIN18. Insertion was checked by EcoRI digestion.

2.7.6.4. Generation of control expression construct

pRRL.SIN18 (LV-ctrl): CMVpRRL.SIN18-caPKGI was digested with ClaI to excise the CMV promoter and caPKGI cDNA. The purified vector was religated.

2.7.7. Generation of lenti-/retrovirus

In order to produce lentiviral or retroviral VSV-G pseudotyped vectors, human embryonic kidney cells (HEK293T) were transiently transfected by a calcium phosphate method with the retroviral (pCLMFG/pBABE) or lentiviral constructs (pRRL.SIN18) and packaging plasmids: pMDLg/pRRE (*gag, pol, polyA signal of β -globin, lentivirus only*), RSV-Rev (*rev, lentivirus only*), pMD.G (*CMV-VSV-G, lenti- and retrovirus*) or CMVgagpol (*gag, pol, retrovirus only*). The supernatant containing the virus was harvested, enriched by centrifugation, and directly used for infection of cells.

2.7.7.1. Calcium phosphate transfection of HEK293-T cells

HEK293-T cells were expanded in growth medium at 37° C and 10% CO₂ in a humidified atmosphere. Cells were grown on 140 mm plates until a confluence of approximately 60% was reached. 2.3 ml of transfection mix was added and cells were incubated o/n at 37° C in 3% CO₂. The next day, the medium was changed and cells were further cultured in growth medium at 37° C and 10% CO₂.

2 x BBS

BES..... 4.26 g pH 6.95

NaCl 6.54 g

Na₂HPO₄..... 0.085 g

filled up to 400 ml with H₂O, sterile filtered

Transfection mix retrovirus (for 1 x 140 mm plate)

<i>Viral plasmid</i>	25 μ g
<i>CMVgagpol</i>	25 μ g
<i>CMV-VSV-G</i>	12.5 μ g

Transfection mix lentivirus (for 1 x 140 mm plate)

<i>Viral plasmid</i>	22.5 μ g
<i>pMDL</i>	14.6 μ g
<i>REV</i>	5.7 μ g
<i>CMV-VSV-G</i>	7.9 μ g

*filled up to 1.17 ml with sterile H₂O, addition of
CaCl₂ (2.5 M)..... 117 μ l
vortexed, addition of
2 x BBS..... 1.17 ml
inverted and incubated 10 - 15 min at RT*

2.7.7.2. Harvest of viral supernatant

First harvest: 24 h after transfection the supernatant was taken off and filtered through a 0.45 μ m filter. 16 ml growth medium was added to the cells which were incubated for additional 24 h at 37° C in 10% CO₂. The filtrate was centrifuged at 50000 x g (SW28 rotor) for 2 h at 17° C and pellets were resuspended in HBSS, vortexed and stored at 4° C.

Second harvest: 48 h after transfection the viral supernatant was taken off and treated as above. For concentration of the virus, pellets of the first and second harvest were combined, mixed with 2 ml of 20% sucrose and centrifuged at 42000 x g (SW55 rotor) for 2 h at 17° C. Pellets were resuspended in HBSS, mixed at 1400 rpm for 45 min at 17° C and spun down. Supernatant was taken off, aliquoted and stored at -80° C.

Hank's Balanced Salt solution (HBSS), Gibco, Karlsruhe (Cat. No. 14175-046)

2.7.7.3. Infection of cells with lenti-/retroviral vectors

The day before infection, 1.5 - 2 x 10⁵ cells were seeded in a 6-well plate and cultured o/n. The next day in the afternoon, 800 μ l growth medium containing 0.5 - 10 μ l of the virus supernatant (2.7.7.2) was added to the cells. The next day, the medium was filled up to 2 ml

and grown again o/n. Cells were either directly subjected to experiments or trypsinized and seeded again on 6-well plates or 100 mm dishes.

2.7.8. Isolation of RNA from cells and tissues and reverse transcription (RT)

Total RNA from cultured cells and tissues was isolated with the TriFast® reagent (Peqlab) and 4 µg RNA were reverse transcribed with the SuperScript®II (Invitrogen) reverse transcriptase using random hexamer primers. RT-PCR analysis was performed using two specific primer combinations (2.7.9.1) and the PCR products were resolved on 2.0% agarose gels.

For Real-time PCR analysis (2.7.9.4) 0.5 µg RNA were reverse transcribed with the Transcriptor First Strand Synthesis Kit (Roche) using random hexamer primers.

PeqGOLD TriFast®, Peqlab, Erlangen (Cat. No. 30-2020)

SuperScript®II First-Strand Synthesis Kit, Invitrogen, Karlsruhe (Cat. No. 12371019)

Transcriptor First Strand Synthesis Kit, Roche, Mannheim (Cat. No. 4896866)

2.7.9. Polymerase chain reaction (PCR)

PCR is a widely used method for enzymatic DNA amplification (Saiki et al., 1988). The reaction is carried out in the presence of three nucleic acid segments (DNA template, primer 1, primer 2), DNA polymerase (*Taq* polymerase) and dNTPs. The amplification occurs in three different steps: denaturation (95° C), annealing of the primers to the DNA template (52 - 65° C, depending on the primer) and DNA synthesis (72° C). For specific primer combinations refer to 2.7.9.1.

2.7.9.1. Primers PCR

All primers were synthesized and purified by MWG, Ebersberg.

Name	Primer sequence	Application
C2f	5' - GTG AAA ATA CTA CTA GGT ATC ATG G - 3'	genotyping PKGI floxed
C2r	5' - CAT GTA CTA AAC ATT AAG GGT AGA G - 3'	genotyping PKGI floxed
C1f	5' - CTA AAT GAG CAA ACA GAA ACT ATG - 3'	genotyping PKGI floxed
NeoPA	5' - GCC TGC TCT TTA CTG AAG GCT CT - 3'	genotyping PKGI k.o.
KISAX	5' - GCC GCT CGA GTA AGG GAA ACT AAT GAG AAA CTG CT - 3'	genotyping PKGI k.o.
Ap-18	5' - GCT CTA CTC GTC CGA AAC CT - 3'	genotyping PKGI k.o.
UCP-1 forward	5' - GTG AAC CCG ACA ACT TCC GAA GTG - 3'	RT-PCR
UCP-1 reverse	5' - CAT GAG GTC ATA TGT CAC CAG CTC - 3'	RT-PCR
PPAR γ forward	5' - ATG CCA TTCTGG CCC ACC AAC TTC - 3'	RT-PCR
PPAR γ reverse	5' - CAT AAA TAA GCT TCA ATC GGA TGG - 3'	RT-PCR
Runx2 forward	5' - CAG GAA GAC TGC AAG AAG GCT CTG G - 3'	RT-PCR
Runx2 reverse	5' - ACA CGG TGT CAC TGC GCT GAA GA - 3'	RT-PCR
Ocn forward	5' - AGG ACC CTC TCT CTG CTC AC - 3'	RT-PCR
Ocn reverse	5' - AAC GGT GGT GCC ATA GAT GC - 3'	RT-PCR
PKGI forward	5' - ACT GTA TGT ACC CCG TGG AAT - 3'	RT-PCR
PKGI reverse	5' - TTG GTG AGT CTT CTC GAG TAA - 3'	RT-PCR
GC-A forward	5' - ATC GGG GTG AAG GAT GAG TAC G - 3'	RT-PCR
GC-A reverse	5' - AGT ACT CAG GAT TAT CGG GTT C - 3'	RT-PCR
GC-B forward	5' - CAT GGC AGG ACA ATC GAA CC - 3'	RT-PCR
GC-B reverse	5' - TGC CTG CAC CCT TGT GAT AG - 3'	RT-PCR
GC-C forward	5' - TCC AGG TGG CCT ACG AAG AC - 3'	RT-PCR
GC-C reverse	5' - GAT TCT CCG AAT GGT GTC AC - 3'	RT-PCR

Name	Primer sequence	Application
sGC forward	5' - TCA CTC TGG CTA ACA AAT TTG AAT C - 3'	RT-PCR
sGC reverse	5' - ACA ATG TGC TGG ATT TTG AGT GCA G - 3'	RT-PCR
PDE3B forward	5' - CAG GAA GGA TTC TCA GTC AG - 3'	RT-PCR
PDE3B reverse	5' - GTA CTC TGG GCG AGA AAG AT - 3'	RT-PCR
nNOS forward	5' - CAA ACG CAA AGT GGG AGG TC - 3'	RT-PCR
nNOS reverse	5' - TTG CCG TCG AGG TCT CTG TC - 3'	RT-PCR
iNOS forward	5' - GTT CTC AGC CCA ACA ATA CA - 3'	RT-PCR
iNOS reverse	5' - AGG CAG TGC ATA CCA CTT CA - 3'	RT-PCR
eNOS forward	5' - CTG GCA AGA CAG ACT ACA CGA - 3'	RT-PCR
eNOS reverse	5' - CGC AAT GTG AGT CCG AAA ATG T - 3'	RT-PCR
GAPDH forward	5' - CGG CAA ATT CAA CGG CAC AGT CA - 3'	RT-PCR
GAPDH reverse	5' - GGT TTC TCC AGG CGG CAC GTC A - 3'	RT-PCR

2.7.9.2. PCR reactions

PCR reactions with two different templates were performed. 1) PCR for genotyping, using genomic tail DNA (2.7.2), 2) RT-PCR, using cDNA reverse-transcribed from RNA (2.7.8). All PCR reactions were carried out using the TaqCORE kit (Qbiogen).

Genotyping PCR

Isolated tail DNA..... 1 μ l
 Primer 1 (10 pmol)..... 1.25 μ l
 Primer 2 (10 pmol)..... 1.25 μ l
 Primer 3 (10 pmol)..... 1.25 μ l
 dNTPs (10 mM)..... 4 μ l
 10 x PCR buffer..... 2.5 μ l with MgCl₂
 Taq polymerase..... 0.25 μ l
 filled up with H₂O to 25 μ l, subjected to PCR (2.7.9.3)

RT-PCR

cDNA..... 1 μ l
 Primer 1 (10 pmol)..... 1.25 μ l
 Primer 2 (10 pmol)..... 1.25 μ l

dNTPs (10 mM) 4 μ l
10 x PCR buffer 2.5 μ l *with MgCl₂*
Taq polymerase 0.25 μ l
filled up with H₂O to 25 μ l, subjected to PCR (2.7.9.3)

TaqCORE Kit, Qbiogen, (Cat. No. EPTQK109)

2.7.9.3. PCR programs

The following PCR programs were used in this study:

Genotyping PKGI floxed PCR

Step	Time (sec)	Temp (° C)
1	120	95
2	30	94
3	30	55 (-1° C/cycle)
4	30	72
steps 2 - 4 were repeated 10 times		
5	30	94
6	30	45
7	30	72
steps 5 - 7 were repeated 35 times		
8	600	72
9	∞	4

Genotyping PKGI k.o. PCR

Step	Time (sec)	Temp (° C)
1	120	95
2	40	94
3	30	65 (-1° C/cycle)
4	40	72
steps 2 - 4 were repeated 10 times		
5	40	94
6	30	55
7	40	72
steps 5 - 7 were repeated 40 times		
8	600	72
9	∞	4

RT-PCR (cDNA)

Step	Time (sec)	Temp (° C)
1	120	94
2	30	94
3	30	52 - 62 depending on the primer annealing temperatures
4	20-60	72 depending on the product size of the amplicon
steps 2 - 4 were repeated 35 times		
5	600	72
6	∞	4

2.7.9.4. Real-time PCR (SYBR Green)

SYBR Green I dye intercalates into double-stranded DNA and produces a fluorescent signal. The intensity of the signal is proportional to the amount of dsDNA present in the reaction. Therefore, at each step of the PCR reaction, the signal intensity increases as the amount of product increases. This provides a very simple and reliable method to monitor PCR reactions in real time.

SYBR Green Real-time PCR was performed using the LightCycler® SYBR Green I Master mix (Roche) on a Roche LightCycler®480 instrument (96-well format). For specific primer combinations refer to 2.7.9.5.

LightCycler® SYBR Green I Master, Roche, Mannheim (Cat. No. 4887352)

2.7.9.5. Primers Real-time PCR

Name	Primer sequence
UCP-1 forward	5' - GGT GAA CCC GAC AAC TTC CGA AGT G - 3'
UCP-1 reverse	5' - GGG TCG TCC CTT TCC AAA GTG TTG A - 3'
PPAR γ forward	5' - TCC GTA GAA GCC GTG CAA GAG ATC A - 3'
PPAR γ reverse	5' - CAG CAG GTT GTC TTG GAT GTC CTC G - 3'
PGC-1 α forward	5' - GCA CAC ACC GCA ATT CTC CCT TGT A - 3'
PGC-1 α reverse	5' - ACG CTG TCC CAT GAG GTA TTG ACC A - 3'
HSL forward	5' - GAG GCT CAG ACG AGA GGG AGA A - 3'
HSL reverse	5' - CTA CGG GAA GGA CAG GAC AGC AAG G - 3'
Plin forward	5' - CTC TGG GAA GCA TCG AGA AGG TGG T - 3'
Plin reverse	5' - CCT TCA GGG CAT CGG ATA GGG ACA T - 3'
Gpd1 forward	5' - TGT TAA ATA CCT GCC AGG GCA CAA GC - 3'
Gpd1 reverse	5' - AGT TGG GTG TCT GCA TCA GGT CCT TC - 3'
Cidea forward	5' - ATT TAA GAG ACG CGG CTT TGG GAC A - 3'
Cidea reverse	5' - TTT GGT TGC TTG CAG ACT GGG ACA T - 3'

Name	Primer sequence
aP2 forward	5' - TGA AAG AAG TGG GAG TGG GCT TTG C - 3'
aP2 reverse	5' - CAC CAC CAG CTT GTC ACC ATC TCG T - 3'
HPRT forward	5' - ACA TTG TGG CCC TCT GTG TGC TCA - 3'
HPRT reverse	5' - CTG GCA ACA TCA ACA GGA CTC CTC GT - 3'

2.7.9.6. Real-time PCR reactions

SYBR® Green PCR

cDNA..... 3 μ l
Primer 1 (5 pmol)..... 1.25 μ l
Primer 2 (5 pmol)..... 1.25 μ l
2 x Master mix..... 4 μ l
subjected to Real-time PCR (2.7.9.7)

2.7.9.7. Real-time PCR program

Real-time PCR (cDNA)

Step ... Time (sec)..Temp (° C)

1..... 600..... 95
 2..... 10..... 95
 3..... 15..... 72
 4..... 90..... 72
 5..... 1..... 82 single acquisition

steps 2 - 5 were repeated 40 times

melting curve:

6..... 1..... 95
 7..... 15..... 65
 8..... ---..... 95 20 acquisitions per ° C from 65° C to 95° C

2.7.9.8. Quantification of Real-time PCR data

Relative quantification of mRNA levels was performed based on the crossing point (CP) values of the amplification curves, determined by the second derivative maximum method. HPRT (hypoxanthine-guanine-phosphoribosyltransferase) served as an internal control. Fold changes were derived from the Δ CP values.

2.7.10. DNA chip hybridization

For the linear T7-based amplification step of sample RNA, 0.5 μ g of each total RNA (2.7.8) sample was used as starting material (RNA from wt and PKGI^{-/-} brown adipocytes differentiated in the presence of 200 μ M cGMP). The further steps were carried out by Milteny Biotec (Gladbach): to produce Cy3- and Cy5-labelled cRNA, the samples were amplified and labelled using Low RNA Input Linear Amp Kit (Agilent Technologies, USA) following the manufacturer's protocol. Yields of cRNA and dye incorporation rate were measured with a ND-1000 spectrophotometer (NanoDrop®Technologies, Thermo Scientific, USA). Samples from PKGI^{-/-} mice were labelled with Cy5 and samples from wild type mice with Cy3. DNA chip hybridization was performed on Agilent Whole Mouse Genome Oligo (60-mer) 4x44K microarrays according to the 60-mer oligo microarray processing protocol of the Gene Expression Hybridization Kit (Agilent, USA). Agilent's Feature Extraction Software was used to read out and process the microarray image files. The software determined feature intensities and ratios after background subtraction and normalization to equal average intensity. Output data consisted of gene lists with the complete raw data sets including absolute intensities, Cy5/Cy3 ratios and fold changes. Grouping of genes was performed by Gene Ontology (GO) annotation.

2.8. Statistical analysis

All values are presented as means \pm standard error of the mean (s.e.m.). Statistical differences were determined using Student's t test. p-values < 0.05 were considered significant. The following definitions were used and are described in the figure legends: * p < 0.05; ** p < 0.01; *** p < 0.001

3. Results

3.1. Characterization of BAT-derived mesenchymal stem cells

Adipocytes originate from multipotent mesenchymal stem cells that among others (1.2.3) differentiate into preadipocytes/lipoblasts, which give rise to either unilocular, white or multilocular, brown adipocytes (Figure 6). To isolate BAT-MSCs from BAT, interscapular brown fat pads were harvested from new born wild type (wt) mice and fractionated into mature adipocytes and stroma-vascular fractions (Nechad, 1983). The cells of the stroma-vascular fraction were immortalized by lentiviral transduction with a vector expressing the SV40 large T antigen. These cells exhibited a fibroblast-like morphology (Figure 8) and flow cytometer analysis using a panel of antibodies against stem cell surface markers (Figure 9A) demonstrated that BAT-MSCs exhibit a phenotype similar to bone marrow-derived MSCs (BM-MSCs) (Breitbach et al., 2007).

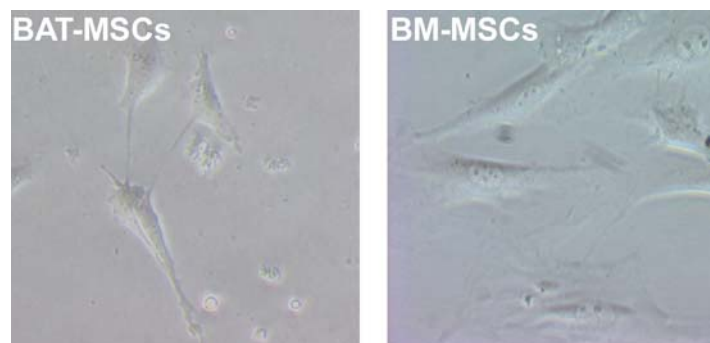


Figure 8. BAT-MSCs and BM-MSCs exhibit a fibroblast-like morphology.

Bright field pictures of undifferentiated BAT-MSCs and BM-MSCs (provided by Prof. Bernd Fleischmann, Universität Bonn); magnification 20 x.

BAT-MSCs were positive for Sca-1, CD44, CD49e, CD105, CD106, but negative for the hematopoietic markers CD45 and CD11b. The multipotent nature and functional integrity of BAT-MSCs was further confirmed by *in vitro* differentiation to (brown) adipogenic and osteoblastic lineages (Figure 9B, C).

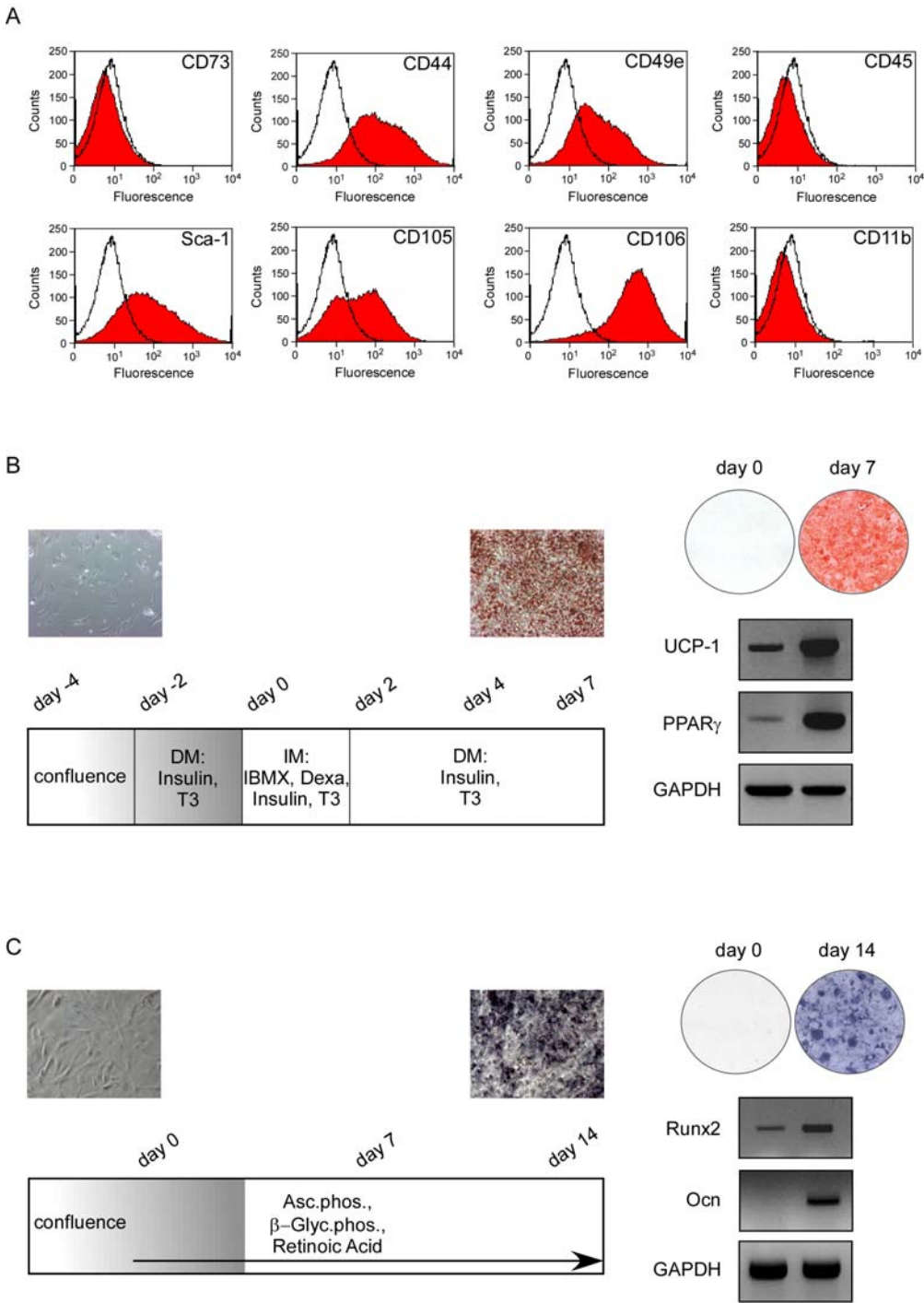


Figure 9. Characterization of BAT-MSCs. (A) Flow cytometry analysis of BAT-MSCs; note the expression of MSC markers (positive for Sca-1, CD44, CD49e, CD105, CD106) and the lack of the haematopoietic cell markers CD45 and CD11b. (B) The protocol for adipogenic differentiation of BAT-MSCs is depicted indicating the different stages of differentiation (day -4 – day 7) and the media (DM, differentiation medium; IM, induction medium; IBMX, isobutylmethylxanthine; T3, triiodothyronine; Dexa, dexamethason) used at the different time points (bottom left). Adipogenic differentiation was confirmed by Oil Red O staining (top left and right) and the expression of UCP-1 and PPAR_γ by RT-PCR (bottom right). (C) The stages of the osteogenic differentiation of BAT-MSCs (day 0 – day 14) are shown (bottom left; Asc.phosph., ascorbate-2-phosphate; β-Glyc.phosph., β-glycero-phosphate). To confirm osteogenic differentiation, alkaline phosphatase staining (top left and right) and RT-PCR of the osteogenic markers Runx2 and osteocalcin (Ocn) were performed (bottom right).

3.1.1. Expression of the NO/cGMP signaling cascade in BAT-MSCs

First, the expression of components of the NO/cGMP signaling cascade in BAT-MSCs was analyzed. RT-PCR analysis showed that endothelial NO synthase (eNOS), soluble and particulate guanylylcyclases (sGC, GC-B, respectively, cGMP generating enzymes) and two major cGMP receptors PKGI and PDE3B were expressed in BAT-MSCs (Figure 10A). Western blot analysis corroborated high levels of PKGI in BAT-MSCs, which further increased during adipocyte differentiation reaching a peak at day 4 (Figure 10B).

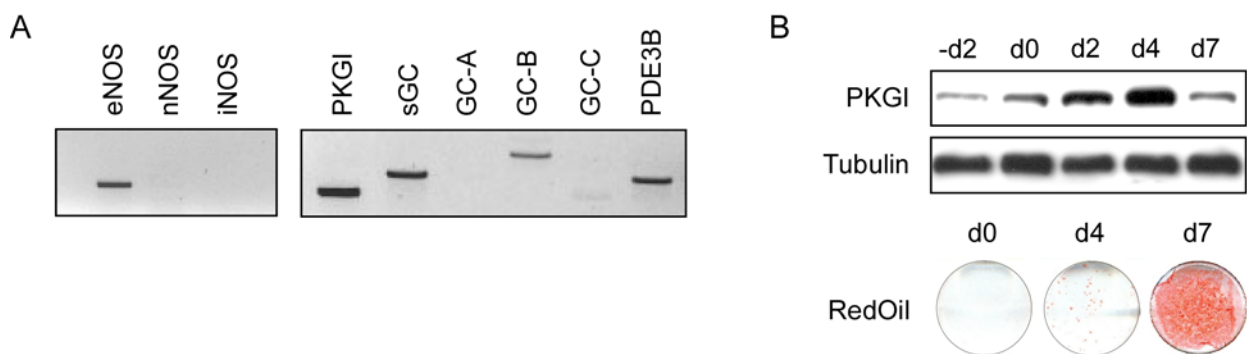


Figure 10. Expression of the NO/cGMP signaling cascade in BAT-MSCs.

(A) Expression analysis (RT-PCR) of the NO-dependent signaling cascade in undifferentiated BAT-MSCs. NOS, NO-synthase; GC, guanylylcyclase; PKGI, protein kinase GI; PDE3B, phosphodiesterase 3B. (B) Western blot analysis of PKGI expression (top) and Oil Red O staining (bottom) during brown fat differentiation.

3.2. PKGI mediates cGMP-induced mitochondrial biogenesis in BAT-MSCs

Mitochondrial content increases during the differentiation process of brown adipocytes and NO has been shown to induce mitochondrial biogenesis via generation of cGMP (Nisoli et al., 2003; Nisoli et al., 1998). However, the mechanism of cGMP-induced mitochondrial biogenesis is unclear. Therefore, mitochondrial content was measured by MitoTracker fluorescence in differentiated cells isolated from wt and PKGI-deficient ($PKGI^{-/-}$) mice (Pfeifer et al., 1998). Consistent with previous studies (Nisoli et al., 2003), treatment of BAT-MSCs with 200 μ M 8-pCPT-cGMP (cGMP) during differentiation increased mitochondrial content by $23 \pm 5\%$ as compared to control wt cells (Figure 11A). In $PKGI^{-/-}$ cells, the basal MitoTracker fluorescence signal was reduced by $33 \pm 10\%$ of wt levels, and cGMP had no effect on mitochondrial biogenesis. Lentiviral expression of a constitutively active mutant of PKGI (caPKGI, LV-caPKGI) (Heil et al., 1987) in wt BAT-MSCs significantly increased the MitoTracker fluorescence signal over wt cells transduced with a control virus (Figure 11A),

demonstrating that activation of PKGI induces mitochondrial biogenesis. Quantitative morphometry revealed that the area of mitochondria of PKGI^{-/-} cells was significantly reduced as compared to wt cells (Figure 11B), explaining the distinct decrease of mitochondrial volume as observed with MitoTracker fluorescence.

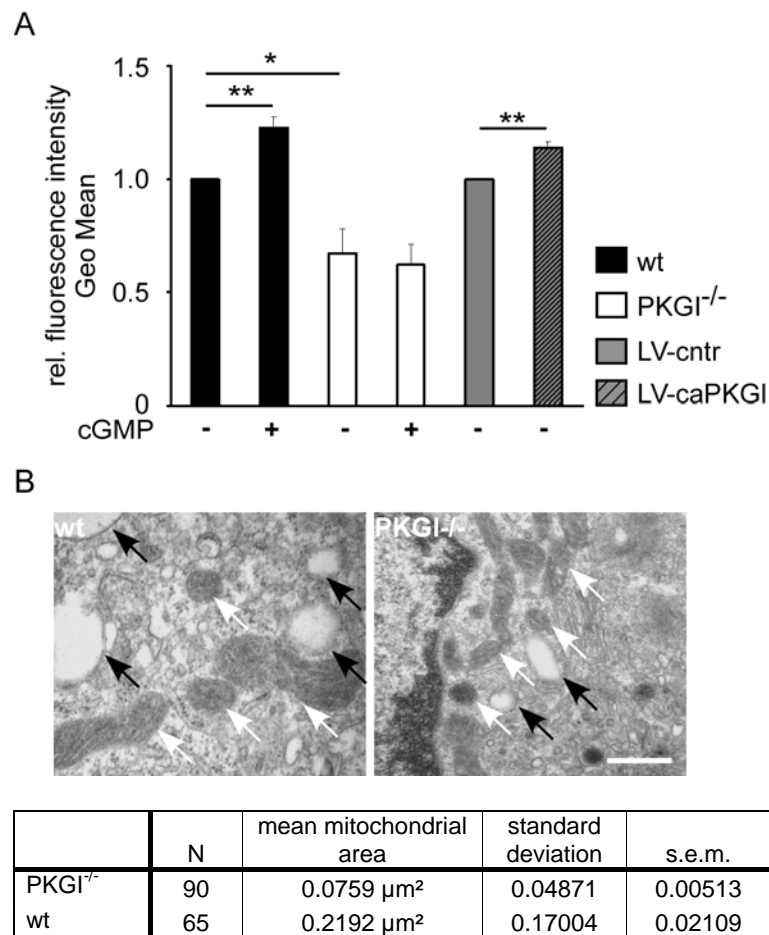


Figure 11. PKGI mediates cGMP-induced mitochondrial biogenesis.

(A) Analysis of MitoTracker fluorescence in wt and PKGI^{-/-} cells differentiated (day 4) in the presence of 200 μM 8-pCPT-cGMP (cGMP) (n=4) and cells transduced with a lentiviral vector containing a constitutively active PKGI (LV-caPKGI) or a control virus (n=3) containing no transgene (LV-cntr) as indicated. Untreated wt and LV-cntr were set as one. Data are given as mean ± s.e.m.; * p < 0.05; ** p < 0.01 compared to untreated wt or LV-cntr. (B) Representative transmission electron microscopy micrographs of wt (upper left) and PKGI^{-/-} brown adipocytes (upper right); magnification 30000 x; scalebar = 450 nm; white arrows indicate mitochondria, black arrows indicate lipid droplets. Table showing mitochondrial areas of wt and PKGI^{-/-} cells (lower panel); p < 0.001 compared to wt.

The transcriptional coactivator peroxisome proliferator-activated receptor γ (PPAR γ) coactivator-1 α (PGC-1 α) is a key regulator of mitochondrial biogenesis and is known to activate UCP-1 expression and mitochondrial respiration (Lehman et al., 2000; Puigserver et al., 1998; Wu et al., 1999). Therefore, I analyzed if PKGI triggers the expression of PGC-1 α and UCP-1 in differentiated brown adipocytes. Quantitative real-time PCR (RQ-PCR) revealed that treatment of wt cells with cGMP induced expression of UCP-1 (to 235 ± 38%)

and PGC-1 α (to $180 \pm 41\%$). In sharp contrast, UCP-1 was barely detectable in PKGI $^{-/-}$ cells and PGC-1 α expression was reduced by $23 \pm 7.5\%$ of wt levels, and cGMP treatment had no effect on UCP-1 and PGC-1 α expression in PKGI $^{-/-}$ cells (Figure 12A). Western blot analysis corroborated reduced UCP-1 protein levels and the loss of cGMP effects in PKGI $^{-/-}$ cells (Figure 12B). Lentiviral expression of caPKGI in wt cells increased UCP-1 and PPAR γ mRNA-levels during the differentiation process (Figure 12C). These data indicate that PKGI mediates the NO/cGMP-dependent induction of mitochondrial biogenesis in brown adipocytes.

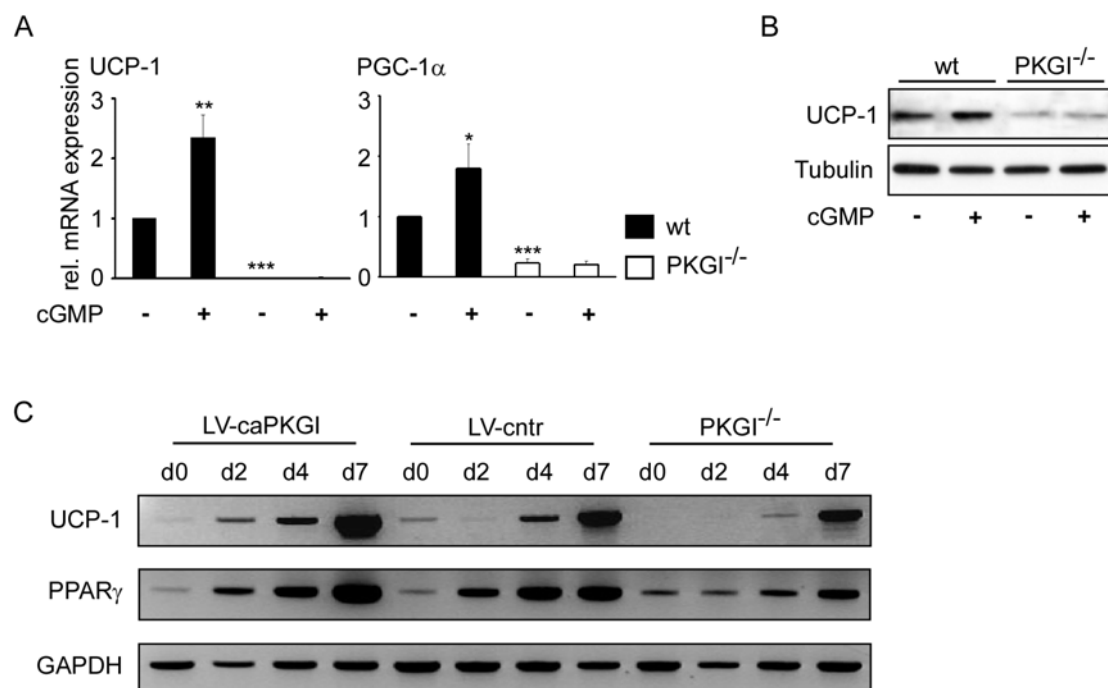


Figure 12. Mitochondrial marker gene expression.

(A) Quantitative real-time PCR (RQ-PCR) analysis of UCP-1 and PGC-1 α of differentiated brown adipocytes (day 7) of wt or PKGI $^{-/-}$ mice treated with 200 μ M cGMP from day -2 to day 7 as indicated (n=5). HPRT was used as an internal control and values are expressed as fold change, untreated wt was set as one. Data are given as mean \pm s.e.m.; * p < 0.05; ** p < 0.01; *** p < 0.001 compared to untreated wt. (B) Western blot of UCP-1 of differentiated brown adipocytes from wt or PKGI $^{-/-}$ mice treated with cGMP as indicated. (C) Time course of UCP-1 and PPAR γ expression (RT-PCR) during differentiation. RNA was isolated at the indicated time points from cells transduced with LV-cntr, LV-caPKGI or PKGI $^{-/-}$ cells.

3.3. PKGI regulates accumulation of fat and expression of adipogenic makers during fat cell differentiation

Given the importance of PGC-1 α and UCP-1 for brown fat energy expenditure (Puigserver et al., 1998), the effect of PKGI on the accumulation of lipids was analyzed in brown adipocytes by Oil Red O staining and quantification of triglycerides (TG). It was speculated that because

of the reduced UCP-1 and mitochondrial contents less fat should be utilized for energy dissipation and that fat storage should be increased in PKGI^{-/-} cells. Surprisingly, less lipid droplets were observed in PKGI^{-/-} cells after 7 days of adipogenic differentiation as compared to wt cells (Figure 13A). The basal TG content was significantly reduced by $56 \pm 4\%$ in PKGI^{-/-} cells (Figure 13B). Furthermore, adipogenic differentiation of wt BAT-MSCs for 7 days in the presence of cGMP resulted in a significantly increased accumulation of lipid droplets and TG content increased by $50 \pm 18\%$. In contrast, cGMP had no significant effect on TG content in PKGI^{-/-} cells (Figure 13A, B).

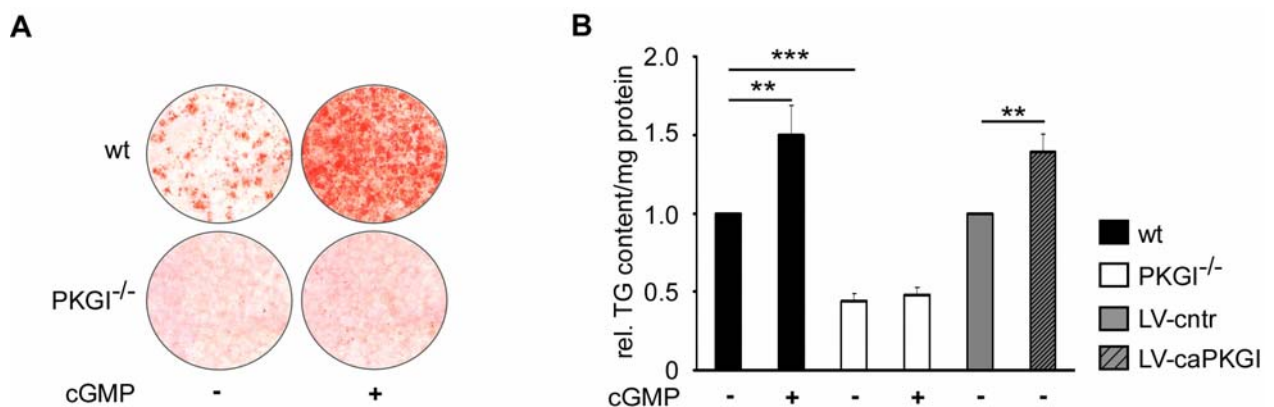


Figure 13. PKGI mediates cGMP-induced lipid accumulation.

(A) Oil Red O staining of differentiated wt and PKGI^{-/-} brown adipocytes treated with 200 μ M cGMP as indicated. (B) Triglyceride (TG) content normalized to the protein content of the sample of differentiated brown adipocytes of wt and PKGI^{-/-} mice (n=6) treated with 200 μ M cGMP or cells infected with LV-cntr and LV-caPKGI (n=4) as indicated, untreated wt and LV-cntr were set as one. Data are given as mean \pm s.e.m.; ** p < 0.01; *** p < 0.001 compared to untreated wt or LV-cntr.

Since constitutive knock out of PKGI might induce compensatory changes in other signaling pathways, conditional PKGI knockout mice (PKGI^{fl/fl}) were generated at the MPI für Biochemie, Martinsried in the laboratory of Prof. Reinhard Fässler. Transduction of BAT-MSCs isolated from PKGI^{fl/fl} mice with a self deleting Cre lentivirus (LV-CreSD) efficiently disrupted the *prkg1* gene (PKGI^{0/0} cells) (Figure 14A). PKGI^{0/0} cells accumulated significantly less fat (Figure 14B, C). Moreover, expression of caPKGI in wt BAT-MSCs resulted in a significant increase in TG content as compared to control (by $39 \pm 12\%$) (Figure 13B). These data indicate that PKGI controls distinct aspects of BAT biology, i.e. (i) normal thermogenic capacity (i.e. UCP-1 expression, high mitochondrial content), and (ii) brown fat cell differentiation.

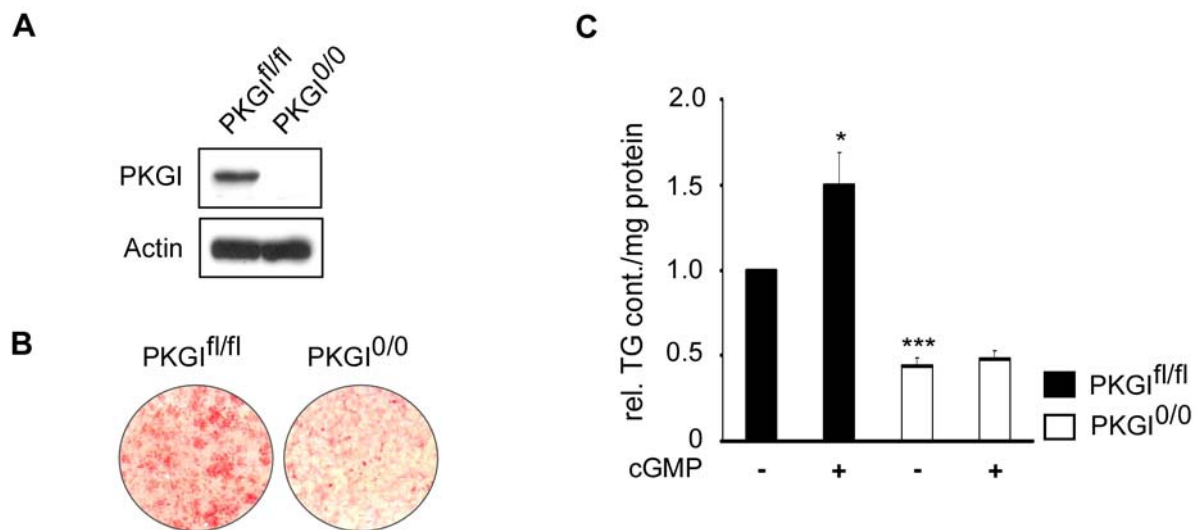


Figure 14. Lipid accumulation is reduced in PKGI^{0/0} cells.

(A) Anti-PKGI Western blot of cells isolated from PKGI^{fl/fl} mice infected with (PKGI^{0/0}) or without (PKGI^{fl/fl}) the Cre-expressing lentivirus LV-CreSD. Actin Western blot was performed to control for loading. (B) Oil Red O staining of differentiated brown adipocytes of PKGI^{fl/fl} and PKGI^{0/0} mice. (C) TG content of differentiated brown adipocytes of PKGI^{fl/fl} and PKGI^{0/0} mice treated with 200 μ M cGMP as indicated was measured and normalized to the protein content of the sample (n=4). Untreated PKGI^{fl/fl} was set as one. Data are given as mean \pm s.e.m.; * p < 0.05; *** p < 0.001 compared to untreated PKGI^{fl/fl}.

3.3.1. Microarray (CHIP) analysis of differentiated brown fat cells

To assess the requirement of PKGI in the global and metabolic transcriptional response to cGMP, microarray analysis was performed of RNA isolated from differentiated wt and PKGI^{-/-} brown adipocytes treated with cGMP. The top 30 genes up and down-regulated more than 3-fold are displayed in Table 3 and Table 4 (6. Appendix) respectively, sorted according to function and magnitude of induction. Differentially expressed genes were grouped according to the gene ontology (GO) annotation. In total, 2199 annotations could be ascribed to the genes that were changed at least 3-fold, of which 857 were up-regulated and 1342 down-regulated in PKGI^{-/-} cells as compared to wt cells. The largest differences between PKGI^{-/-} and wt cells were found in transcripts related to signaling (160 up-regulated, 289 down-regulated in PKGI^{-/-} versus wt cells) and metabolism (93 up-regulated, 278 down-regulated in PKGI^{-/-} versus wt cells). Expression of genes involved in lipid, energy, carbohydrate and other metabolism were down-regulated by 87%, 82%, 80% and 64%, respectively (Figure 15).

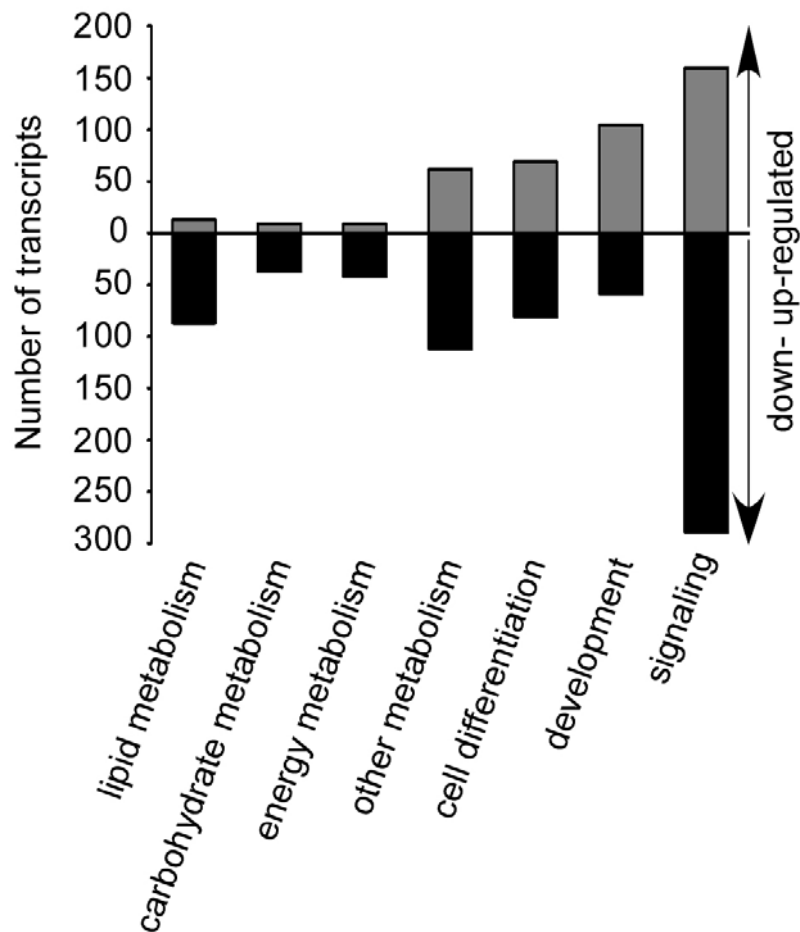


Figure 15. Gene expression analysis.

Microarray analysis of differentiated wt and PKGI^{-/-} brown adipocytes treated with cGMP. Grouping was performed by GO annotation.

To further confirm these findings, RQ-PCR expression analysis in differentiated brown adipocytes was performed of a panel of adipogenic genes, including glycerol-3-phosphate dehydrogenase (Gpd1), perilipin (Plin), PPAR γ , hormone sensitive lipase (HSL), fatty acid binding protein 4 (aP2), and cell death-inducing DNA fragmentation factor α subunit-like effector A (Cidea). Incubation of wt cells with cGMP caused an increase in the levels of Gpd1 (to $209 \pm 45\%$), perilipin (to $162 \pm 22\%$), PPAR γ (to $153 \pm 26\%$), HSL (to $161 \pm 19\%$), aP2 (to $282 \pm 185\%$) and Cidea (to $328 \pm 152\%$). Conversely, the mRNAs of these adipogenic marker genes were suppressed in PKGI^{-/-} cells (Figure 16).

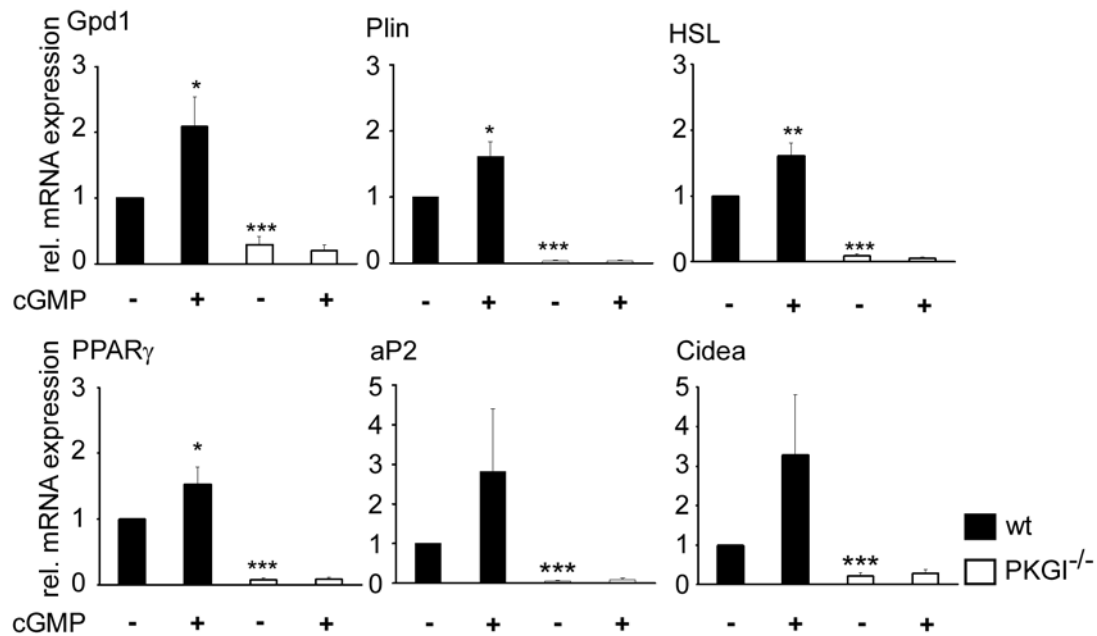


Figure 16. RQ-PCR quantification of fat cell markers.

RQ-PCR of Gpd1, Plin, HSL, PPAR γ , aP2 and Cidea was performed in brown adipocytes of wt and PKGI^{-/-} mice treated with 200 μ M cGMP as indicated (n=5). HPRT was used as an internal control and values are expressed as fold change, untreated wt was set as one. Data are given as mean \pm s.e.m.; * p < 0.05; ** p < 0.01; *** p < 0.001 compared to untreated wt.

In addition, also early and late adipogenic markers were analyzed by Western blotting: CCAAT/enhancer-binding protein β (C/EBP β) is a crucial factor during early stages of fat differentiation (Hamm et al., 2001). Induction of C/EBP β protein expression with induction medium (IM) at day 0 of differentiation was significantly reduced in PKGI^{-/-} cells (by 19 \pm 1.6%) (Figure 17A) and PKGI^{0/0} cells (Figure 17B). In addition, caPKGI increased C/EBP β protein content (Figure 17C). According to the microarray and RQ-PCR data, reduced PPAR γ and aP2 protein levels were found in PKGI^{-/-} cells and treatment with cGMP caused only an increase of the respective protein levels in wt cells (Figure 17D). Reduced UCP-1 and PPAR γ mRNA levels could be confirmed in differentiated PKGI^{0/0} cells (Figure 17E). Thus, the microarray, RQ-PCR and Western blot data further point to a pivotal role of PKGI not only for brown fat mitochondrial biogenesis but also for brown fat cell differentiation.

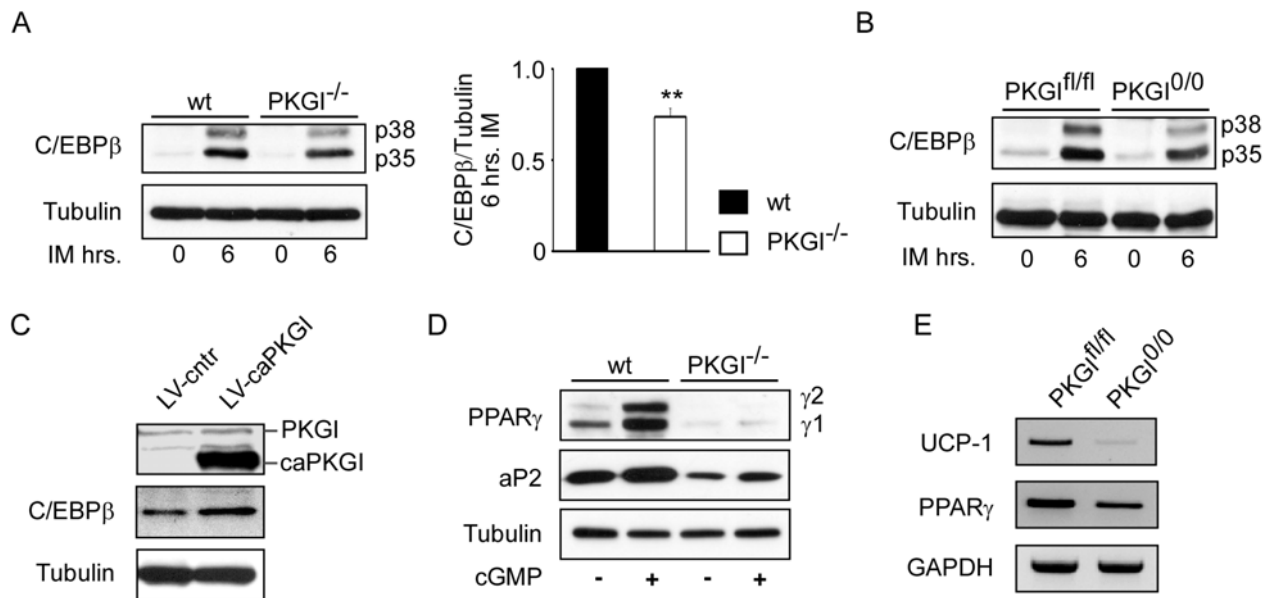


Figure 17. Expression of early and late adipogenic markers.

(A) Western blot analysis showing the induction of C/EBP β expression in wt and PKGI $^{-/-}$ cells after treatment with induction medium (IM) for 6 h at day 0 as indicated (left). Densitometric analysis of C/EBP β expression after 6 h of treatment with IM in wt versus PKGI $^{-/-}$ cells (n=3, right). Data are given as mean \pm s.e.m.; ** p < 0.01 compared to wt. (B) Western blot showing the induction of C/EBP β expression in PKGI $^{fl/fl}$ and PKGI $^{0/0}$ cells after treatment with induction medium (IM) for 6 h at day 0 as indicated. (C) Western blot showing the expression of C/EBP β and caPKGI 72 h post infection with LV-caPKGI. (D) Western blots of PPAR γ and aP2 of differentiated brown adipocytes of wt and PKGI $^{-/-}$ mice treated with cGMP as indicated. (E) Expression of UCP-1 and PPAR γ in differentiated PKGI $^{fl/fl}$ and PKGI $^{0/0}$ brown adipocytes as assessed by RT-PCR.

3.4. PKGI effects on adipogenic differentiation are mediated via the RhoA/ROCK pathway

To gain insight into the molecular mechanisms of PKGI-mediated cGMP effects on BAT differentiation, I focused on the signaling cascade downstream of PKGI. I hypothesized that the small GTPase RhoA might be involved in the cGMP/PKGI-dependent differentiation of brown adipocytes, as RhoA was shown to play a role in mesenchymal stem cell lineage commitment as well as adipogenic differentiation of 3T3-L1 cells and mouse embryonic fibroblasts (MEFs) (McBeath et al., 2004; Sordella et al., 2003), and as RhoA activity can be negatively regulated by PKGI in vascular smooth muscle cells (VSMCs) (Begum et al., 2002; Rolli-Derkinderen et al., 2005; Sauzeau et al., 2000). To test this hypothesis, RhoA-GTP levels were measured and were found to be elevated in PKGI $^{-/-}$ as compared to wt BAT-MSCs before and even more pronounced after serum treatment (Figure 18A). In addition, RhoA mutants were used to enhance or suppress RhoA signaling. Retroviral expression of the dominant-negative mutant Myc-RhoN19 increased TG levels in wt cells by $20 \pm 5.4\%$ as compared to untreated cells. Expression of Myc-RhoN19 in PKGI $^{-/-}$ cells (Figure 18C) rescued lipid droplet accumulation and induced an increase in TG content to $81 \pm 4.7\%$ of wt

levels, while expression of a constitutively active Myc-RhoL63 mutant (Figure 18C) reduced TG accumulation by $66 \pm 3.8\%$ in wt but had no significant effect in PKGI^{-/-} cells (Figure 18B).

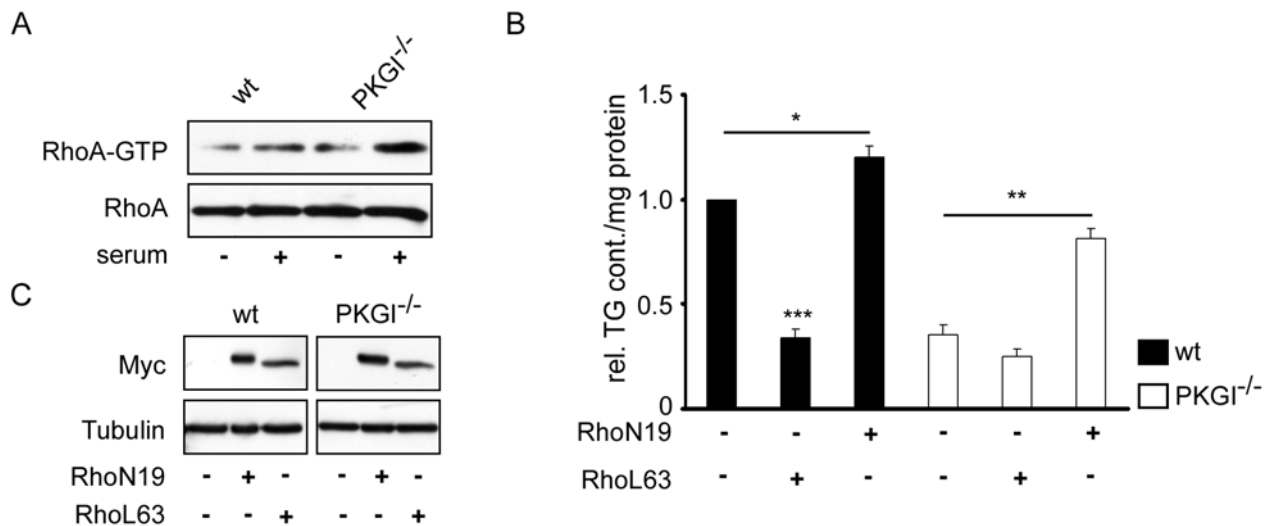


Figure 18. Effects of PKGI on RhoA signaling.

(A) Anti-RhoA immunoblot of total cell lysates (RhoA) and GST-Rhotekin pull-downs (RhoA-GTP) from serum starved wt and PKGI^{-/-} BAT-MSCs stimulated with serum for 3 min as indicated. (B) Differentiated wt and PKGI^{-/-} brown adipocytes expressing RhoA mutants as indicated were analyzed for their TG levels normalized to the protein content of the sample (n=3). Data are given as mean \pm s.e.m.; * $p < 0.05$; ** $p < 0.01$; *** $p < 0.001$ compared to untreated wt or PKGI^{-/-}. (C) Expression analysis of RhoA mutants 72 h post infection of wt or PKGI^{-/-} cells with the myc-tagged RhoA mutants RhoN19 and RhoL63. Western blots with an anti-myc antibody were performed. Tubulin Western blot was performed to control for loading.

Rho-kinases (ROCKs) are serine/threonine kinases and important RhoA downstream effector proteins that mediate a broad spectrum of RhoA effects including the formation of actin stress fibers in adherent cells (Ridley and Hall, 1992). Serum-induced stress fiber formation was inhibited by treatment of wt BAT-MSCs with cGMP. PKGI^{-/-} cells already showed more stress fibers in the serum starved state and stress fiber formation was not reduced by pre-incubation of PKGI^{-/-} cells with cGMP (Figure 19A), indicating that loss of PKGI is indeed leading to increased RhoA and ROCK activation in BAT-MSCs. Interestingly, pharmacological inhibition of ROCK with 30 μ M Y-27632 during differentiation resulted in a strong increase of TG accumulation (Figure 19B) and induction of fat specific and mitochondrial marker gene expression in wt cells (Figure 19 C, D). Furthermore, Y-27632 treatment rescued TG accumulation, adipogenic and mitochondrial marker gene expression in PKGI^{-/-} cells (Figure 19 B-D). Altogether, the data suggest that the effects of PKGI on brown adipocyte differentiation and mitochondrial biogenesis are mediated through inhibition of RhoA/ROCK signaling.

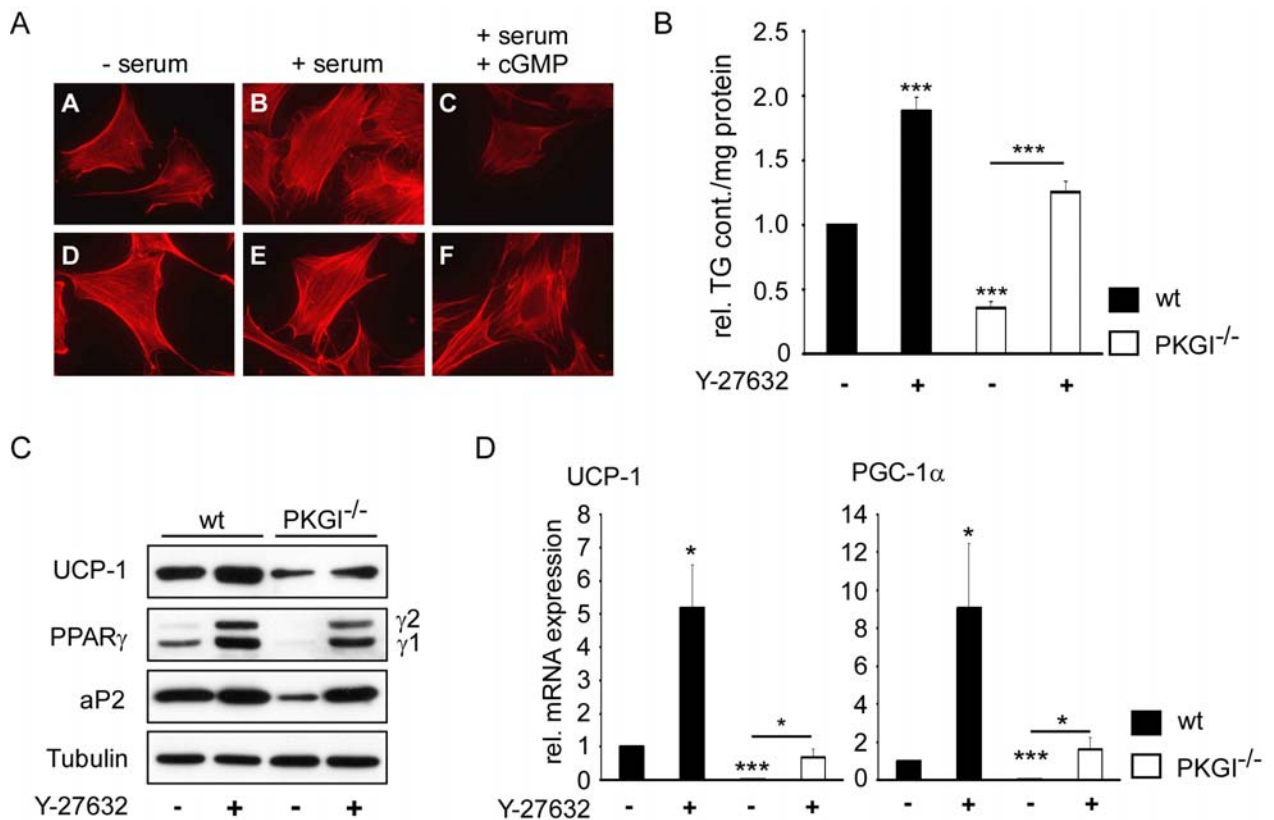


Figure 19. PKGI inhibits RhoA/ROCK signaling.

(A) Phalloidin staining of F-Actin stress fibers in wt (A, B, C) and PKGI^{-/-} (D, E, F) BAT-MSCs plated on fibronectin-coated glass coverslips. (B) TG content normalized to the protein content of the sample of differentiated brown adipocytes of wt and PKGI^{-/-} mice treated with 30 μ M of the ROCK inhibitor Y-27632 as indicated (n=3). (C) Western blot analysis of UCP-1, PPAR γ and aP2 expression in differentiated brown adipocytes of wt and PKGI^{-/-} mice treated with 30 μ M Y-27632 as indicated. (D) RQ-PCR analysis of UCP-1 and PGC-1 α expression in differentiated brown adipocytes of wt and PKGI^{-/-} mice treated with 30 μ M Y-27632 as indicated (n=3). HPRT was used as an internal control and values are expressed as fold change, untreated wt was set as one. Data are given as mean \pm s.e.m.; * p < 0.05; *** p < 0.001 compared to untreated wt or PKGI^{-/-}.

3.5. Insulin signaling is impaired in PKGI^{-/-} brown adipocytes

To explore potential downstream targets of the cGMP/PKGI/RhoA/ROCK pathway, the time course of cGMP effects during BAT differentiation was analyzed. cGMP treatment from days -2 to +2 was sufficient to enhance lipid accumulation, whereas no major effect was observed during days 2 to 4 and 4 to 7 (Figure 20A). Incubation with cGMP for only two days starting at day -2 enhanced lipid accumulation almost to the same extend as incubation for 4 days (days -2 to 2) (Figure 20B). Interestingly, this time point coincided with the first addition of insulin (Figure 9B, bottom left), pointing to a potential involvement of PKGI in insulin signaling in brown fat cells.

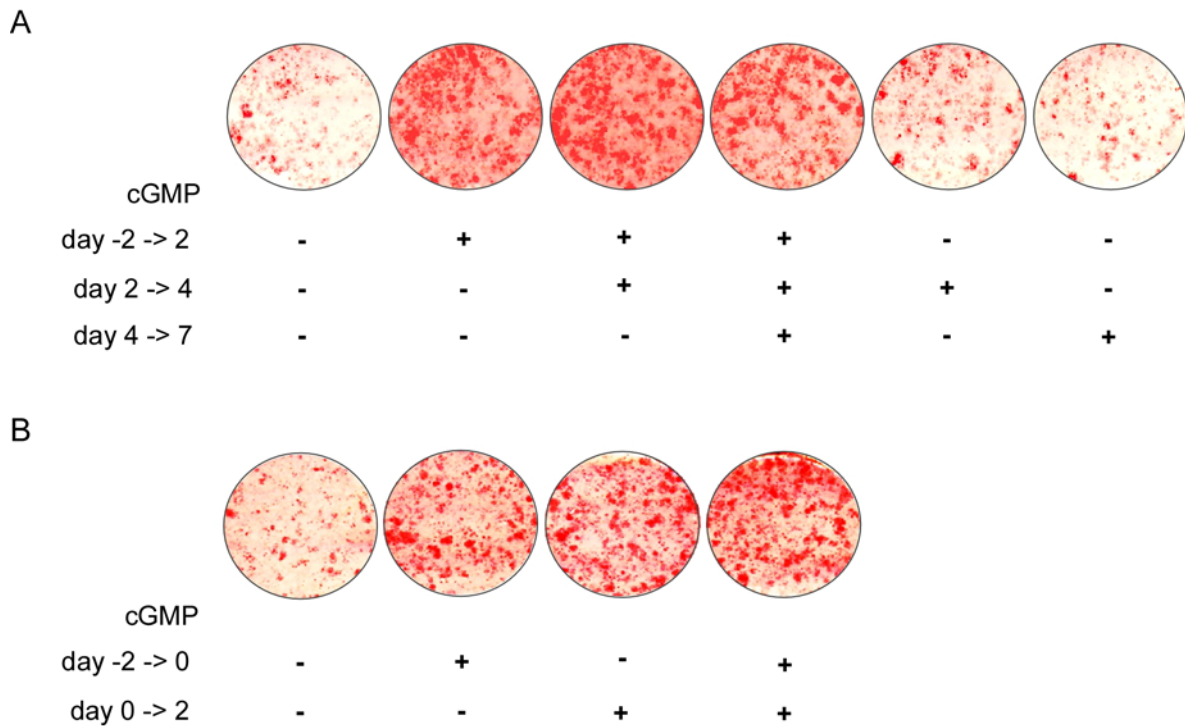


Figure 20. Effect of cGMP on brown adipocytes lipid accumulation.

(A) Red O staining of wt cells at 7 days of differentiation after treatment with 200 μ M cGMP for the indicated periods between day -2 and day 7. (B) Analysis of cGMP effects on lipid accumulation during insulin induction of differentiation (day -2 to 2). Oil Red O staining after 7 days of differentiation of wt cells treated with 200 μ M cGMP for the indicated periods. Note the effect of cGMP coincides with the insulin treatment starting at day -2.

Insulin positively regulates brown adipogenesis (Teruel et al., 1996) and activates the thermogenic program through induction of UCP-1 expression (Lorenzo et al., 1993). Interestingly, it has previously been shown in muscle cells that ROCK directly associates with insulin receptor substrate-1 (IRS-1) and phosphorylates serine residues (Begum et al., 2002; Furukawa et al., 2005) leading to reduced insulin-induced tyrosine phosphorylation of IRS-1 and phosphoinositide 3-kinase (PI3K) activation (Begum et al., 2002). Similar results were obtained with 3T3-L1 white adipocytes (Noguchi et al., 2007). To directly investigate whether RhoA/ROCK links cGMP/PKGI with insulin signaling in brown fat cells, the phosphorylation status of IRS-1 was analyzed. Insulin stimulation of BAT-MSCs led to enhanced phosphorylation of the inhibitory serine residues 636/639 of IRS-1 in PKGI^{-/-} cells ($44 \pm 21\%$ increase in insulin-treated PKGI^{-/-} as compared to insulin-treated wt cells) (Figure 21A) and PKGI^{0/0} cells (Figure 21B).

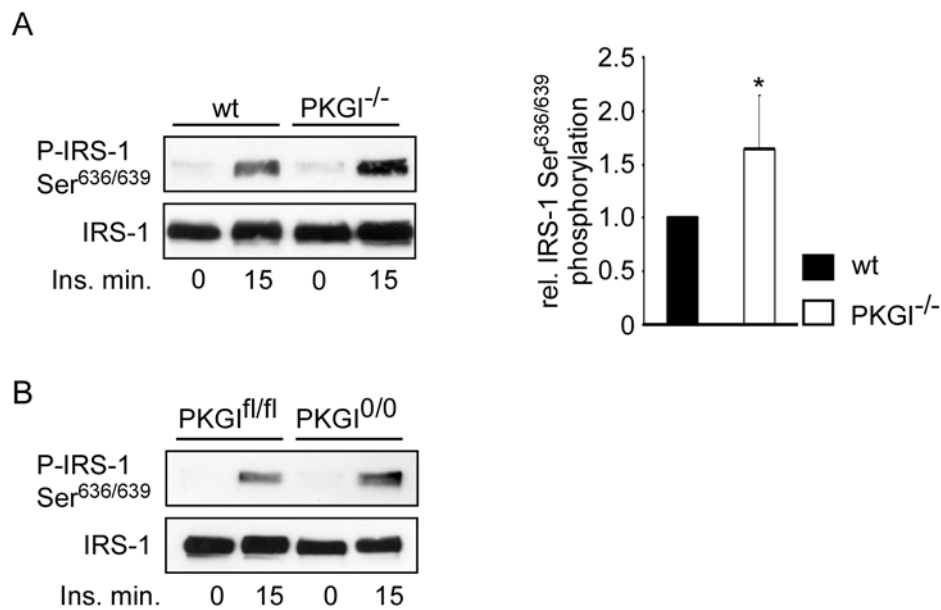


Figure 21. Analysis of the phosphorylation status of IRS-1.

(A) Serum starved wt and PKGI^{-/-} BAT-MSCs were treated with 100 nM insulin for 15 min as indicated and subjected to Western blotting using a phospho-specific (Ser636/639) antibody. The same membrane was probed with an IRS-1 antibody (left). Densitometric analysis of phospho-IRS-1 Ser636/639 phosphorylation after 15 min of treatment with 100 nM insulin in wt versus PKGI^{-/-} cells (n=3, right). Data are given as mean \pm s.e.m.; * $p < 0.05$ compared to wt. (B) The same experiment as in (A, left) was repeated with PKGI^{fl/fl} and PKGI^{0/0} cells.

Consistently, tyrosine phosphorylation and PI3K p85 α subunit association to IRS-1 were reduced in PKGI^{-/-} cells after insulin treatment (Figure 22A). Similar results were obtained with PKGI^{0/0} cells (Figure 22B).

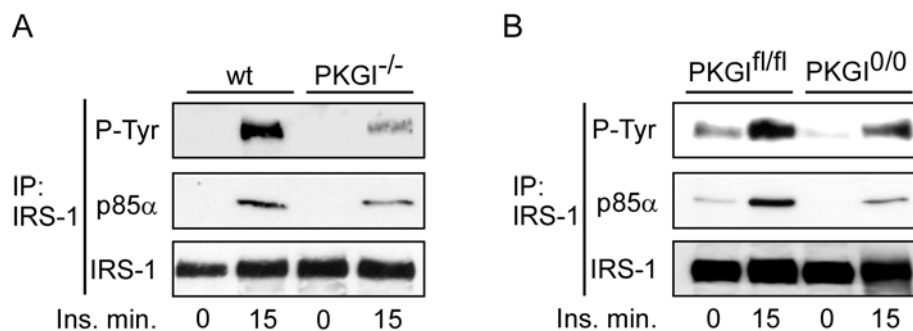


Figure 22. IRS-1 activation and p85 α association is reduced in PKGI^{-/-} BAT-MSCs.

(A) IRS-1 was immunoprecipitated from protein lysates of wt and PKGI^{-/-} BAT-MSCs treated with 100 nM insulin for 15 min as indicated and probed with phospho-tyrosine and p85 α antibodies. IRS-1 Western blot was performed to control for loading. (B) The same experiment as in (A) was repeated with PKGI^{fl/fl} and PKGI^{0/0} cells.

Reduced IRS-1 tyrosine phosphorylation and p85 α association should lead to diminished insulin/IRS-1 signaling in PKGI^{-/-} cells. To confirm this hypothesis, insulin-induced activation of Akt/protein kinase B, an important downstream target of the IRS-1/PI3K signaling cascade (White and Kahn, 1994) was studied. Insulin treatment of BAT-MSCs induced a

phosphorylation of Akt that was reduced in PKGI^{-/-} (Figure 23A) and PKGI^{0/0} cells (Figure 23B), indicating that PKGI exerts a permissive effect on insulin signaling. Importantly, Y-27632 induced Akt phosphorylation in wt cells and enhanced phosphorylation of the kinase in PKGI^{-/-} cells (Figure 23A). The IRS-1 phosphorylation data and the effect of the ROCK inhibitor on Akt activation indicate that RhoA/ROCK links cGMP/PKGI with the insulin pathway.

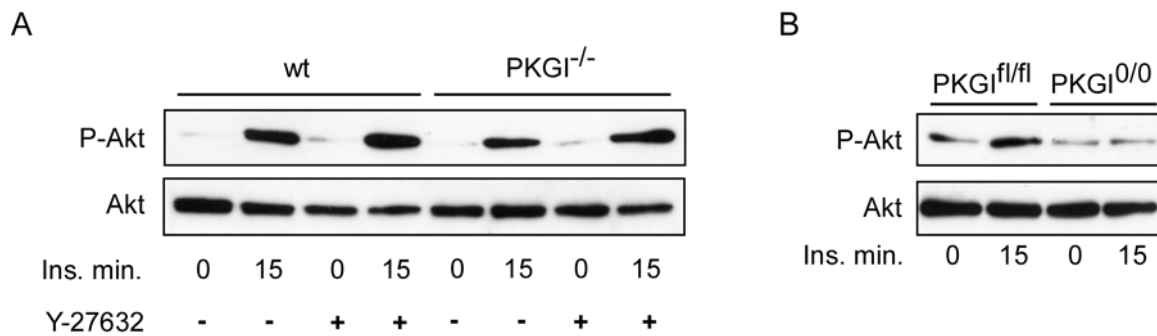


Figure 23. Insulin induced Akt activation.

(A) Insulin-induced Akt (Ser473) phosphorylation after 15 min incubation with 100 nM insulin as revealed by immunoblotting of wt and PKGI^{-/-} BAT-MSCs. Prior to insulin stimulation, cells were serum starved and pre-incubated with 30 μ M Y-27632 for 15 min as indicated. The same membrane was probed with an Akt antibody to control for loading. (B) Phospho-Akt (Ser473) immunoblot after 15 min incubation with 100 nM insulin as indicated of serum starved PKGI^{fl/fl} and PKGI^{0/0} BAT-MSCs. The same membrane was probed with an Akt antibody to control for loading.

To further corroborate that the effects of cGMP/PKGI are indeed mediated through IRS-1/PI3K/Akt, a constitutively active, myristoylated Akt (Myr-Akt) (Boehm et al., 2007) was expressed in PKGI^{-/-} cells using retrovirus. Expression of Myr-Akt induced a 2.58 ± 4.2 fold increase in TG content (Figure 24A) and increased aP2 and PPAR γ protein levels (Figure 24B). In addition, mitochondrial biogenesis and UCP-1 and PGC-1 α gene expression were enhanced by Myr-Akt in wt cells (Figure 24C, D). Importantly, Myr-Akt expression rescued TG accumulation, adipogenic marker gene expression, mitochondrial biogenesis and at least in part mitochondrial marker gene expression in PKGI^{-/-} cells (Figure 24 A-D).

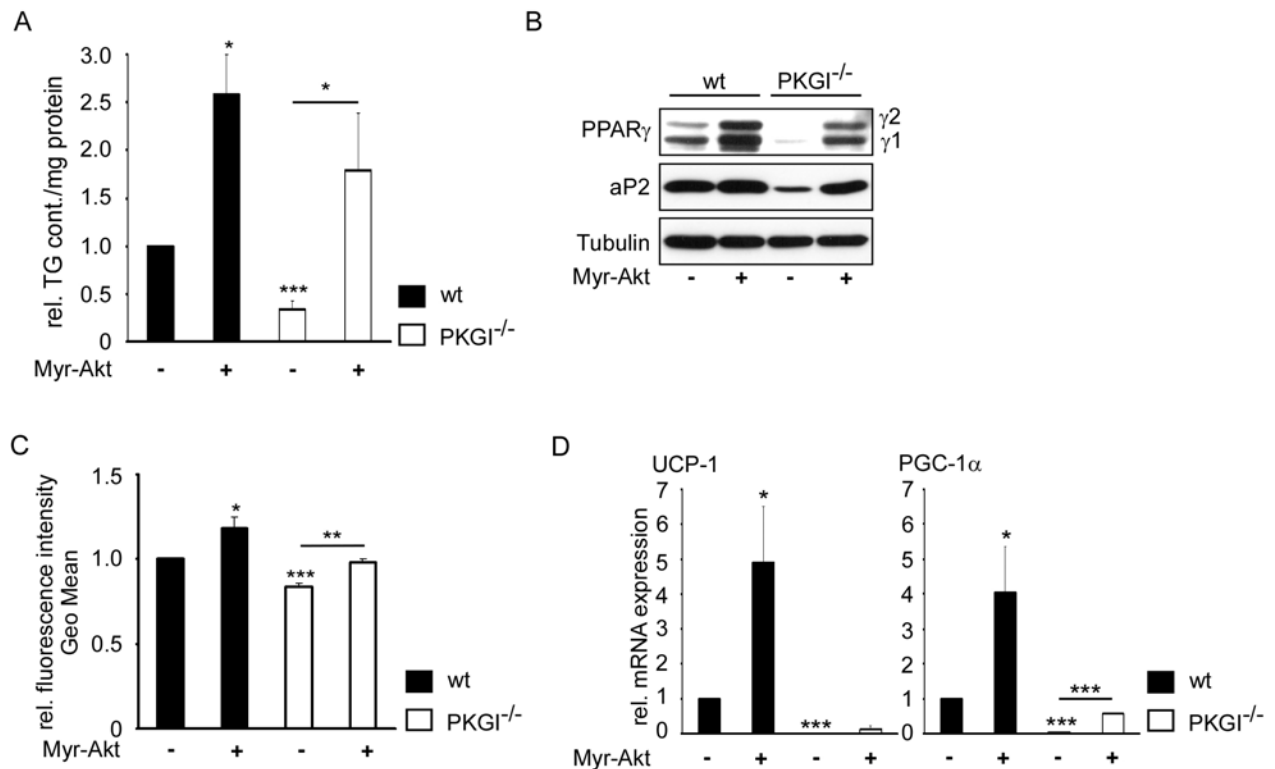


Figure 24. Myristoylated Akt rescues the PKGI^{-/-} phenotype.

(A) TG content normalized to the protein content of the sample of differentiated brown adipocytes of wt and PKGI^{-/-} mice transduced with a viral vector expressing myristoylated Akt (Myr-Akt) as indicated (n=3), untreated wt was set as one. (B) Western blots of PPAR γ and aP2 of differentiated brown adipocytes of wt and PKGI^{-/-} mice transduced with Myr-Akt virus as indicated. (C) Analysis of MitoTracker fluorescence in wt and PKGI^{-/-} cells expressing Myr-Akt as indicated at day 4 of differentiation (n=3), untreated wt was set as one. (D) RQ-PCR analysis of UCP-1 and PGC-1 α expression of differentiated wt and PKGI^{-/-} brown adipocytes infected with Myr-Akt virus as indicated (n=3). HPRT was used as an internal control and values are expressed as fold change, untreated wt was set as one. Data are given as mean \pm s.e.m.; * p < 0.05; ** p < 0.01; *** p < 0.001 compared to untreated wt or PKGI^{-/-}.

3.6. Akt downstream signaling is impaired in PKGI^{-/-} brown adipocytes

Since p38 MAPK and cAMP response element-binding protein (CREB) represent important downstream targets of the insulin/Akt signaling pathway (Valverde et al., 2005) and are known to be required for adipogenesis, mitochondrial biogenesis and UCP-1 expression (Cao et al., 2004; Engelman et al., 1999; Engelman et al., 1998), it was tested whether PKGI also regulates insulin-triggered p38 MAPK and CREB activation. Consistent with a link between PKGI, p38 MAPK and CREB activation, it was found that insulin treatment induced p38 MAPK and CREB phosphorylation to a lesser extent in PKGI^{-/-} cells as compared to wt cells (Figure 25).

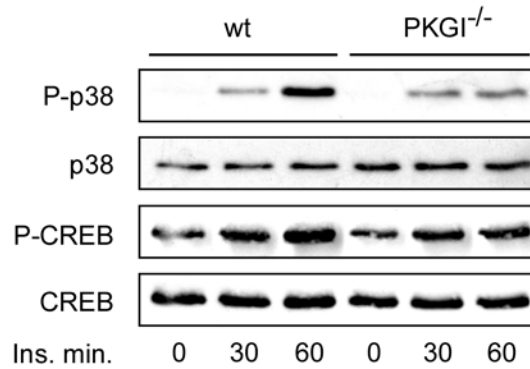


Figure 25. Insulin-induced Akt downstream signaling is impaired in PKGI^{-/-} cells.

Time course of insulin (100 nM) induced p38 MAPK (Thr180/Tyr182) and CREB (Ser133) phosphorylation in serum starved wt and PKGI^{-/-} BAT-MSCs as revealed by immunoblotting with phospho-p38 MAPK and phospho-CREB antibodies. p38 MAPK and CREB immunoblots were performed to control for loading.

p38 MAPK regulates UCP-1 gene transcription through a coordinated activation of nuclear factors on two separate elements (PPRE and CRE2) of the UCP-1 enhancer region (Cao et al., 2004). Expression of caPKGI activated a 3.1 kb UCP-1 promoter fragment by 3 - 4-fold in transient transfection assays in HIB1B preadipocytes and this effect was even more pronounced after insulin treatment (Figure 26A). Additionally, an induction of the PGC-1 α and the PPAR γ 2 promoters by caPKGI was found while the PPAR γ 1 promoter remained unaffected (Figure 26B, C).

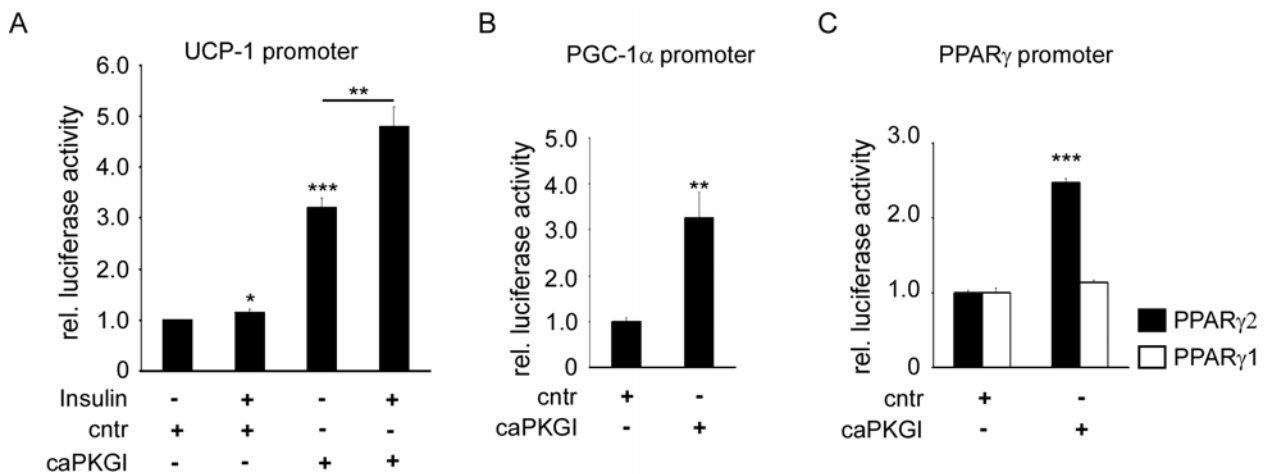


Figure 26. Luciferase reporter assays.

(A) Relative luciferase activity of the UCP-1 promoter (3.1 Kb) in HIB1B preadipocytes transiently transfected with a lentiviral expression vector containing either caPKGI or a control vector containing no transgene (cntr) (n=9), cntr was set as one. After serum starvation cells were incubated with or without 500 nM insulin for 18 hours prior to the assay. (B-C) Relative luciferase activity of the PGC-1 α and PPAR γ promoter in HIB1B preadipocytes transiently transfected with an expression vector containing either caPKGI or cntr (n=6), cntr was set as one. Data are given as mean \pm s.e.m.; * p < 0.05; ** p < 0.01; *** p < 0.001 compared to untreated cntr or caPKGI.

3.7. Brown adipose tissue of PKGI^{-/-} mice exhibits reduced fat accumulation and expression of fat specific markers

Finally, it was analyzed whether PKGI also affects brown fat *in vivo*. Similarly like in cultured BAT-MSCs (Figure 10A) all components of the NO/cGMP signaling cascade were found to be expressed in interscapular BAT of newborn mice (Figure 27A). The expression of PKGI in BAT was further confirmed by Western blot (Figure 27B) and immunohistochemistry (Figure 27C). Importantly, a significantly reduced fat accumulation was observed in interscapular BAT of 1 week old PKGI-deficient mice. Lipid droplets were reduced and smaller in size (Figure 27D).

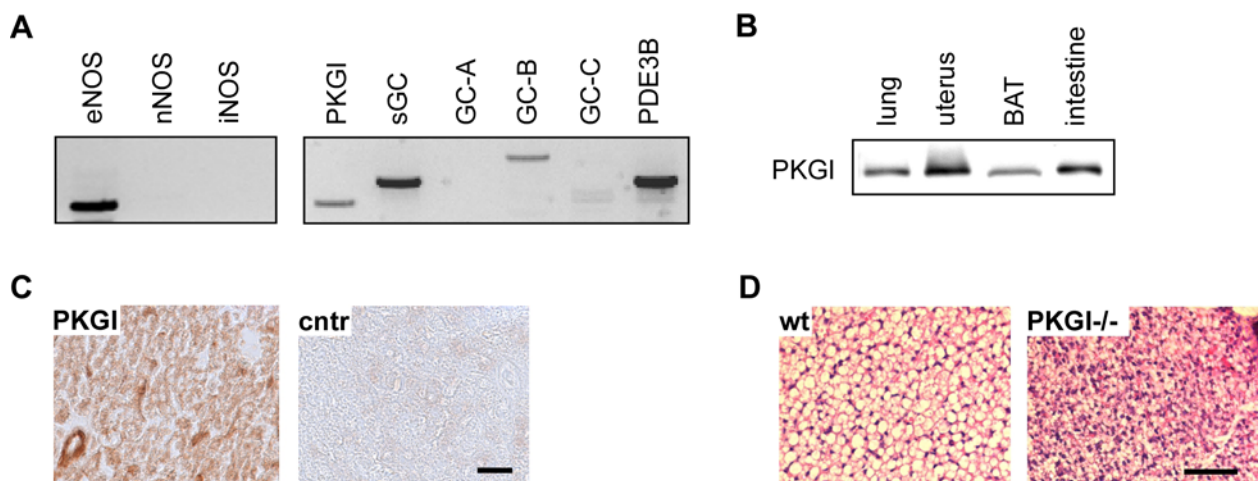


Figure 27. Expression of the NO/cGMP signaling cascade in BAT.

(A) Expression analysis (RT-PCR) of NO-synthases (eNOS, iNOS, nNOS), guanylyl cyclases (sGC, GC-A, GC-B, GC-C) and cGMP receptors (PKGI and PDE3B) in interscapular BAT from new born wt mice. (B) Western blot analysis of the expression of PKGI in BAT as compared to lung, uterus and intestine of wt mice. (C) Immunohistochemical analysis of PKGI expression in BAT isolated from new born wild type mice. Detection of PKGI by immunohistochemistry (polyclonal anti-PKGI staining, brown). Control (right) was incubated with secondary antibody alone; scalebar = 20 μ m. (D) Hematoxylin-eosin staining of paraffin embedded sections (4 μ m) of BAT from one week old wt and PKGI^{-/-} littermates; scalebar = 50 μ m. Note the reduced size and number of lipid droplets in BAT from PKGI^{-/-} mice.

Since loss of PKGI causes insulin resistance with reduced Akt activation in isolated brown adipocytes, also the phosphorylation status of Akt in BAT of PKGI^{-/-} mice and their wt littermates was analyzed. Consistent with the *in vitro* data, reduced levels of phosphorylated Akt were found in BAT of PKGI^{-/-} mice (Figure 28A). Next, adipogenic gene expression in BAT was investigated. PPAR γ protein levels were reduced by $19 \pm 11.2\%$ in BAT of PKGI^{-/-} mice suggesting that PKGI regulates brown fat cell differentiation also *in vivo*. Furthermore, the expression of UCP-1 was significantly lower in BAT of PKGI^{-/-} mice demonstrating that

Results

PKGI also regulates thermogenic gene expression in BAT (Figure 28B). In addition, expression of aP2 and perilipin were reduced by $27 \pm 17\%$ and $64 \pm 21\%$ in BAT of PKGI^{-/-} mice (Figure 28C).

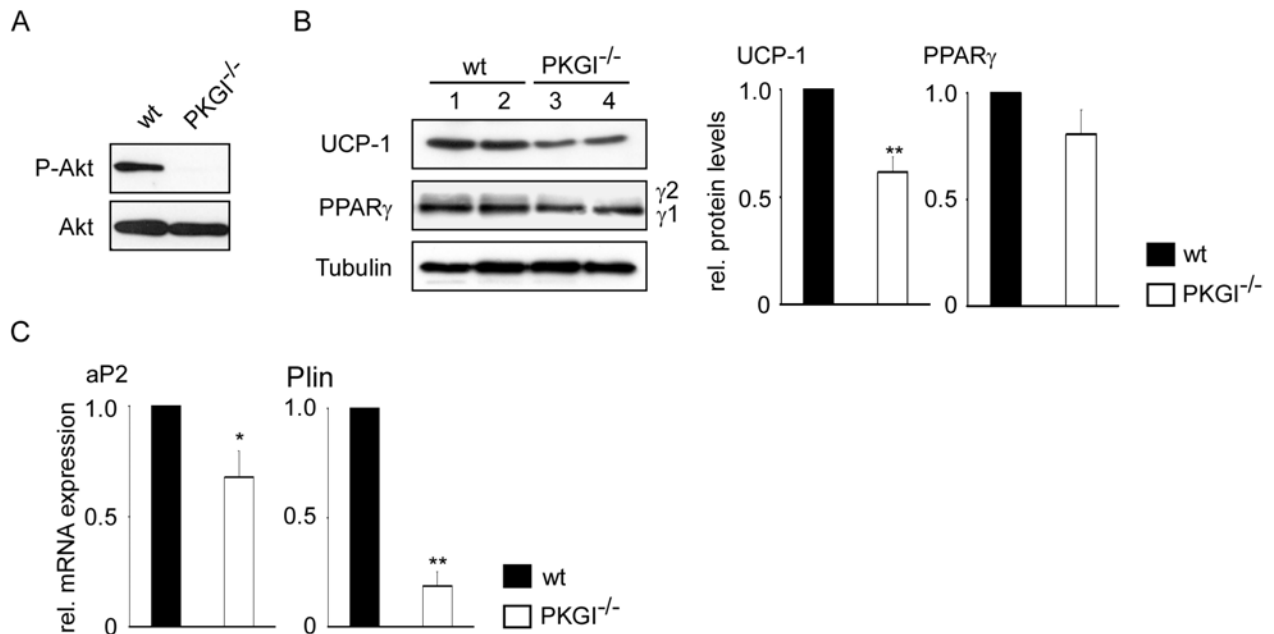


Figure 28. Analysis of PKGI signaling in BAT of PKGI^{-/-} mice.

(A) Western blot analysis of phosphorylation of Akt (Ser473) in wt and PKGI^{-/-} BAT of new born mice. The same membrane was probed with an Akt antibody to control for loading. (B) Western blots showing the expression of UCP-1 and PPAR γ protein levels (left) in BAT isolated from newborn wt and PKGI^{-/-} mice (lane 1 and 2 wt mice, lane 3 and 4 PKGI^{-/-} mice, littermates). Tubulin Western blot was performed to control for loading. Densitometric analysis of the expression of UCP-1 and PPAR γ protein levels (right) normalized to the expression of tubulin (n=7 wt and PKGI^{-/-} mice). (C) RQ-PCR analysis of aP2 and perilipin in BAT of wt and PKGI^{-/-} mice (n=7 wt and PKGI^{-/-} mice). HPRT was used as an internal control and values are expressed as fold change, wt was set as one. Data are given as mean \pm s.e.m.; * p < 0.05; ** p < 0.01 compared to wt.

4. Discussion

4.1. NO/cGMP effects on mitochondrial biogenesis and thermogenesis

The recent finding that NO/cGMP can regulate mitochondrial biogenesis (Nisoli et al., 2003) raised the question about the downstream signaling cascade activated by cGMP. The cAMP/PKA signaling pathway in BAT is well characterized and is a major regulator of BAT thermogenesis. The cAMP pathway is activated by the sympathetic nervous system (Cannon and Nedergaard, 2004). A major mediator of cAMP effects is PKA, the prototypic serine/threonine protein kinase (Su et al., 1995). Through phosphorylation of various target enzymes, the activated PKA mediates adrenergic effects (also see Figure 3): 1) PKA phosphorylates and activates the transcription factor CREB in BAT (Thonberg et al., 2002). CREB then binds to cAMP-response elements (CREs) on the UCP-1 promoter and activates its expression (Cao et al., 2004). 2) HSL activity can be positively regulated by adrenergic stimulation via PKA leading to lipolysis and the release of free fatty acids (Shih and Taberner, 1995), which in turn promote UCP-1 activation (Matthias et al., 2000). 3) p38 MAPK is activated by PKA subsequently leading to the activation and phosphorylation of PGC-1 α and CREB (Cao et al., 2004), the main transcription factors involved in regulation of mitochondrial biogenesis and UCP-1 expression.

NO and cGMP have been shown to increase PGC-1 α and UCP-1 expression in isolated brown adipocytes (Nisoli et al., 2003; Nisoli et al., 1998). *In vivo* experiments on eNOS-deficient mice showed that these mice, when fed at normal chow diet, exhibited increased body weight as compared to their wt littermates (Nisoli et al., 2003). These findings implicate that eNOS-deficient mice have reduced energy expenditure that can lead to obesity. However, the underlying mechanisms of NO/cGMP-induced thermogenesis remain still unclear.

4.2. Potential cGMP-activated signaling pathways

The analysis of the cGMP signaling molecules in BAT clearly showed that PKGI and PDE3B are expressed in murine brown adipocytes. Given the recent findings and the important role of the cAMP signaling cascade in BAT, three scenarios for cGMP signaling in brown adipocytes were possible (Figure 29):

- 1) cGMP cross activates PKA what would lead to the above described effects on thermogenesis and lipolysis. *In vitro* studies in muscle cells (Chao et al., 1994; Jiang et al., 1992; Lincoln et al., 1990) led to the hypothesis of a cross-talk between the cGMP and cAMP signaling cascades at the level of cyclic nucleotide-dependent protein kinases, i.e. cross-activation of PKGI by cAMP, or vice versa. Thus, high cGMP levels in BAT might directly activate PKA. This hypothesis was further supported by biochemical analyses which showed that autophosphorylation of PKGI lowers cyclic nucleotide concentrations needed for activation (Landgraf et al., 1986; Smith et al., 1996).

- 2) cGMP regulates PDE3B leading to indirect activation of the cAMP/PKA cascade. PDE3B has high affinities to both cAMP and cGMP (K_m values between 0.1 - 0.8 μ M). However, the V_{max} for cAMP is 4 -10 times higher than that for cGMP which is hydrolyzed poorly by PDE3B (Conti et al., 1995; Manganiello et al., 1995). As cAMP and cGMP are competitive substrates, high cGMP concentrations lead to inhibition of cAMP hydrolysis by PDE3B. PDE3B is the predominant isoform expressed in white and brown fat and activation of PDE3B is a major mechanism by which insulin antagonizes cAMP-induced lipolysis (Degerman et al., 1997). Inhibition of PDE3B by cGMP could result in increased cAMP levels and activation of PKA, which on one hand could lead to enhanced mitochondrial biogenesis and on the other hand to increased lipolysis.

- 3) cGMP directly activates PKGI. PKGI has been shown to be the mediator of NO/cGMP effects in the cardiovascular system including vascular smooth muscles and platelets (Pfeifer et al., 1998; Pfeifer et al., 1999). So far, not much was known about potential roles of PKGI in metabolism and fat cells. A recent study by (Sengenès et al., 2003) indicated that in WAT the ANP-induced lipolysis is mediated by PKGI.

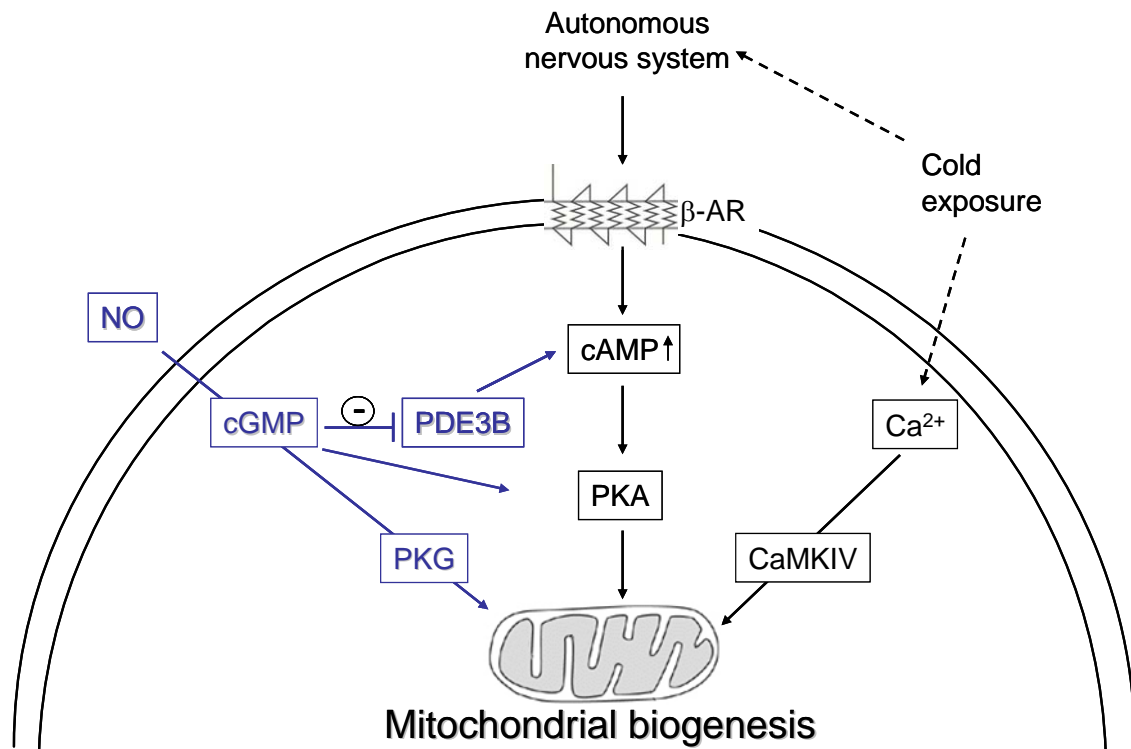


Figure 29. Possible scenarios for cGMP signaling in BAT.

4.3. cGMP effects on mitochondrial biogenesis and UCP-1 expression are mediated by PKGI

This study clearly establishes a cGMP/PKGI signaling pathway in BAT that controls brown adipocyte mitochondrial biogenesis and thermogenesis. Using constitutive and conditional PKGI knock out mice as well as lentiviral vectors to overexpress PKGI in brown adipocytes, it could be demonstrated that NO/cGMP effects in BAT are indeed mediated by PKGI. PKGI-deficient cells had lower mitochondrial contents and mitochondria were smaller in size. Additionally, incubation with cGMP only increased mitochondrial biogenesis in wt cells, but had no effect in the mutant cells. Similarly, RQ-PCR and Western blot analysis of PGC-1 α and UCP-1 expression demonstrated that both are induced by cGMP only in the presence PKGI. Expression of constitutively active PKGI in wt cells increased mitochondrial biogenesis to a similar extend as cGMP treatment, emphasizing the role of PKGI in mediating cGMP effects in brown adipocytes. These data underline the unique role for PKGI in mediating NO/cGMP effects in BAT. Taken together my findings could rule out other, indirect cGMP signaling mechanisms that are based on cross activation of the cAMP/PKA pathway as discussed under 4.2 points 1) and 2).

So far the major focus of the analysis of the physiological role of PKGI was on the cardiovascular and neuronal system. In the present work, a novel function of PKGI in the regulation of mitochondrial biogenesis and function was identified. Preliminary experiments using HeLa and HEK293-T cells indicate that this function of PKGI might not be restricted to brown adipocytes.

4.4. PKGI is necessary for brown fat cell differentiation

An important question addressed in the present thesis was whether the effects of PKGI in brown adipocytes are restricted to regulation of mitochondrial biogenesis and UCP-1 expression. Recent studies on PGC-1 α -deficient cells demonstrated that thermogenesis and brown fat differentiation (adipogenesis) can be differentially regulated (Uldry et al., 2006). Despite the lack of PGC-1 α , the mutant cells differentiated normally and accumulated fat, indicating that two independent programs driving mitochondrial biogenesis and adipogenesis in BAT exist. Given these findings, differentiation of PKGI-deficient cells was analyzed. Surprisingly, despite low mitochondrial contents and UCP-1 levels of PKGI-deficient cells, reduced lipid accumulation and TG contents during differentiation were observed. For a detailed characterization of the PKGI-null phenotype the global and metabolic transcriptional response to cGMP was analyzed. To this end, microarray analysis was performed of RNA isolated from differentiated wt and PKGI^{-/-} brown adipocytes. This CHIP analysis revealed a strong down-regulation of metabolic and differentiation-related genes pointing to a pivotal role of PKGI not only on mitochondrial biogenesis but also on BAT differentiation. Expression of genes involved in lipid, energy, carbohydrate and other metabolism were down-regulated by 87%, 82%, 80% and 64%, respectively in PKGI-deficient cells. To complement the CHIP data, further experiments were performed to analyze the differentiation defect of PKGI-deficient cells. Using RQ-PCR and Western blotting, the down-regulation of a large number of adipogenic and metabolic genes was confirmed. Among these were such important regulators of adipogenesis like PPAR γ , aP2, Cidea or HSL. Thus, the cGMP effects on PKGI are not only restricted to induction of the thermogenic but also to the regulation of the adipogenic program.

4.5. PKGI at the cross-roads of three signaling pathways

The search for the signaling pathway downstream of PKGI discovered an interaction of the cGMP/PKGI pathway with the insulin signaling cascade. Insulin has an outstanding importance for normal development of fat cells. The main pathway involved in adipogenesis and thermogenesis is the insulin IRS-1/PI3K/Akt cascade (Valverde et al., 2005).

In the present study, I identified a crosstalk between the NO/cGMP/PKGI signaling cascade, the RhoA/ROCK pathway and insulin signaling in brown adipocytes, which controls both cell differentiation and the thermogenic program. Several lines of evidence presented herein suggest that PKGI enhances insulin signaling in brown adipocytes through antagonizing the inhibitory effects of the RhoA/ROCK pathway. Previous work in smooth muscle cells provides evidence that phosphorylation of RhoA at Ser188 by PKGI induces translocation from membranes to the cytosol, enhances Rho GDP-dissociation inhibitor (RhoGDI) binding and, thereby, inactivates RhoA (Sawada et al., 2001). Analysis of RhoA-GTP levels using rhotekin pull down assays for the detection of active GTP-bound RhoA revealed that PKGI-deficient cells exhibited increased RhoA activity. Furthermore, expression of a dominant negative RhoA mutant as well as inhibition of ROCK, which is a major downstream effector of RhoA (Wojciak-Stothard and Ridley, 2003), rescued both the adipogenic differentiation as well as the thermogenic program in PKGI-deficient cells. ROCK has been shown to negatively regulate insulin signaling in 3T3-L1 white adipocytes and mouse embryonic fibroblasts (Noguchi et al., 2007; Sordella et al., 2003) by increasing phosphorylation of IRS-1 at serine residues (Furukawa et al., 2005). Studies on IRS-1-deficient cells have shown that the IRS-1/PI3K/Akt pathway plays an important role in brown fat cell differentiation and thermogenic gene expression. IRS-1 is upstream of PPAR γ and C/EBP α (Valverde et al., 2005). Interestingly, IRS-1 has been suggested to be also the major mediator of insulin effects in human WAT, because its expression is reduced in patients with type-2 diabetes mellitus (Rondinone et al., 1997). Type-2 diabetes is a complex metabolic disease that occurs when insulin secretion can no longer compensate insulin resistance in peripheral tissues (DeFronzo, 1997). At the molecular level, insulin resistance correlates with impaired insulin signaling. Increased IRS-1 serine phosphorylation is one of the major mechanisms thought to be responsible for insulin resistance (Hotamisligil et al., 1996; Sykiotis and Papavassiliou, 2001). However, conflicting results have been published on the effect of RhoA/ROCK on IRS-1 signaling. Both ROCK-dependent inhibition (Noguchi et al., 2007; Sordella et al., 2003) via IRS-1 serine phosphorylation as well as activation of the IRS-1/PI3K/Akt cascade via ROCK have been described for 3T3-L1 white adipocytes (Furukawa et al., 2005).

In PKGI-deficient BAT-MSCs, we found increased ser636/639 phosphorylation of IRS-1, and IRS-1 was found to be less tyrosine phosphorylated after insulin treatment as compared to wt controls. Importantly, immunoprecipitation assays of IRS-1 demonstrated a diminished association of the regulatory subunit p85 α of PI3K to IRS-1. Reduced p85 α association leads to reduced PI3K activity and, therefore, to diminished downstream substrate activation. One of the major PI3K downstream targets is the kinase Akt/PKB. I found reduced activation of Akt, i.e. reduced levels of Ser473 phosphorylated Akt after insulin treatment in the mutant cells. Furthermore, treatment with the ROCK inhibitor Y-27632 rescued Insulin-induced Akt activation showing that RhoA/ROCK signaling is linked to the insulin pathway in brown adipocytes. In addition, PKGI-deficient cells had reduced levels of phosphorylated p38 MAPK and CREB, two important downstream targets of IRS-1/PI3K/Akt, which are regulators of PGC-1 α and UCP-1 expression as well as inducers of adipogenic differentiation (Cao et al., 2004; Engelman et al., 1999; Engelman et al., 1998). Most importantly, myristoylated Akt that is constitutively active rescued the brown fat cell differentiation defect, as measured by TG content and marker gene expression, as well as the thermogenic phenotype of PKGI-deficient cells. Luciferase reporter assays in the HIB1B brown preadipocyte cell line revealed a significant enhancement of UCP-1 promoter activity by insulin after cotransfection with constitutively active PKGI. Thus, showing that PKGI effects are not only restricted to one cell line.

Taken together my data show that the NO/cGMP signaling cascade is linked to the insulin signaling pathway through RhoA/ROCK, thereby, placing PKGI functions at the cross-roads of three signaling systems: The NO/cGMP signal activates PKGI, which in turn inhibits the small GTPase RhoA and the RhoA downstream effector ROCK. ROCK inhibits the insulin signaling cascade in brown adipocytes. Thus, inhibition of RhoA/ROCK by PKGI leads to enhanced insulin-dependent activation of PI3K and Akt/PKB (Figure 30). Consequently, loss of PKGI leads to insulin resistance and prohibits expression of a genetic program finally resulting in normal brown fat cell differentiation.

4.6. Role of PKGI in BAT *in vivo*

PKGI-deficient mice were crucial for the analysis of the cardiovascular functions of PKGI. PKGI-deficient mice display a severe cardiovascular and intestinal phenotype due to impaired smooth muscle relaxation (Pfeifer et al., 1998). In addition, PKGI has also been implicated in regulation of platelet aggregation (Gambaryan et al., 2004; Marshall et al., 2004; Massberg et

al., 1999). The PKG-deficient mice were also valuable for analysis of the function of PKGI in BAT.

I analyzed the NO/cGMP signaling cascade expressed in BAT. Histological analysis of PKGI-deficient BAT revealed reduced lipid accumulation and lipid droplets were smaller in size. More detailed analysis of PKGI-deficient BAT showed that, according to the cell culture findings, UCP-1 and adipogenic marker expression was significantly reduced. Given the finding of insulin resistance of PKGI-deficient brown adipocytes (4.5) the Akt phosphorylation status in BAT was investigated. Akt phosphorylation (Ser473) was barely detectable in BAT of PKGI-deficient mice, which is in sharp contrast to wt mice, leading to the conclusion that insulin signaling is also disturbed *in vivo*.

An important point for the *in vivo* studies is the plethora of phenotypes including intestinal dysfunction, because of disturbed motility, observed in PKGI-deficient mice. Therefore, the conditional PKGI knock out mice are a valuable tool that will be used in future studies. Using transgenic mice carrying an UCP-1 driven Cre-recombinase, one could obtain mice with a BAT-specific ablation of PKGI. Our group already obtained UCP-1 Cre-deleter mice however, the transgenic UCP-1-Cre/PKGI^{fl/fl} mouse line did not express Cre-recombinase in BAT.

5. Summary

A hallmark of BAT is its ability to increase energy expenditure through thermogenesis, which is mediated by the expression of UCP-1. Induction of UCP-1 expression via the transcriptional coactivator PGC-1 α is stimulated by external stimuli such as food intake and changes in temperature. Food intake and exposure to cold induce sympathetic activation and the release of NA which, in turn, activates adrenergic receptors on brown fat cells. Another pathway leading to mitochondrial biogenesis and thermogenesis has recently been identified; NO has been demonstrated to induce mitochondrial biogenesis in brown adipose tissue through cGMP-dependent mechanisms (Nisoli et al., 2003; Nisoli et al., 1998). In addition, calorie restriction induces eNOS expression in a variety of tissues including fat (Nisoli et al., 2005).

The data presented in this study identify the role of PKGI in NO/cGMP-induced regulation of mitochondrial biogenesis and differentiation of BAT. Initially, several signaling molecules that form the NO/cGMP signaling cascades including PDE3B and PKGI were identified in BAT-MSCs. Differentiation of BAT-MSCs into brown adipocytes showed that PKGI-deficient cells had reduced mitochondrial contents. Furthermore, levels of PGC-1 α and UCP-1 were significantly reduced in PKGI-deficient cells. Conversely, expression of a constitutively active PKGI during differentiation in wt BAT-MSCs and pharmacological treatment with cGMP had the opposite effects. Thus far, it was not clear whether cGMP regulates brown adipocyte differentiation. Low UCP-1 levels and mitochondrial content should lead to reduced energy expenditure, however, differentiated PKGI-deficient cells accumulated less lipids and had reduced TG contents. Therefore, the signaling molecules downstream of PKGI were analyzed. Loss of PKGI in BAT-MSCs led to increased RhoA activity. PKGI-deficient cells exhibited increased levels of active GTP-bound RhoA, due to loss of RhoA inhibition by PKGI. Expression of a dominant-negative version of RhoA as well as pharmacological inhibition with Y-27632 of the RhoA downstream effector ROCK rescued brown adipogenesis and brown adipogenic marker expression during differentiation of PKGI-deficient BAT-MSCs. I addressed the question how RhoA can regulate BAT mitochondrial biogenesis and differentiation. Loss of PKGI led to reduced insulin-induced activation of the IRS-1/PI3K/Akt signaling cascade, a major pathway involved in brown adipogenesis (Lorenzo et al., 1993; Teruel et al., 1996), which has been shown to be modulated by RhoA/ROCK in 3T3-L1 cells and MEFs (McBeath et al., 2004; Sordella et al., 2003). Analysis of the phosphorylation status of IRS-1 revealed that inhibitory serine residues

(ser636/639) were hyperphosphorylated in BAT-MSCs of PKGI-deficient mice. As a consequence, insulin-induced activation of IRS-1 by tyrosine phosphorylation and PI3K p85 α subunit association were diminished. The PI3K downstream target Akt was found to be less activated after insulin stimulation in BAT-MSCs of PKGI-deficient mice. Importantly, treatment with the ROCK inhibitor Y-27632 reduced the loss of activation of the kinase. Further analysis showed that expression of a constitutively active myristoylated Akt restored brown fat cell differentiation, mitochondrial biogenesis and brown fat specific marker expression in PKGI-deficient BAT-MSCs. In addition, the Akt downstream effectors p38 MAPK and CREB, which are known to be required for adipogenesis and mitochondrial biogenesis (Cao et al., 2004; Engelman et al., 1999), were less activated in PKGI-deficient BAT-MSCs after insulin treatment. Consistently with these findings, luciferase reporter assays with brown preadipocytes transiently transfected with caPKGI showed increased UCP-1, PGC-1 α and PPAR γ 2 promoter activations.

Finally, the role of PKGI was analyzed *in vivo*. Similar to cultured BAT-MSCs, all components of the NO/cGMP signaling cascade were expressed in interscapular BAT of newborn mice. Analysis of BAT revealed that Akt phosphorylation was barely detectable in BAT of PKGI-deficient mice, which is in sharp contrast to wt mice. Consistent with the *in vitro* data, lipid accumulation, expression of UCP-1 and adipogenic markers was reduced in PKGI-deficient BAT.

In summary these data show, that PKGI is essential for brown fat thermogenesis as well as brown adipocyte differentiation and plays a permissive role in insulin signaling *in vitro* and *in vivo* (Figure 30).

The cGMP/PKGI pathway plays an outstanding role in cardiovascular physiology and pharmacology (Ignarro et al., 2002; Munzel et al., 2003; Murad, 2006; Pfeifer et al., 1998; Pfeifer et al., 1999) including blood pressure regulation and thrombocyte aggregation. Given the recent finding that adult humans possess metabolically active BAT (Nedergaard et al., 2007), the cGMP/PKGI pathway might, thereby, serve as a novel therapeutic target in obesity-related cardiovascular and metabolic disorders like type-2 diabetes.

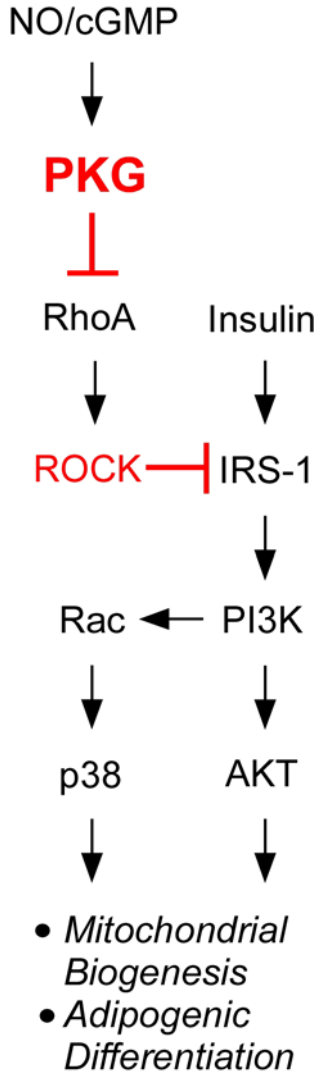


Figure 30. Scheme depicting the cross talk of PKGI with the RhoA and insulin pathways in brown fat cells.

6. Appendix

Table 3. Whole genome DNA chip results. Top 30 genes up-regulated in wt vs PKGI^{-/-} mice (+cGMP), sorted according to (putative) function and magnitude of induction. Gene function was derived from information in the CoreNucleotide or OMIM database (www.ncbi.nlm.nih.gov) unless otherwise indicated.

Nr	Abbrev	Sequence Name	Accession	Fold Change	Description
Genes with a specific function in adipocytes and/or metabolism					
1	Acvr1c	activin A receptor, type 1C	NM_001033369	86.58459	receptor for activin A and activin B; known as a marker for adipocyte differentiation; Activins are pleiotropic growth factors with a broad tissue distribution
2	Fabp4	fatty acid binding protein 4, adipocyte	NM_024406	78.40028	also called aP2; known to be induced during adipocyte differentiation
3	Cfd	complement factor D (adipsin)	NM_013459	78.24822	adipsin is a serine protease that is secreted by adipocytes into the bloodstream. It is deficient in several animal models of obesity
4	Cidec	cell death-inducing DFFA-like effector c	NM_178373	48.84889	closely related to Cidea (see below); Cidec is an adipocyte lipid droplet protein that negatively regulates lipolysis and promotes triglyceride accumulation.
5	Gpd1	glycerol-3-phosphate dehydrogenase 1 (soluble)	NM_010271	40.47907	metabolic enzyme
6	S3-12	plasma membrane associated protein, S3-12	NM_020568	37.2589	coat protein for newly synthesized triacylglycerol vesicles
7	Adipoq	adiponectin, C1Q and collagen domain containing	NM_009605	35.00502	hormone secreted by adipocytes that regulates energy homeostasis and glucose and lipid metabolism; shares significant similarity to collagens X and VIII
8	Pnpla3	patatin-like phospholipase domain containing 3	NM_054088	30.67456	also called adiponutrin, a transmembrane protein corresponding to a dietary- and obesity-linked mRNA
9	Rbp4	retinol binding protein 4, plasma	NM_011255	26.87439	experiments suggest that RBP4 causes insulin resistance, the underlying mechanisms is not fully understood
10	Pck1	phosphoenolpyruvate carboxykinase 1, cytosolic	NM_011044	25.043	Pck1 is a main target for regulation of gluconeogenesis
11	Lep	leptin	NM_008493	24.88337	hormone regulating energy homeostasis
12	Slc36a2	solute carrier family 36 (proton/amino acid symporter), member 2	NM_153170	24.53498	transporter that actively exports neutral amino acids from lysosomes
13	Lgals12	lectin, galactose binding, soluble 12	NM_019516	24.37544	lectin, galactose binding, required for adipogenic signaling and adipocyte differentiation
14	Ucp1	uncoupling protein-1 (mitochondrial, proton carrier)	NM_009463	21.99985	enables thermogenesis in BAT
15	Plin	perilipin	NM_175640	21.75883	results of studies with Plin KO mice demonstrate a role in reining basal HSL activity and regulating lipolysis and energy balance
16	Acs11	acyl-CoA synthetase long-chain family member 1	NM_007981	19.57816	metabolic enzyme
17	Apoc1	apolipoprotein C-I	NM_007469	19.11507	thought to be involved in atherogenesis like apolipoprotein E

18	Klb	klotho beta	NM_031180	19.06122	co-factor required for FGF (fibroblast growth factor)-21 and -23 binding to FGF receptors; Klb also regulates bile acid secretion
19	Tshr	thyroid stimulating hormone receptor	NM_011648	18.27109	hormone receptor
20	Cidea	cell death-inducing DNA fragmentation factor, alpha subunit-like effector A	NM_007702	18.00561	highly expressed in BAT; Cidea-null mice have higher metabolic rates, lipolysis, and core body temperature during cold treatment. They are lean and resistant to diet-induced obesity/diabetes

Other genes

1	Xist	Mouse nuclear-localized inactive X-specific transcript	L04961	64.26028	involved in X chromosome inactivation; no specific role in adipocytes known
2	Aqp7	aquaporin 7	AB010100	43.25714	no specific function in adipocytes known
3	Car3	carbonic anhydrase 3	NM_007606	38.48983	enzyme involved in CO ₂ /carbonate handling; Car3 is mainly expressed in skeletal muscle and has lower enzyme activity than the other isoforms; no specific function in adipocytes known
4	Otop1	otopettrin 1	NM_172709	36.17683	membrane protein; expressed in the developing inner ear; function in adipocytes not known
5	Orm1	orosomuroid 1	NM_008768	26.87725	loss leads to deafness; role in adipocytes unknown
6	Mrap	melanocortin 2 receptor accessory protein	NM_029844	23.77011	mutations cause familial glucocorticoid deficiency
7	H60	histocompatibility 60	NM_010400	22.87177	immunologic functions; no specific role in adipocytes described
8	Orm2	orosomuroid 2	NM_011016	17.9898	no specific function in adipocytes known
9	Mup1	major urinary protein 1	NM_031188	17.53765	no specific function in adipocytes known
10	Fgf10	fibroblast growth factor 10	NM_008002	17.17731	ligand of FGF receptor 2b; mutations of FGF receptor 2 cause Apert syndrome (disturbed limb development, craniofacial abnormalities)

Table 4. Whole genome DNA chip results. Top 30 genes down-regulated in wt vs PKGI^{-/-} mice (+cGMP), sorted according to (putative) function and magnitude of induction. Gene function was derived from information in the CoreNucleotide or OMIM database (www.ncbi.nlm.nih.gov) unless otherwise indicated.

Nr	Abbrev	Sequence Name	Accession	Fold Change	Description
Genes (putatively) involved in cartilage / bone development					
1	C1qtnf3	C1q and tumor necrosis factor related protein 3	NM_030888	-21.80621	also called cartducin; structurally similar to adiponectin; reported to play a role in chondrogenic differentiation
2	Cart1	cartilage homeo protein 1	NM_172553	-18.18627	involved in chondrogenesis during embryonic development
3	Cpxm2	carboxypeptidase X 2 (M14 family)	NM_018867	-15.89631	specific function unknown; a closely related protein (carboxypeptidase 1) was reported to be highly expressed in fetal primordial cartilage and skeletal structures
4	Hoxa11	homeo box A11	NM_010450	-14.58918	required to globally pattern the mammalian skeleton
5	Myf5	myogenic factor 5	NM_008656	-11.47078	targeted inactivation Myf-5 results in abnormal rib development
6	Barx1	BarH-like homeobox 1	NM_007526	-11.26572	involved in the development of head and neck
7	Col8a1	procollagen, type VIII, alpha 1	NM_007739	-10.47507	expressed in skin, endothelium, eye lens and in mesenchymal cells surrounding cartilage and calvarial bone
8	Ctgf	connective tissue growth factor	NM_010217	-10.03685	involved in secondary ossification
Other developmental genes					
1	Pax6	paired box gene 6	BC036957	-11.9885	involved in eye development
2	Dppa3	developmental pluripotency-associated 3	NM_139218	-10.53046	involved in germ cell development
3	Isl1	ISL1 transcription factor, LIM/homeodomain	NM_021459	-9.00521	involved in the development of endocrine cells, heart and retina
Signaling					
1	Prkg2	protein kinase, cGMP-dependent, type II (PKGII)	NM_008926	-21.80695	PKGII is highly concentrated in brain, lung, and intestinal mucosa and mediates intestinal water and electrolyte secretion; up-regulated in PKGI ^{-/-} mice to partly compensate the loss of PKGI
2	Asb5	ankyrin repeat and SOCs box-containing protein 5	NM_029569	-18.13529	Asb proteins function as suppressors of cytokine signaling
3	Jakmip2	janus kinase and microtubule interacting protein 2, transcript variant 1	XM_129010	-13.09763	involved in intracellular signaling; specific function not known
4	Iqsec3	IQ motif and Sec7 domain 3	NM_001033 354	-11.6672	function not known, probably involved in intracellular signaling since it contains a Sec7 domain (found in guanine-nucleotide-exchange factors) and a PH domain (found on many cellular signaling proteins)
5	Il5ra	interleukin 5 receptor, alpha	NM_008370	-10.0924	cytokine receptor; no specific function in adipocytes known
6	Npy6r	neuropeptide Y receptor Y6	NM_010935	-9.68283	receptor for intestinal peptides
7	ORF63	open reading frame 63	NM_144854	-8.20289	structurally similar to TGF-beta-activated kinase

Other genes					
1	Msln	mesothelin	NM_018857	-9.84161	may play a role in cellular adhesion
2	Perp	TP53 apoptosis effector	NM_022032	-9.69898	target of the tumour suppressor gene p53; no specific function in adipocytes known
3	Slc1a6	solute carrier family 1 (high affinity aspartate/glutamate transporter), member 6	NM_009200	-9.35135	no specific function in adipocytes known
4	Glrb	glycine receptor, beta subunit	NM_010298	-9.18247	neurotransmitter receptor in the CNS; no specific function in adipocytes known
5	Rab27b	RAB27b, member RAS oncogene family	NM_030554	-8.93891	involved in exocytosis; no specific function in adipocytes known
6	Tcra	SJL-7A5 T cell receptor alpha chain	U07662	-8.82356	immunologic function; no specific function in adipocytes known
7	C85627	expressed sequence C85627	NM_001033	-8.60155	function not known
			794		
8	Car8	carbonic anhydrase 8	NM_007592	-8.51432	seems to play an important role in the cerebellum; no specific function in adipocytes known
9	Ccdc68	coiled-coil domain containing 68	NM_201362	-8.30616	function not known
10	Grik1	glutamate receptor, ionotropic, kainate 1	NM_146072	-8.14363	neurotransmitter receptor in the CNS; no specific function in adipocytes known
11	Gjb2	gap junction membrane channel protein beta 2	NM_008125	-8.00103	no specific function in adipocytes known
12	Olr1	oxidized low density lipoprotein (lectin-like) receptor 1	NM_138648	-7.64712	role in atherogenesis if expressed on vascular cells; no specific function in adipocytes known

7. Curriculum vitae

Name: Bernd-Bodo Haas
Geburtsdatum: 15. Oktober 1976
Geburtsort: Erbach
Staatsangehörigkeit: deutsch
Familienstand: verheiratet

Schulausbildung:

1983 - 1987 Grundschule Michelstadt
1987 - 1989 Förderstufe (Theodor-Litt-Schule Michelstadt)
1989 - 1996 Gymnasium Michelstadt
Abschluss: Abitur

Zivildienst:

1996 - 1997 Odenwaldklinik, Bad-König

Studium:

Oktober 1997 Beginn des Studiums der Pharmazie an der Universität Heidelberg
März 2000 Abschluss des 1. Staatsexamens
April 2002 Abschluss der 2. Staatsexamens
Mai 2002 - November 2002 1. Teil des praktischen Jahres bei Merck, Mexiko-Stadt, Mexiko
November 2002 - April 2003 2. Teil des praktischen Jahres in der Stern-Apotheke, Heidelberg
Juni 2003 Abschluss des 3. Staatsexamens
August 2003 Approbation als Apotheker

Wissenschaftliche Tätigkeiten:

Juni - August 2000 Forschungspraktikum an der School of Pharmacy, University of London, Thema: "*Isoform expression of PKA during development in rat brain*"

Curriculum vitae

- März 2001 - April 2001 Forschungspraktikum am Centro de Investigación Biomedica de Occidente, IMSS, Guadalajara, Mexiko
- Dezember 2003 - August 2006 Wissenschaftlicher Mitarbeiter am Zentrum für Pharmaforschung, Department Pharmazie der Ludwig-Maximilians-Universität in München
- September 2006 - Juli 2008 Wissenschaftlicher Mitarbeiter am Institut für Pharmakologie und Toxikologie der Rheinischen Friedrich-Wilhelm Universität Bonn

München, den 04.06.2008

8. Publications and Abstracts

8.1. Publications

Haas B, Mayer P, Jennissen K, Ahmad M, Berriel Diaz M, Bloch W, Herzig S, Fässler R & Pfeifer A (2008)

Protein Kinase G Controls Insulin-Induced Brown Fat Cell Differentiation and Mitochondrial Biogenesis - submitted

Massoumi R, Kuphal S, Hellerbrand C, **Haas B**, Wild P, Spruss T, Pfeifer A, Fässler R & Bosserhoff AK (2008)

Downregulation of CYLD expression by Snail promotes tumor progression in malignant melanoma - submitted

8.2. Abstracts

Haas B, Jennissen K, Pfeifer A (2008)

Protein kinase G regulates differentiation of mesenchymal stem cells

Frühjahrstagung der DGPT, March 2008, Mainz; Naunyn Schmiedebergs Arch. Pharmacol. 2008 Mar; 377 (Suppl. 1): 72

Syttkus B, **Haas B**, Hofmann A, Pfeifer A (2008)

Analysis of microRNA effects on MSC differentiation to adipocytes

Frühjahrstagung der DGPT, March 2008, Mainz; Naunyn Schmiedebergs Arch. Pharmacol. 2008 Mar; 377 (Suppl. 1): 309

Haas B, Hennecke K, Fässler R, Pfeifer A (2007)

Role of cGMP in mesenchymal stem cell differentiation

Bonner Forum Biomedizin - Semester Meeting - February 2007, Bad Breisig

9. References

- Alioua, A., Tanaka, Y., Wallner, M., Hofmann, F., Ruth, P., Meera, P., and Toro, L. (1998). The large conductance, voltage-dependent, and calcium-sensitive K⁺ channel, Hslo, is a target of cGMP-dependent protein kinase phosphorylation in vivo. *J Biol Chem* 273, 32950-32956.
- Arancio, O., Kandel, E.R., and Hawkins, R.D. (1995). Activity-dependent long-term enhancement of transmitter release by presynaptic 3',5'-cyclic GMP in cultured hippocampal neurons. *Nature* 376, 74-80.
- Aszodi, A., Pfeifer, A., Ahmad, M., Glauner, M., Zhou, X.H., Ny, L., Andersson, K.E., Kehrel, B., Offermanns, S., and Fassler, R. (1999). The vasodilator-stimulated phosphoprotein (VASP) is involved in cGMP- and cAMP-mediated inhibition of agonist-induced platelet aggregation, but is dispensable for smooth muscle function. *EMBO J* 18, 37-48.
- Backer, J.M., Myers, M.G., Jr., Shoelson, S.E., Chin, D.J., Sun, X.J., Miralpeix, M., Hu, P., Margolis, B., Skolnik, E.Y., Schlessinger, J., and et al. (1992). Phosphatidylinositol 3'-kinase is activated by association with IRS-1 during insulin stimulation. *EMBO J* 11, 3469-3479.
- Baksh, D., Song, L., and Tuan, R.S. (2004). Adult mesenchymal stem cells: characterization, differentiation, and application in cell and gene therapy. *J Cell Mol Med* 8, 301-316.
- Barnard, T. (1977). Brown adipose tissue as an effector of nonshivering thermogenesis. *Experientia* 33, 1124-1126.
- Begum, N., Sandu, O.A., Ito, M., Lohmann, S.M., and Smolenski, A. (2002). Active Rho kinase (ROK-alpha) associates with insulin receptor substrate-1 and inhibits insulin signaling in vascular smooth muscle cells. *J Biol Chem* 277, 6214-6222.
- Bieback, K., Kern, S., Kluter, H., and Eichler, H. (2004). Critical parameters for the isolation of mesenchymal stem cells from umbilical cord blood. *Stem Cells* 22, 625-634.
- Biel, M., Zong, X., Ludwig, A., Sautter, A., and Hofmann, F. (1999). Structure and function of cyclic nucleotide-gated channels. *Rev Physiol Biochem Pharmacol* 135, 151-171.
- Boehm, J.S., Zhao, J.J., Yao, J., Kim, S.Y., Firestein, R., Dunn, I.F., Sjostrom, S.K., Garraway, L.A., Weremowicz, S., Richardson, A.L., Greulich, H., Stewart, C.J., Mulvey, L.A., Shen, R.R., Ambrogio, L., Hirozane-Kishikawa, T., Hill, D.E., Vidal, M., Meyerson, M., Grenier, J.K., Hinkle, G., Root, D.E., Roberts, T.M., Lander, E.S., Polyak, K., and Hahn, W.C. (2007). Integrative genomic approaches identify IKBKE as a breast cancer oncogene. *Cell* 129, 1065-1079.
- Bradford, M.M. (1976). A rapid and sensitive method for the quantitation of microgram quantities of protein utilizing the principle of protein-dye binding. *Anal Biochem* 72, 248-254.

- Breitbach, M., Bostani, T., Roell, W., Xia, Y., Dewald, O., Nygren, J.M., Fries, J.W., Tiemann, K., Bohlen, H., Hescheler, J., Welz, A., Bloch, W., Jacobsen, S.E., and Fleischmann, B.K. (2007). Potential risks of bone marrow cell transplantation into infarcted hearts. *Blood* 110, 1362-1369.
- Campagnoli, C., Roberts, I.A., Kumar, S., Bennett, P.R., Bellantuono, I., and Fisk, N.M. (2001). Identification of mesenchymal stem/progenitor cells in human first-trimester fetal blood, liver, and bone marrow. *Blood* 98, 2396-2402.
- Cannon, B., and Nedergaard, J. (2004). Brown adipose tissue: function and physiological significance. *Physiol Rev* 84, 277-359.
- Cao, W., Daniel, K.W., Robidoux, J., Puigserver, P., Medvedev, A.V., Bai, X., Floering, L.M., Spiegelman, B.M., and Collins, S. (2004). p38 mitogen-activated protein kinase is the central regulator of cyclic AMP-dependent transcription of the brown fat uncoupling protein 1 gene. *Mol Cell Biol* 24, 3057-3067.
- Carey, M., and Lisberger, S. (2002). Embarrassed, but not depressed: eye opening lessons for cerebellar learning. *Neuron* 35, 223-226.
- Chao, A.C., de Sauvage, F.J., Dong, Y.J., Wagner, J.A., Goeddel, D.V., and Gardner, P. (1994). Activation of intestinal CFTR Cl⁻ channel by heat-stable enterotoxin and guanylin via cAMP-dependent protein kinase. *EMBO J* 13, 1065-1072.
- Chao, D.S., Silvagno, F., Xia, H., Cornwell, T.L., Lincoln, T.M., and Bredt, D.S. (1997). Nitric oxide synthase and cyclic GMP-dependent protein kinase concentrated at the neuromuscular endplate. *Neuroscience* 76, 665-672.
- Chen, C., and Tonegawa, S. (1997). Molecular genetic analysis of synaptic plasticity, activity-dependent neural development, learning, and memory in the mammalian brain. *Annu Rev Neurosci* 20, 157-184.
- Cinti, S. (2005). The adipose organ. *Prostaglandins Leukot Essent Fatty Acids* 73, 9-15.
- Conti, M., Nemoz, G., Sette, C., and Vicini, E. (1995). Recent progress in understanding the hormonal regulation of phosphodiesterases. *Endocr Rev* 16, 370-389.
- DeFronzo, R.A. (1997). Insulin resistance: a multifaceted syndrome responsible for NIDDM, obesity, hypertension, dyslipidaemia and atherosclerosis. *Neth J Med* 50, 191-197.
- Degerman, E., Belfrage, P., and Manganiello, V.C. (1997). Structure, localization, and regulation of cGMP-inhibited phosphodiesterase (PDE3). *J Biol Chem* 272, 6823-6826.
- Draijer, R., Vaandrager, A.B., Nolte, C., de Jonge, H.R., Walter, U., and van Hinsbergh, V.W. (1995). Expression of cGMP-dependent protein kinase I and phosphorylation of its substrate, vasodilator-stimulated phosphoprotein, in human endothelial cells of different origin. *Circ Res* 77, 897-905.
- Dull, T., Zufferey, R., Kelly, M., Mandel, R.J., Nguyen, M., Trono, D., and Naldini, L. (1998). A third-generation lentivirus vector with a conditional packaging system. *J Virol* 72, 8463-8471.

References

- Engelman, J.A., Berg, A.H., Lewis, R.Y., Lin, A., Lisanti, M.P., and Scherer, P.E. (1999). Constitutively active mitogen-activated protein kinase kinase 6 (MKK6) or salicylate induces spontaneous 3T3-L1 adipogenesis. *J Biol Chem* 274, 35630-35638.
- Engelman, J.A., Lisanti, M.P., and Scherer, P.E. (1998). Specific inhibitors of p38 mitogen-activated protein kinase block 3T3-L1 adipogenesis. *J Biol Chem* 273, 32111-32120.
- Etter, E.F., Eto, M., Wardle, R.L., Brautigan, D.L., and Murphy, R.A. (2001). Activation of myosin light chain phosphatase in intact arterial smooth muscle during nitric oxide-induced relaxation. *J Biol Chem* 276, 34681-34685.
- Feil, R., Hartmann, J., Luo, C., Wolfsgruber, W., Schilling, K., Feil, S., Barski, J.J., Meyer, M., Konnerth, A., De Zeeuw, C.I., and Hofmann, F. (2003). Impairment of LTD and cerebellar learning by Purkinje cell-specific ablation of cGMP-dependent protein kinase I. *J Cell Biol* 163, 295-302.
- Fukao, M., Mason, H.S., Britton, F.C., Kenyon, J.L., Horowitz, B., and Keef, K.D. (1999). Cyclic GMP-dependent protein kinase activates cloned BKCa channels expressed in mammalian cells by direct phosphorylation at serine 1072. *J Biol Chem* 274, 10927-10935.
- Furchgott, R.F., and Vanhoutte, P.M. (1989). Endothelium-derived relaxing and contracting factors. *FASEB J* 3, 2007-2018.
- Furukawa, N., Ongusaha, P., Jahng, W.J., Araki, K., Choi, C.S., Kim, H.J., Lee, Y.H., Kaibuchi, K., Kahn, B.B., Masuzaki, H., Kim, J.K., Lee, S.W., and Kim, Y.B. (2005). Role of Rho-kinase in regulation of insulin action and glucose homeostasis. *Cell Metab* 2, 119-129.
- Gambaryan, S., Geiger, J., Schwarz, U.R., Butt, E., Begonja, A., Oberfell, A., and Walter, U. (2004). Potent inhibition of human platelets by cGMP analogs independent of cGMP-dependent protein kinase. *Blood* 103, 2593-2600.
- Gamm, D.M., and Uhler, M.D. (1995). Isoform-specific differences in the potencies of murine protein kinase inhibitors are due to nonconserved amino-terminal residues. *J Biol Chem* 270, 7227-7232.
- Garbers, D.L., and Lowe, D.G. (1994). Guanylyl cyclase receptors. *J Biol Chem* 269, 30741-30744.
- Geiselhoring, A., Gaisa, M., Hofmann, F., and Schlossmann, J. (2004). Distribution of IRAG and cGKI-isoforms in murine tissues. *FEBS Lett* 575, 19-22.
- Guilak, F., Awad, H.A., Fermor, B., Leddy, H.A., and Gimble, J.M. (2004). Adipose-derived adult stem cells for cartilage tissue engineering. *Biorheology* 41, 389-399.
- Hamm, J.K., Park, B.H., and Farmer, S.R. (2001). A role for C/EBPbeta in regulating peroxisome proliferator-activated receptor gamma activity during adipogenesis in 3T3-L1 preadipocytes. *J Biol Chem* 276, 18464-18471.

References

- Hattori, H., Sato, M., Masuoka, K., Ishihara, M., Kikuchi, T., Matsui, T., Takase, B., Ishizuka, T., Kikuchi, M., and Fujikawa, K. (2004). Osteogenic potential of human adipose tissue-derived stromal cells as an alternative stem cell source. *Cells Tissues Organs* 178, 2-12.
- Hauser, W., Knobloch, K.P., Eigenthaler, M., Gambaryan, S., Krenn, V., Geiger, J., Glazova, M., Rohde, E., Horak, I., Walter, U., and Zimmer, M. (1999). Megakaryocyte hyperplasia and enhanced agonist-induced platelet activation in vasodilator-stimulated phosphoprotein knockout mice. *Proc Natl Acad Sci U S A* 96, 8120-8125.
- Heil, W.G., Landgraf, W., and Hofmann, F. (1987). A catalytically active fragment of cGMP-dependent protein kinase. Occupation of its cGMP-binding sites does not affect its phosphotransferase activity. *Eur J Biochem* 168, 117-121.
- Herzig, S., Long, F., Jhala, U.S., Hedrick, S., Quinn, R., Bauer, A., Rudolph, D., Schutz, G., Yoon, C., Puigserver, P., Spiegelman, B., and Montminy, M. (2001). CREB regulates hepatic gluconeogenesis through the coactivator PGC-1. *Nature* 413, 179-183.
- Hofmann, F., Ammendola, A., and Schlossmann, J. (2000). Rising behind NO: cGMP-dependent protein kinases. *J Cell Sci* 113 (Pt 10), 1671-1676.
- Hofmann, F., Dostmann, W., Keilbach, A., Landgraf, W., and Ruth, P. (1992). Structure and physiological role of cGMP-dependent protein kinase. *Biochim Biophys Acta* 1135, 51-60.
- Hofmann, F., and Sold, G. (1972). A protein kinase activity from rat cerebellum stimulated by guanosine-3':5'-monophosphate. *Biochem Biophys Res Commun* 49, 1100-1107.
- Hotamisligil, G.S., Peraldi, P., Budavari, A., Ellis, R., White, M.F., and Spiegelman, B.M. (1996). IRS-1-mediated inhibition of insulin receptor tyrosine kinase activity in TNF- α - and obesity-induced insulin resistance. *Science* 271, 665-668.
- Ignarro, L.J., Napoli, C., and Loscalzo, J. (2002). Nitric oxide donors and cardiovascular agents modulating the bioactivity of nitric oxide: an overview. *Circ Res* 90, 21-28.
- In 't Anker, P.S., Scherjon, S.A., Kleijburg-van der Keur, C., de Groot-Swings, G.M., Claas, F.H., Fibbe, W.E., and Kanhai, H.H. (2004). Isolation of mesenchymal stem cells of fetal or maternal origin from human placenta. *Stem Cells* 22, 1338-1345.
- Jiang, H., Shabb, J.B., and Corbin, J.D. (1992). Cross-activation: overriding cAMP/cGMP selectivities of protein kinases in tissues. *Biochem Cell Biol* 70, 1283-1289.
- Joyce, N.C., DeCamilli, P., Lohmann, S.M., and Walter, U. (1986). cGMP-dependent protein kinase is present in high concentrations in contractile cells of the kidney vasculature. *J Cyclic Nucleotide Protein Phosphor Res* 11, 191-198.
- Junqueira, L. and Carneiro, J. (2002). *Basic histology*. McGraw-Hill Professional; 10th Edition; ISBN: 0071215654.
- Kasuga, M., Karlsson, F.A., and Kahn, C.R. (1982). Insulin stimulates the phosphorylation of the 95,000-dalton subunit of its own receptor. *Science* 215, 185-187.

References

- Keilbach, A., Ruth, P., and Hofmann, F. (1992). Detection of cGMP dependent protein kinase isozymes by specific antibodies. *Eur J Biochem* 208, 467-473.
- Kleppisch, T., Pfeifer, A., Klatt, P., Ruth, P., Montkowski, A., Fassler, R., and Hofmann, F. (1999). Long-term potentiation in the hippocampal CA1 region of mice lacking cGMP-dependent kinases is normal and susceptible to inhibition of nitric oxide synthase. *J Neurosci* 19, 48-55.
- Kleppisch, T., Wolfgruber, W., Feil, S., Allmann, R., Wotjak, C.T., Goebbels, S., Nave, K.A., Hofmann, F., and Feil, R. (2003). Hippocampal cGMP-dependent protein kinase I supports an age- and protein synthesis-dependent component of long-term potentiation but is not essential for spatial reference and contextual memory. *J Neurosci* 23, 6005-6012.
- Komalavilas, P., and Lincoln, T.M. (1996). Phosphorylation of the inositol 1,4,5-trisphosphate receptor. Cyclic GMP-dependent protein kinase mediates cAMP and cGMP dependent phosphorylation in the intact rat aorta. *J Biol Chem* 271, 21933-21938.
- Kumar, R., Joyner, R.W., Komalavilas, P., and Lincoln, T.M. (1999). Analysis of expression of cGMP-dependent protein kinase in rabbit heart cells. *J Pharmacol Exp Ther* 291, 967-975.
- Kuo, J.F., and Greengard, P. (1970). Cyclic nucleotide-dependent protein kinases. VI. Isolation and partial purification of a protein kinase activated by guanosine 3',5'-monophosphate. *J Biol Chem* 245, 2493-2498.
- Laemmli, U.K. (1970). Cleavage of structural proteins during the assembly of the head of bacteriophage T4. *Nature* 227, 680-685.
- Landgraf, W., Hullin, R., Gobel, C., and Hofmann, F. (1986). Phosphorylation of cGMP-dependent protein kinase increases the affinity for cyclic AMP. *Eur J Biochem* 154, 113-117.
- Lehman, J.J., Barger, P.M., Kovacs, A., Saffitz, J.E., Medeiros, D.M., and Kelly, D.P. (2000). Peroxisome proliferator-activated receptor gamma coactivator-1 promotes cardiac mitochondrial biogenesis. *J Clin Invest* 106, 847-856.
- Lincoln, T.M., Cornwell, T.L., and Taylor, A.E. (1990). cGMP-dependent protein kinase mediates the reduction of Ca²⁺ by cAMP in vascular smooth muscle cells. *Am J Physiol* 258, C399-407.
- Lloyd-Jones, D.M., and Bloch, K.D. (1996). The vascular biology of nitric oxide and its role in atherogenesis. *Annu Rev Med* 47, 365-375.
- Lohmann, S.M., Walter, U., Miller, P.E., Greengard, P., and De Camilli, P. (1981). Immunohistochemical localization of cyclic GMP-dependent protein kinase in mammalian brain. *Proc Natl Acad Sci U S A* 78, 653-657.
- Lorenzo, M., Valverde, A.M., Teruel, T., and Benito, M. (1993). IGF-I is a mitogen involved in differentiation-related gene expression in fetal rat brown adipocytes. *J Cell Biol* 123, 1567-1575.

- Loscalzo, J., and Welch, G. (1995). Nitric oxide and its role in the cardiovascular system. *Prog Cardiovasc Dis* 38, 87-104.
- Manganiello, V.C., Murata, T., Taira, M., Belfrage, P., and Degerman, E. (1995). Diversity in cyclic nucleotide phosphodiesterase isoenzyme families. *Arch Biochem Biophys* 322, 1-13.
- Marshall, S.J., Senis, Y.A., Auger, J.M., Feil, R., Hofmann, F., Salmon, G., Peterson, J.T., Burslem, F., and Watson, S.P. (2004). GPIIb-dependent platelet activation is dependent on Src kinases but not MAP kinase or cGMP-dependent kinase. *Blood* 103, 2601-2609.
- Massberg, S., Gruner, S., Konrad, I., Garcia Arguinzonis, M.I., Eigenthaler, M., Hemler, K., Kersting, J., Schulz, C., Muller, I., Besta, F., Nieswandt, B., Heinzmann, U., Walter, U., and Gawaz, M. (2004). Enhanced in vivo platelet adhesion in vasodilator-stimulated phosphoprotein (VASP)-deficient mice. *Blood* 103, 136-142.
- Massberg, S., Sausbier, M., Klatt, P., Bauer, M., Pfeifer, A., Siess, W., Fassler, R., Ruth, P., Krombach, F., and Hofmann, F. (1999). Increased adhesion and aggregation of platelets lacking cyclic guanosine 3',5'-monophosphate kinase I. *J Exp Med* 189, 1255-1264.
- Matthias, A., Ohlson, K.B., Fredriksson, J.M., Jacobsson, A., Nedergaard, J., and Cannon, B. (2000). Thermogenic responses in brown fat cells are fully UCP1-dependent. UCP2 or UCP3 do not substitute for UCP1 in adrenergically or fatty acid-induced thermogenesis. *J Biol Chem* 275, 25073-25081.
- McBeath, R., Pirone, D.M., Nelson, C.M., Bhadriraju, K., and Chen, C.S. (2004). Cell shape, cytoskeletal tension, and RhoA regulate stem cell lineage commitment. *Dev Cell* 6, 483-495.
- Munzel, T., Feil, R., Mulsch, A., Lohmann, S.M., Hofmann, F., and Walter, U. (2003). Physiology and pathophysiology of vascular signaling controlled by guanosine 3',5'-cyclic monophosphate-dependent protein kinase [corrected]. *Circulation* 108, 2172-2183.
- Murad, F. (2006). Shattuck Lecture. Nitric oxide and cyclic GMP in cell signaling and drug development. *N Engl J Med* 355, 2003-2011.
- Nechad, M. (1983). Development of brown fat cells in monolayer culture. II. Ultrastructural characterization of precursors, differentiating adipocytes and their mitochondria. *Exp Cell Res* 149, 119-127.
- Nedergaard, J., Bengtsson, T., and Cannon, B. (2007). Unexpected evidence for active brown adipose tissue in adult humans. *Am J Physiol Endocrinol Metab* 293, E444-452.
- Nisoli, E., Clementi, E., Paolucci, C., Cozzi, V., Tonello, C., Sciorati, C., Bracale, R., Valerio, A., Francolini, M., Moncada, S., and Carruba, M.O. (2003). Mitochondrial biogenesis in mammals: the role of endogenous nitric oxide. *Science* 299, 896-899.
- Nisoli, E., Clementi, E., Tonello, C., Sciorati, C., Briscini, L., and Carruba, M.O. (1998). Effects of nitric oxide on proliferation and differentiation of rat brown adipocytes in primary cultures. *Br J Pharmacol* 125, 888-894.

References

- Nisoli, E., Tonello, C., Cardile, A., Cozzi, V., Bracale, R., Tedesco, L., Falcone, S., Valerio, A., Cantoni, O., Clementi, E., Moncada, S., and Carruba, M.O. (2005). Calorie restriction promotes mitochondrial biogenesis by inducing the expression of eNOS. *Science* 310, 314-317.
- Noguchi, M., Hosoda, K., Fujikura, J., Fujimoto, M., Iwakura, H., Tomita, T., Ishii, T., Arai, N., Hirata, M., Ebihara, K., Masuzaki, H., Itoh, H., Narumiya, S., and Nakao, K. (2007). Genetic and pharmacological inhibition of Rho-associated kinase II enhances adipogenesis. *J Biol Chem* 282, 29574-29583.
- Palmer, R.M., Ferrige, A.G., and Moncada, S. (1987). Nitric oxide release accounts for the biological activity of endothelium-derived relaxing factor. *Nature* 327, 524-526.
- Pfeifer, A., Brandon, E.P., Kootstra, N., Gage, F.H., and Verma, I.M. (2001). Delivery of the Cre recombinase by a self-deleting lentiviral vector: efficient gene targeting in vivo. *Proc Natl Acad Sci U S A* 98, 11450-11455.
- Pfeifer, A., Klatt, P., Massberg, S., Ny, L., Sausbier, M., Hirneiss, C., Wang, G.X., Korth, M., Aszodi, A., Andersson, K.E., Krombach, F., Mayerhofer, A., Ruth, P., Fassler, R., and Hofmann, F. (1998). Defective smooth muscle regulation in cGMP kinase I-deficient mice. *Embo J* 17, 3045-3051.
- Pfeifer, A., Ruth, P., Dostmann, W., Sausbier, M., Klatt, P., and Hofmann, F. (1999). Structure and function of cGMP-dependent protein kinases. *Rev Physiol Biochem Pharmacol* 135, 105-149.
- Pittenger, M.F., Mackay, A.M., Beck, S.C., Jaiswal, R.K., Douglas, R., Mosca, J.D., Moorman, M.A., Simonetti, D.W., Craig, S., and Marshak, D.R. (1999). Multilineage potential of adult human mesenchymal stem cells. *Science* 284, 143-147.
- Prunet-Marcassus, B., Cousin, B., Caton, D., Andre, M., Penicaud, L., and Casteilla, L. (2006). From heterogeneity to plasticity in adipose tissues: site-specific differences. *Exp Cell Res* 312, 727-736.
- Pryzwansky, K.B., Kidao, S., Wyatt, T.A., Reed, W., and Lincoln, T.M. (1995). Localization of cyclic GMP-dependent protein kinase in human mononuclear phagocytes. *J Leukoc Biol* 57, 670-678.
- Puigserver, P., Wu, Z., Park, C.W., Graves, R., Wright, M., and Spiegelman, B.M. (1998). A cold-inducible coactivator of nuclear receptors linked to adaptive thermogenesis. *Cell* 92, 829-839.
- Qian, Y., Chao, D.S., Santillano, D.R., Cornwell, T.L., Nairn, A.C., Greengard, P., Lincoln, T.M., and Brecht, D.S. (1996). cGMP-dependent protein kinase in dorsal root ganglion: relationship with nitric oxide synthase and nociceptive neurons. *J Neurosci* 16, 3130-3138.
- Reid, T., Bathorn, A., Ahmadian, M.R., and Collard, J.G. (1999). Identification and characterization of hPEM-2, a guanine nucleotide exchange factor specific for Cdc42. *J Biol Chem* 274, 33587-33593.
- Ren, X.D., Kioussis, W.B., and Schwartz, M.A. (1999). Regulation of the small GTP-binding protein Rho by cell adhesion and the cytoskeleton. *EMBO J* 18, 578-585.

- Ridley, A.J., and Hall, A. (1992). The small GTP-binding protein rho regulates the assembly of focal adhesions and actin stress fibers in response to growth factors. *Cell* 70, 389-399.
- Rolli-Derkinderen, M., Sauzeau, V., Boyer, L., Lemichez, E., Baron, C., Henrion, D., Loirand, G., and Pacaud, P. (2005). Phosphorylation of serine 188 protects RhoA from ubiquitin/proteasome-mediated degradation in vascular smooth muscle cells. *Circ Res* 96, 1152-1160.
- Rondinone, C.M., Wang, L.M., Lonroth, P., Wesslau, C., Pierce, J.H., and Smith, U. (1997). Insulin receptor substrate (IRS) 1 is reduced and IRS-2 is the main docking protein for phosphatidylinositol 3-kinase in adipocytes from subjects with non-insulin-dependent diabetes mellitus. *Proc Natl Acad Sci U S A* 94, 4171-4175.
- Rothwell, N.J., and Stock, M.J. (1979). A role for brown adipose tissue in diet-induced thermogenesis. *Nature* 281, 31-35.
- Ruth, P., Pfeifer, A., Kamm, S., Klatt, P., Dostmann, W.R., and Hofmann, F. (1997). Identification of the amino acid sequences responsible for high affinity activation of cGMP kinase Ialpha. *J Biol Chem* 272, 10522-10528.
- Ruth, P., Wang, G.X., Boekhoff, I., May, B., Pfeifer, A., Penner, R., Korth, M., Breer, H., and Hofmann, F. (1993). Transfected cGMP-dependent protein kinase suppresses calcium transients by inhibition of inositol 1,4,5-trisphosphate production. *Proc Natl Acad Sci U S A* 90, 2623-2627.
- Safford, K.M., Safford, S.D., Gimble, J.M., Shetty, A.K., and Rice, H.E. (2004). Characterization of neuronal/glial differentiation of murine adipose-derived adult stromal cells. *Exp Neurol* 187, 319-328.
- Saiki, R.K., Gelfand, D.H., Stoffel, S., Scharf, S.J., Higuchi, R., Horn, G.T., Mullis, K.B., and Erlich, H.A. (1988). Primer-directed enzymatic amplification of DNA with a thermostable DNA polymerase. *Science* 239, 487-491.
- Salmon, P., Oberholzer, J., Occhiodoro, T., Morel, P., Lou, J., and Trono, D. (2000). Reversible immortalization of human primary cells by lentivector-mediated transfer of specific genes. *Mol Ther* 2, 404-414.
- Sauzeau, V., Le Jeune, H., Cario-Toumaniantz, C., Smolenski, A., Lohmann, S.M., Bertoglio, J., Chardin, P., Pacaud, P., and Loirand, G. (2000). Cyclic GMP-dependent protein kinase signaling pathway inhibits RhoA-induced Ca²⁺ sensitization of contraction in vascular smooth muscle. *J Biol Chem* 275, 21722-21729.
- Sawada, N., Itoh, H., Yamashita, J., Doi, K., Inoue, M., Masatsugu, K., Fukunaga, Y., Sakaguchi, S., Sone, M., Yamahara, K., Yurugi, T., and Nakao, K. (2001). cGMP-dependent protein kinase phosphorylates and inactivates RhoA. *Biochem Biophys Res Commun* 280, 798-805.
- Schlossmann, J., Ammendola, A., Ashman, K., Zong, X., Huber, A., Neubauer, G., Wang, G.X., Allescher, H.D., Korth, M., Wilm, M., Hofmann, F., and Ruth, P. (2000). Regulation of intracellular calcium by a signalling complex of IRAG, IP3 receptor and cGMP kinase Ibeta. *Nature* 404, 197-201.

References

- Schmidt, H., Werner, M., Heppenstall, P.A., Henning, M., More, M.I., Kuhbandner, S., Lewin, G.R., Hofmann, F., Feil, R., and Rathjen, F.G. (2002). cGMP-mediated signaling via cGKIalpha is required for the guidance and connectivity of sensory axons. *J Cell Biol* 159, 489-498.
- Schmidt, H.H., and Walter, U. (1994). NO at work. *Cell* 78, 919-925.
- Sengenès, C., Bouloumie, A., Hauner, H., Berlan, M., Busse, R., Lafontan, M., and Galitzky, J. (2003). Involvement of a cGMP-dependent pathway in the natriuretic peptide-mediated hormone-sensitive lipase phosphorylation in human adipocytes. *J Biol Chem* 278, 48617-48626.
- Shibuki, K., and Okada, D. (1991). Endogenous nitric oxide release required for long-term synaptic depression in the cerebellum. *Nature* 349, 326-328.
- Shih, D.T., Lee, D.C., Chen, S.C., Tsai, R.Y., Huang, C.T., Tsai, C.C., Shen, E.Y., and Chiu, W.T. (2005). Isolation and characterization of neurogenic mesenchymal stem cells in human scalp tissue. *Stem Cells* 23, 1012-1020.
- Shih, M.F., and Taberner, P.V. (1995). Selective activation of brown adipocyte hormone-sensitive lipase and cAMP production in the mouse by beta 3-adrenoceptor agonists. *Biochem Pharmacol* 50, 601-608.
- Skolnik, E.Y., Lee, C.H., Batzer, A., Vicentini, L.M., Zhou, M., Daly, R., Myers, M.J., Jr., Backer, J.M., Ullrich, A., White, M.F., and et al. (1993). The SH2/SH3 domain-containing protein GRB2 interacts with tyrosine-phosphorylated IRS1 and Shc: implications for insulin control of ras signalling. *EMBO J* 12, 1929-1936.
- Smith, J.A., Francis, S.H., Walsh, K.A., Kumar, S., and Corbin, J.D. (1996). Autophosphorylation of type Ibeta cGMP-dependent protein kinase increases basal catalytic activity and enhances allosteric activation by cGMP or cAMP. *J Biol Chem* 271, 20756-20762.
- Sonnenburg, W.K., and Beavo, J.A. (1994). Cyclic GMP and regulation of cyclic nucleotide hydrolysis. *Adv Pharmacol* 26, 87-114.
- Sordella, R., Jiang, W., Chen, G.C., Curto, M., and Settleman, J. (2003). Modulation of Rho GTPase signaling regulates a switch between adipogenesis and myogenesis. *Cell* 113, 147-158.
- Su, Y., Dostmann, W.R., Herberg, F.W., Durick, K., Xuong, N.H., Ten Eyck, L., Taylor, S.S., and Varughese, K.I. (1995). Regulatory subunit of protein kinase A: structure of deletion mutant with cAMP binding domains. *Science* 269, 807-813.
- Sun, X.J., Crimmins, D.L., Myers, M.G., Jr., Miralpeix, M., and White, M.F. (1993). Pleiotropic insulin signals are engaged by multisite phosphorylation of IRS-1. *Mol Cell Biol* 13, 7418-7428.
- Sun, X.J., Wang, L.M., Zhang, Y., Yenush, L., Myers, M.G., Jr., Glasheen, E., Lane, W.S., Pierce, J.H., and White, M.F. (1995). Role of IRS-2 in insulin and cytokine signalling. *Nature* 377, 173-177.

- Surks, H.K., Mochizuki, N., Kasai, Y., Georgescu, S.P., Tang, K.M., Ito, M., Lincoln, T.M., and Mendelsohn, M.E. (1999). Regulation of myosin phosphatase by a specific interaction with cGMP- dependent protein kinase I α . *Science* 286, 1583-1587.
- Sykiotis, G.P., and Papavassiliou, A.G. (2001). Serine phosphorylation of insulin receptor substrate-1: a novel target for the reversal of insulin resistance. *Mol Endocrinol* 15, 1864-1869.
- Taniguchi, J., Furukawa, K.I., and Shigekawa, M. (1993). Maxi K⁺ channels are stimulated by cyclic guanosine monophosphate-dependent protein kinase in canine coronary artery smooth muscle cells. *Pflugers Arch* 423, 167-172.
- Teruel, T., Valverde, A.M., Benito, M., and Lorenzo, M. (1996). Insulin-like growth factor I and insulin induce adipogenic-related gene expression in fetal brown adipocyte primary cultures. *Biochem J* 319 (Pt 2), 627-632.
- Thonberg, H., Fredriksson, J.M., Nedergaard, J., and Cannon, B. (2002). A novel pathway for adrenergic stimulation of cAMP-response-element-binding protein (CREB) phosphorylation: mediation via α 1-adrenoceptors and protein kinase C activation. *Biochem J* 364, 73-79.
- Uldry, M., Yang, W., St-Pierre, J., Lin, J., Seale, P., and Spiegelman, B.M. (2006). Complementary action of the PGC-1 coactivators in mitochondrial biogenesis and brown fat differentiation. *Cell Metab* 3, 333-341.
- Ullrich, A., Bell, J.R., Chen, E.Y., Herrera, R., Petruzzelli, L.M., Dull, T.J., Gray, A., Coussens, L., Liao, Y.C., Tsubokawa, M., and et al. (1985). Human insulin receptor and its relationship to the tyrosine kinase family of oncogenes. *Nature* 313, 756-761.
- Valverde, A.M., Benito, M., and Lorenzo, M. (1992). Hormonal regulation of malic enzyme and glucose-6-phosphate-dehydrogenase expression in fetal brown-adipocyte primary cultures under non-proliferative conditions. *Eur J Biochem* 203, 313-319.
- Valverde, A.M., Benito, M., and Lorenzo, M. (2005). The brown adipose cell: a model for understanding the molecular mechanisms of insulin resistance. *Acta Physiol Scand* 183, 59-73.
- Waldmann, R., Bauer, S., Gobel, C., Hofmann, F., Jakobs, K.H., and Walter, U. (1986). Demonstration of cGMP-dependent protein kinase and cGMP-dependent phosphorylation in cell-free extracts of platelets. *Eur J Biochem* 158, 203-210.
- White, M.F. (2003). Insulin signaling in health and disease. *Science* 302, 1710-1711.
- White, M.F., and Kahn, C.R. (1994). The insulin signaling system. *J Biol Chem* 269, 1-4.
- Wojciak-Stothard, B., and Ridley, A.J. (2003). Shear stress-induced endothelial cell polarization is mediated by Rho and Rac but not Cdc42 or PI 3-kinases. *J Cell Biol* 161, 429-439.
- Wooldridge, A.A., MacDonald, J.A., Erdodi, F., Ma, C., Borman, M.A., Hartshorne, D.J., and Haystead, T.A. (2004). Smooth muscle phosphatase is regulated in vivo by exclusion of phosphorylation of threonine 696 of MYPT1 by phosphorylation of Serine 695 in response to cyclic nucleotides. *J Biol Chem* 279, 34496-34504.

References

- Wu, Z., Puigserver, P., Andersson, U., Zhang, C., Adelmant, G., Mootha, V., Troy, A., Cinti, S., Lowell, B., Scarpulla, R.C., and Spiegelman, B.M. (1999). Mechanisms controlling mitochondrial biogenesis and respiration through the thermogenic coactivator PGC-1. *Cell* 98, 115-124.
- Zhuo, M., Hu, Y., Schultz, C., Kandel, E.R., and Hawkins, R.D. (1994). Role of guanylyl cyclase and cGMP-dependent protein kinase in long-term potentiation. *Nature* 368, 635-639.
- Zuk, P.A., Zhu, M., Ashjian, P., De Ugarte, D.A., Huang, J.I., Mizuno, H., Alfonso, Z.C., Fraser, J.K., Benhaim, P., and Hedrick, M.H. (2002). Human adipose tissue is a source of multipotent stem cells. *Mol Biol Cell* 13, 4279-4295.
- Zuk, P.A., Zhu, M., Mizuno, H., Huang, J., Futrell, J.W., Katz, A.J., Benhaim, P., Lorenz, H.P., and Hedrick, M.H. (2001). Multilineage cells from human adipose tissue: implications for cell-based therapies. *Tissue Eng* 7, 211-228.